Palestine Polytechnic University

College of Engineering

Artificial Neural Networks - Based Protection System

Prepared by:

Karma Shehadeh **Mahmoud Tamimi**

Supervisor:

Dr.Fouad Zaro

Submitted to the College of Engineering
in partial fulfillment of the requirements for the
Bachelor degree in Power Engineering

Hebron, May 2018

Palestine Polytechnic University

Hebron - Palestine
College of Engineering
Department of Electrical Engineering

Project:

Artificial Neural Networks - Based Protection System

Team:

Karma Shehadeh **Mahmoud Tamimi**

By the guidance of our supervisor, and by the acceptance of all members in the testing committee this project is delivered to the Electrical Engineering Department in the College of Engineering to be as a fulfillment of the requirements for the Bachelor degree in Power Technology Engineering.

Supervisor signature

The head of department signature

Acknowledgment

A part of our effort and the successes of any project depends largely on the encouragements of others.

We take this opportunity to express our regards and gratitude to those people who were part of completing this project.

We would like to show our appropriation to our supervisor Dr.Fouad Zaro, for his support and guidelines that he gave us throughout the year .We would also like to thank Eng. Elias Maharmeh , Eng.Motaz Jawa'deh, Eng.Muhammad Tamimi and Eng.Samer Sultan for their help. And we are so grateful to our parents for their support.

Abstract

In order to ensure Stability and security of the power system , it's extremely important to detect , and locate different types of faults as fast as possible.

This project is a framework of a protection system that based on artificial intelligence, specifically **Artificial Neural Networks** . This protection system consists of several networks that can detect , classify and locate different types of faults .

The artificial neural networks of our project have been designed using MATLAB. And have been tested using MATLAB data , SIMULINK system data and practical data from HEPCO .

الملخص

بهدف المحافظة على اتزان النظام و تقليل الخسائر الهائلة التي من الممكن ان تسببها الاخطاء الكهربائية ،فإنه من الضروري وجود نظام حماية دقيق ، قادر على استكشاف الاخطاء ، و التعرف على انواعها ، و تحديد مكانها في الشبكة ، لاتخاذ اجراء بناءً على ذلك.

هذا المشروع عبارة عن تصميم اطار نظري لنظام حماية باستخدام احدى تقنيات الذكاء الإصطناعي ، و هي شبكة الأعصاب الصناعية (ANN)، هذا النظام مكون من عدة شبكات قادرة على اكتشاف ، و تصنيف ، و تحديد أماكن مختلف أنواع الأعطال .

تم تصميم هذه الشبكات باستخدام برنامج ال MATLAB و تم اختبارها باستخدام بيانات مصدرها ال SIMULINK و اخرى مصدرها شركة كهرباء الخليل .

Table of Contents

Subject	Page
CONTENTS	**I**
LIST OF FIGURES	**III**
LIST OF EQUATIONS	IV
CHAPTER ONE: Introduction	
1.1. Introduction	**2**
1.2. Project Objectives	**3**
1.3. Importance	**3**
1.4. Methodology	**3**
1.5. Literature Review	**4**
CHAPTER TWO: Power System Faults	
2.1. Introduction	**7**
2.2. Power System Faults	**7**
2.2.1. Causes of Faults	**7**
2.2.2. Effects of Power System Faults	**9**
2.2.3. Classification of Faults	**11**
2.2.4. Method of Analysis	**12**
CHAPTER THREE: Artificial Neural Network	
3.1 Artificial Neural Network	**20**
3.2 History of Artificial Neural Networks	**20**
3.3 Structure Neural Networks	**25**
3.5 Working algorithm of ANN'	**27**
3.5.1 Learning in Artificial Neural Networks	**30**

3.6 Number of layers and neurons that should be used in an ANN	**31**
3.7 ANN's Advantages	**32**
CHAPTER FOUR : Project Design	
4.1 Introduction	**36**
4.2 Ideal Design	**36**
4.2.1 Fault Detection Neural Network	**36**
4.2.2 Fault Classification Neural Network	**39**
4.2.3 L-G Fault Locating Neural Network	**41**
4.2.4 L-L Fault Locating Neural Network	**44**
4.2.5 LL-G Fault Locating Neural Network	**46**
4.2.6 Three Phase Fault Locating Neural Network	**48**
4.3 Fourteen Bus System Based Neural Network	**50**
4.3.1 Fault Detection Neural Network	**51**
4.3.2 Fault Classification Neural Network	**53**
4.3.3 L-G Fault Locating Neural Network	**55**
4.3.4 L-L Fault Locating Neural Network	**57**
4.3.5 LL-G Fault Locating Neural Network	**59**
4.3.6 Three Phase Fault Locating Neural Network	**61**
4.3.7 Distance Neural Network	**63**
4.4 Thirty Bus System Based Neural Network	**69**
4.4.1 Fault Detection Neural Network	**71**
4.4.2 Fault Classification Neural Network	**72**
4.4.3 L-G Fault Locating Neural Network	**74**
4.4.4 L-L Fault Locating Neural Network	**76**

4.4.5 LL-G Fault Locating Neural Network	**78**
4.4.6 Three Phase Fault Locating Neural Network	**80**
CHAPTER FIVE :Project Results And Analysis	
5.1 Introduction	**84**
5.2 Ideal Design Analysis	**84**
5.3 14-Bus System Based Design Analysis	**86**
Conclusion and Recommendations	**88**
References	**89**

List of Tables

Table	Page
Table (4.1) : Detection Data Sample	**37**
Table (4.2) : Classification Data Sample	**40**
Table (4.3) : L-G Data Sample	**42**
Table (4.4) : L-L Fault Locating Data Sample	**45**
Table (4.5) : LL-G Fault Locating Data Sample	**47**
Table (4.6) : Three Phase Fault Locating Data Sample	**49**
Table (4.7) : Detection Data Sample	**52**
Table (4.8) : Fault Classification Data Sample	**54**
Table (4.9) : L-G Fault Locating Data Sample	**56**
Table (4.10) : L-L Fault Locating Data Sample	**58**
Table (4.11) : LL-G Fault Locating Data Sample	**60**

Table (4.12) : Three Phase Fault Locating Data Sample	**62**
Table (5.1) : Ideal Locating Network Testing Sample (Ideal System)	**85**
Table (5.2) : Ideal Locating Network Testing Sample (14-Bus System)	**86**
Table (5.3) : 14-Bus System Classification Network Testing Sample.	**87**

List of Figures

Figure	Page
Figure (2.1) : lightening strike - Transmission Tower	**8**
Figure (2.2): A squirrel chewed into a power line in Trumbull, Connecticut, where the Nasdaq's computer center is located, shutting down trading for 34 minutes.	**8**
Figure (2.3) : Two Snakes That Died In An Electric Box	**8**
Figure (2.4) : Tree Distances From Overhead Transmission Lines	**9**
Figure (2.5) : Positive sequence components	**13**
Figure (2.6) : Negative sequence components	**14**
Figure (2.7) : Zero sequence components	**15**
Figure (3.1) : Basic two-layer architecture of a feed forward ANN	**26**
Figure (3.2) : Step activation function	**28**
Figure (3.3) : Piece wise linear activation function	**28**
Figure (3.4) : Sigmoid unipolar activation function	**28**
Figure (3.5) : Typical model of a neuron	**29**
Figure (3.6) : Single neuron	**31**
Figure (4.1) : Detection Network Design	**37**
Figure (4.2): Detecting Network performance	**38**
Figure (4.3) : Classification Network Design	**39**

Figure (4.4) : Classification Network Performance	**41**
Figure (4.5) : L-G Locating Network Design	**42**
Figure (4.6) : L-G Fault Locating Network Performance	**43**
Figure (4.7) : L-L Locating Network Design	**44**
Figure (4.8) : L-L Fault Locating Network Performance	**45**
Figure (4.9) : LL-G Locating Network Design	**46**
Figure (4.10) : LL-G Fault Locating Network Performance	**47**
Figure (4.11) : 3-Phase Faults Locating Network	**48**
Figure (4.12) : Symmetrical Faults Locating Network Performance	**49**
Figure (4.13) : IEEE 14 Bus System Standard	**50**
Figure (4.14) : Fault Detection Network Design	**51**
Figure (4.15) : Fault Detection Network Performance	**52**
Figure (4.16) : Fault Classification Network Design	**53**
Figure (4.17) : Fault Classification Network Performance	**54**
Figure (4.18) : L-G Fault Locating Network Design	**55**
Figure (4.19) : L-G Fault Locating Network	**56**
Figure (4.20) : L-L Fault Locating Network	**57**
Figure (4.21) : L-L Locating Network Performance	**58**
Figure (4.22) : LL-G Locating Network	**59**
Figure (4.23) : LL-G Fault Locating Network Performance	**60**
Figure (4.24) : 3-Phase Faults Locating Network	**61**
Figure (4.25) : Three Phase Fault Locating Network Performance	**62**
Figure (4.26) : Distance Network Design	**63**
Figure (4.27) : Distance Network Performance	**64**

Figure (4.28) : IEEE 30 Bus System Standard	**70**
Figure (4.29) : Fault Detection Network Design	**71**
Figure (4.30) : Fault Detection Network Performance	**72**
Figure (4.31) : Fault Classification Network Design	**73**
Figure (4.32) : Fault Classification Network Performance	**74**
Figure (4.33) : L-G Fault Locating Network Design	**75**
Figure (4.34) : L-G Fault Locating Network	**76**
Figure (4.35) : L-L Fault Locating Network	**77**
Figure (4.36) : L-L Locating Network Performance	**78**
Figure (4.37) : LL-G Locating Network	**79**
Figure (4.38) : LL-G Fault Locating Network Performance	**80**
Figure (4.39) : 3-Phase Faults Locating Network	**81**
Figure (4.40) : Three Phase Fault Locating Network Performance	**82**

List Of Equations

Equations	Page
Equation(2.1):Symmetrical components Va	**15**
Equation(2.2):Symmetrical components Vb	**15**
Equation(2.3): Symmetrical components Vc	**15**
Equation(2.4): The “a” operator	**16**
Equation(2.5): The square of “a” operator	**16**
Equation(2.6): The cubic of “a” operator	**16**
Equation(2.7): Zero sequence components	**16**

Equation(2.8): Positive sequence components	**16**
Equation(2.9): Positive sequence components	**16**
Equation(2.10):Negative sequence components	**16**
Equation(2.11): Negative sequence components	**16**
Equation(2.12): Va phasor	**16**
Equation(2.13): Vb in terms of phase a	**16**
Equation(2.14): Vc in terms of phase a	**16**
Equation(2.15): Matrix form	**17**
Equation(2.16): A matrix	**17**
Equation(2.17): Matrix form with A	**17**
Equation(2.18): Reversed equation for the positive , negative and zero sequences	**17**
Equation(2.19): The inverse matrix of A	**17**
Equation(3.1): The output of the neuron	**29**
Equation(3.2): Propagation function output	**29**
Equation(3.3): The weights vector	**29**
Equation(3.4):The inputs vector	**29**
Equation(3.5): The output of the activation function	**30**
Equation(3.6): Sigmoid as an activation function	**30**
Equation(3.7):The output equation .	**31**
Equation(3.8): The error value	**31**

Equation(3.9):The error gradient	**31**
Equation(3.10):Error gradient	**31**
Equation(3.11):Weight delta	**31**
Equation(3.12):Threshold value delta	**31**
Equation(3.13):The new value of the weight	**31**
Equation(3.14):The new value of the threshold	**31**

1

Chapter One Introduction

1.1 Introduction

1.2 Project Objectives

1.3 Importance

1.4 Methodology

1.5 Literature Review

Chapter one

Introduction

1.1 Introduction

Power transmission lines are considered to be the pivotal links that give the intrinsic continuity of service from power plants to customers. Because of exposing transmission lines to environment, the possibility of experiencing faults on them is higher than other power system components. The most common faults are line faults which could be caused by many environmental factors, such as lightning strikes, trees which may fall across lines, dirty insulators which could cause flash over, and many other factors.

In order to ensure stability and security of the power system, it's extremely important to have an accurate protection system that can detect, classify, and locate different types of faults as fast as possible, to minimize the system damage as much as it could be minimized without any interrupting over healthy circuits in the system .

Our project is a frame work of a protection system that is based on using artificial neural networks techniques which have the ability of learning by training and generalizing what have been learned. According to these abilities using artificial neural networks in detecting, classifying, and locating of power system different types of faults will obtain a very accurate protection system.

1.2 Project Objectives

The main objectives of this project are:

- To design an artificial neural networks that can efficiently detect, classify, and locate power system faults.

- To implement our networks in a local power system and to achieve satisfying results.

1.3 Importance

The main goal of fault detector is to locate a fault in the power system with the highest achievable accuracy. When the dimensions and the size of the transmission lines are considered, the accuracy with which the designed fault locator locates faults in the power system becomes very important in terms of the amount of money and time that can b saved

.

1.4 Methodology

In this project we designed an intelligent protection system that can detect, locate and classify faults in power transmission lines , using artificial neural networks. We used MATLAB for simulating different types of power system faults , and for building artificial neural networks based on data that have been taken from faults simulation . We used artificial neural networks for fault detection , classification and locating based on using the value of input voltages and input

currents are normalized with respect to the pre-fault values of the voltages and currents respectively.

1.5 Literature Review

The study of this project depended on some previous studies that we are going to mention in this section.

A fault location and realization method for overhead high voltage power transmission, This paper focused on presenting and discussing the main used methods of determining power system fault location, that are used in china and in other parts of the world. The main three methods are: traveling wave location, single terminal location and two terminal locations [1].

Classification of Faults in power system using signal processing approach, this paper presented an efficient method for power system fault classification, based on Voltage and current signals are processed using S-transform technique. The multi-resolution S-transform is based on a variable width window, which changes with frequency. Energy levels on the basis of Parseval's theorem are calculated to distinguish the different types of faults [2].

Wavelet-based neural network for recognition of faults at NHABE power substation of the Vietnam power system. A new study has been presented for power system faults recognition. The study focused on using an artificial neural network , depending on wavelet multi resolution analysis (MRA) These techniques were applied to recognize different faults in the supply voltage of the Southern Vietnam power system at NHABE substation. The research results proved that the techniques can be used to detect and classify different types of power system faults [3].

Efficient processing of alarms avalanche using artificial neural networks and classification techniques , this paper shows an efficient processing of alarms avalanche and classification technique based on artificial neural network based on a multilayer perceptron formed by an input vector consisting of the 58 predefined protection signal [4].

Artificial neural network applications for power system protection, this paper covered the already used artificial neural networks techniques in the protection system for different components of power system including transmission lines , transformers , and generators protection techniques [5].

Fault classification using artificial neural network in combined underground cable and overhead line, this paper focused on the design of an artificial neural network depending on the fundamental components of currents and voltages that been measured from the sending end , zero sequence currents , cable parameters , and sequence components of overhead transmission lines [6].

Artificial neural network technique for transmission line protection on nigerian power system **,** this paper presented an artificial neural network based protection system that have been applied on a part of Nigerian power system , a 132 kV transmission line. The objective of this paper was to evaluate the performance of an artificial neural network relays that are connected on line both sides. PSCAD/EMTP used for simulating power system and its faults , MATLAB also used for applying training and testing data of the artificial neural network that has been designed[7] .

2

Chapter Two Power System Faults

2.1 Introduction

2.2 Power System Faults

2.2.1 Causes of Faults

2.2.2 Effects of Power System Faults

2.2.3 Classification of Faults

2.2.4 Method of Analysis

Chapter two

Power System Faults

2.1 Introduction

This chapter focuses on the theoretical background of power system faults analysis .

2.2 Power System Faults

The steady state operating mode of a power system is balanced three-phase ac .However, due to sudden external or internal changes in the system, this condition is disrupted .When the insulation of the system fails at one or more points, a conducting object comes into contact with a live point, a short circuit, or a fault occurs. A fault is any abnormal condition in a power system [8].

2.2.1 Causes of Faults

- Lightning
- Heavy winds
- Trees falling across lines
- Vehicles colliding with towers or poles
- Birds shorting lines
- Aircraft colliding with lines
- Vandalism
- Small animals entering switchgear

- Line breaks due to excessive loading
- Insulators flash over .

Figure 2.1: lightening strike - Transmission Tower

Figure2.2: A squirrel chewed into a power line in Trumbull, Connecticut, where the Nasdaq's computer center is located, shutting down trading for 34 minutes.

Figure 2.3: Two Snakes That Died In An Electric Box .

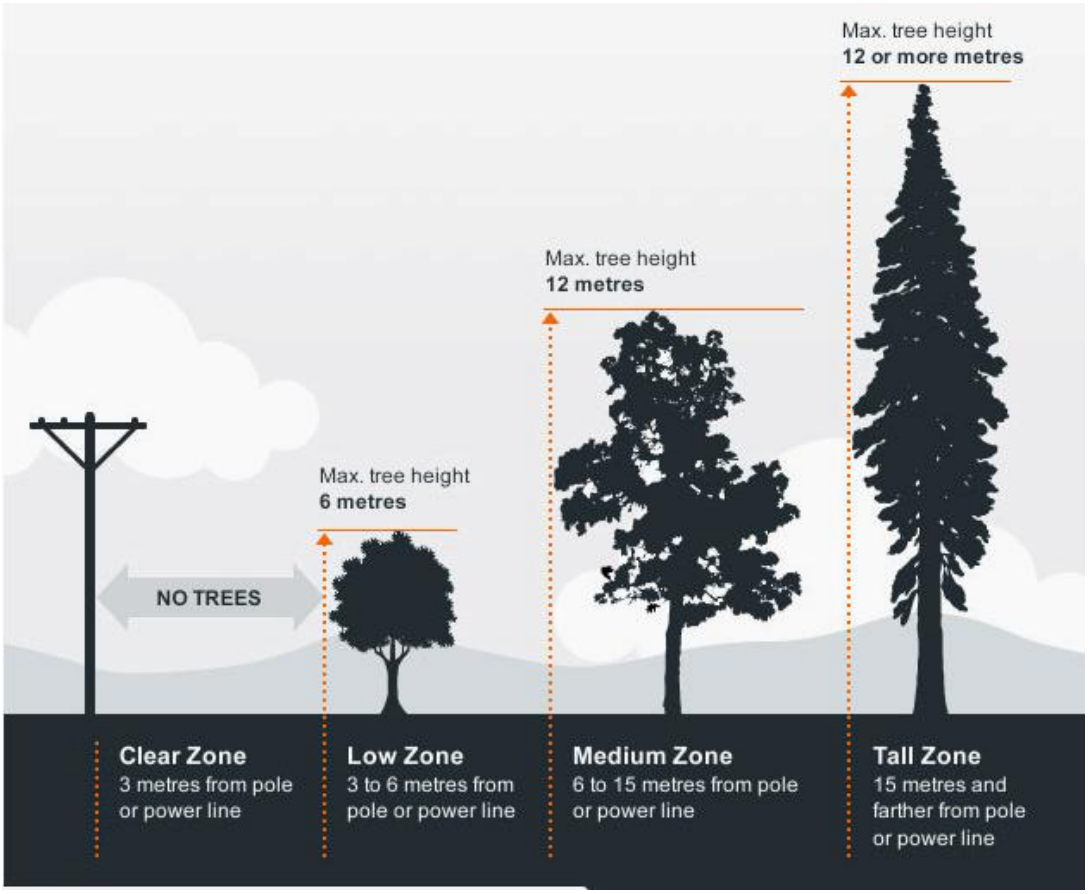

Figure 2.4: Tree Distances From Overhead Transmission Lines

2.2.2 Effects of Power System Faults

Faults may lead to fire breakout that consequently results into loss of property, loss of life and destruction of a power system network. Faults also leads to cut of supply in are as beyond the fault point in a transmission and distribution network leading to power blackouts; this interferes with industrial and commercial activities that support economic growth. Therefore faults should be cleared as quickly as potential.

- Heavy currents due to the short circuit currents results in the excessive heating of the lines, cables and windings resulting in melting down of the above and even can result in fire or explosion.
- Sometimes the short circuit takes the form of the arc that may cause considerable damage to the elements of the power system. For example an arc on an over-head transmission lines if not cleared quickly will burn the conductors causing it to break resulting in long time interruption of the supply.

- Stability of the power system may be adversely affected and can even lead to complete shutdown or cascade tripping of the power system.

- Damage to other apparatus in the power system due to short circuit currents may be caused due to the over-heating and also due to abnormal mechanical stresses or forces set up by the fault.

- A reduction in the voltage in power system due to faults will be sometimes so large that the relays having pressure coils tends to fail.

- There may be an interruption in the power supply to the consumers when power circuits or generating units are switched out with resultant outage of the connected consumer equipment and in number of cases formidable breakdowns.

- Sometimes in an interconnected systems, when a fault develops it is followed by a fall in voltage and frequency. This may result in loads such as motors which normally takes the power from the supply will start to feed or deliver the power to the fault locations. During the faults, induction motors and synchronous motors feed the fault[9].

2.2.3 Classification of Faults

Faults in power system are classified into two main types according to system symmetry.

A. Symmetrical faults

In the balanced system the system impedance in each phase are identical and the three-phase voltages and currents through the system are completely balanced. These are very severe faults and occur infrequently in the power systems. Only 2-5 percent of system faults are symmetrical faults. If these faults occur, system remains balanced but results in severe damage to the electrical power system equipment's.

Faults under symmetrical conditions are caused in the system accidently through:

1. Insulation failure of equipment.
2. Flash over of lines initiated by lighting stroke.
3. Accidental faulty operation.

B. Asymmetrical Faults

Unbalanced system could be a result of asymmetrical faults; then system operation may also become unbalanced when the loads of the three phases are not balanced.

Asymmetrical faults are classified as follow:

I. Single line to ground fault (L-G).

II. Line to line fault (L-L).

III. Double line to ground fault (L-L-G).

These are very common and less severe than symmetrical faults. Line to ground fault (L-G) is most common fault and 65-70 percent of faults are of this type It causes the conductor to make contact with earth or ground. 15 to 20 percent of faults are double line to ground and causes the two conductors to make contact with ground. Line to line faults occur when two conductors make contact with each other mainly while swinging of lines due to winds and 5- 10 percent of the faults are of this type.

2.2.4 Method of Analysis

A three-phase balanced fault can be defined as a short circuit with fault impedance (Z_f) between the ground and each phase. A fault is called solid fault when Z_f equals zero.

In order to analyze any unbalanced power system, Charles Legeyt Fortescue introduced a method called symmetrical components in 1918 to solve such systems using a balanced representation. This method is considered to be the base of all traditional fault analysis approaches of solving unbalanced power systems. The theory suggests that any unbalanced system can be represented by a number of balanced systems equal to the number of its phases.

The balanced systems representations are called symmetrical components. In three-phase system, there are three sets of balanced symmetrical components that can be obtained; positive, negative and zero sequence components [8].

- **Positive Sequence Components**

The positive sequence components are equal in magnitude and displayed from each other by 120^o with the same sequence as the original phases. The positive sequence currents and voltages follow the same cycle order of the original source. In the case of typical counter clockwise rotation electrical system, the positive sequence phasor are shown in Fig 2.5.

The same case applies for the positive current phasors. This sequence is also called the "abc" sequence and usually denoted by the symbol "+" or "1".

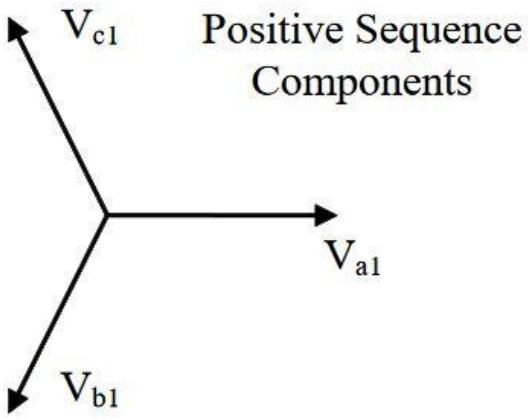

Figure 2.5: Positive sequence components

- **Negative Sequence Components**

This sequence has components that are also equal in magnitude and displayed from each other by 120o similar to the positive sequence components. However, it has an opposite phase sequence from the original system.

The negative sequence is identified as the "acb" sequence and usually denoted by the symbol "-" or "2".The phasors of this sequence are shown in Fig 2.6 where the phasors rotate counter clockwise. This sequence occurs only in case of an unsymmetrical fault in addition to the positive sequence components.

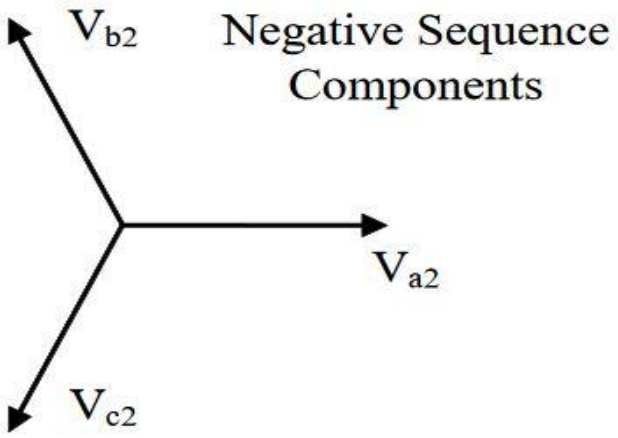

Figure 2.6: Negative sequence components.

- **Zero Sequence Components**

In this sequence, its components consist of three phasors which are equal in magnitude as before but with a zero displacement. The phasor components are in phase with each other. This is illustrated in Fig 2.7. Under an asymmetrical fault condition, this sequence symbolizes the residual electricity in the system in terms of voltages and currents where a ground or a fourth wire exists. It happens when ground currents return to the power system through any grounding point in the electrical system. In this type of faults, the positive and the negative components are also present. This sequence is known by the symbol “0”.

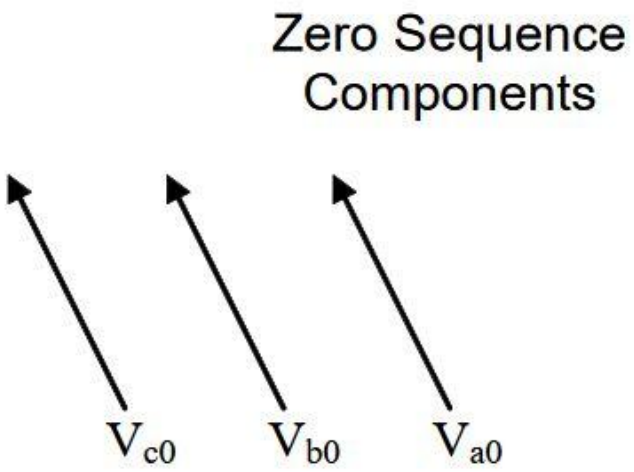

Figure 2.7: Zero sequence components.

The following are three sets of components to represent three-phase system voltages as positive, negative and zero components:

- Positive V_{a1} V_{b1} V_{c1}
- Negative V_{a2} V_{b2} V_{c2}
- Zero V_{a0} V_{b0} V_{c0}

The addition of all symmetrical components will present the original system phase components V_a , V_b and V_c as it seen below:

$$V_a = V_{a0} + V_{a1} + V_{a2} \quad (2.1)$$

$$V_b = V_{b0} + V_{b1} + V_{b2} \quad (2.2)$$

$$V_c = V_{c0} + V_{c1} + V_{c2} \quad (2.3)$$

The “a” operator is defined below:

$$a = 1\angle 120° \quad (2.4)$$

The following relations can be driven from 2.1.4:

$$a^2 = 1\angle -120^o \quad (2.5)$$

$$a^3 = 1 \quad (2.6)$$

From the above definition and using the “a” operator, it can be translated into a set of equations to represents each sequence:

1. Zero sequence components:

$$V_{a0} = V_{b0} = V_{c0} \quad (2.7)$$

2. Positive sequence components:

$$V_{b1} = a^2 V_{a1} \quad (2.8)$$

$$V_{c1} = a\, V_{a1} \quad (2.9)$$

3. Negative sequence components:

$$V_{b2} = aV_{a2} \quad (2.10)$$

$$V_{c2} = a^2 V_{a2} \quad (2.11)$$

The original system phasors V_a, V_b and V_c can be expressed in terms of phase “a” components only. Equation (2.1) can be written as follows:

$$V_a = V_{a0} + V_{a1} + V_{a2} \quad (2.12)$$

$$V_b = V_{a0} + a^2 V_{a1} + aV_{a2} \quad (2.13)$$

$$V_c = V_{a0} + a\, V_{a1} + a^2 V_a \quad (2.14)$$

Writing the above equations can be accomplished in a matrix form:

$$\begin{bmatrix} V_a \\ V_b \\ V_c \end{bmatrix} = \begin{bmatrix} 1 & 1 & 1 \\ 1 & a^2 & a \\ 1 & a & a^2 \end{bmatrix} \begin{bmatrix} V_{a0} \\ V_{a1} \\ V_{a2} \end{bmatrix} \quad (2.15)$$

Defining A as:

$$A = \begin{bmatrix} 1 & 1 & 1 \\ 1 & a^2 & a \\ 1 & a & a^2 \end{bmatrix} \quad (2.16)$$

Equation 2.15 can be written as:

$$\begin{bmatrix} V_a \\ V_b \\ V_c \end{bmatrix} = A \begin{bmatrix} V_{a0} \\ V_{a1} \\ V_{a2} \end{bmatrix} \quad (2.17)$$

This equation can be reversed in order to obtain the positive, negative and zero sequences from the system phasors:

$$\begin{bmatrix} V_{a0} \\ V_{a1} \\ V_{a2} \end{bmatrix} = A^{-1} \begin{bmatrix} V_a \\ V_b \\ V_c \end{bmatrix} \quad (2.18)$$

Where A^{-1} equals the following:

$$A^{-1} = \frac{1}{3} \begin{bmatrix} 1 & 1 & 1 \\ 1 & a^2 & a \\ 1 & a & a^2 \end{bmatrix} \quad (2.19)$$

These equations can be applied for the phase voltages and currents. In addition, it can express the line currents and the line-to-line voltages of any power system under fault conditions.

3

Chapter Three Artificial Neural Network

3.1 Artificial Neural Networks

3.2 History of Artificial Neural Networks

3.3 ANN's Structure

3.4 Components of Neural Networks

3.5 Working algorithm of ANN'

3.6 Number of layers and neurons that should be used in an ANN

3.7 ANN's Advantages

Chapter Three

Artificial Neural Network

3.1 Artificial Neural Network

An Artificial Neural Network is a model that is biologically inspired, which can be computerized to perform a specific certain task ,in order to solve specific problems that cannot be solved using traditional methods .

The importance of the ANN's is mainly recognized in the fact that it can be learned by the observed data . An ANN takes a sample of observed data , and deal with those data as training and testing tools. Based on that ANN's can make interpolations and extrapolations for different data , that wasn't on the training process , which means that it can expect and detect problems that may be happen for the first time[14].

3.2 History of Artificial Neural Networks

The neural networks field has a long history of developments with many ups and downs .The history of the neural networks started in the early 1940's , and nearly at the same time that the programmable computer history started in .

The beginning :

- As soon as 1943 Warren McCulloch and Walter Pitts introduced models of

neurological networks, recreated threshold switches based on neurons and showed

that even simple networks of this kind are able to calculate nearly any logic or arithmetic function [17].

- 1947: Walter Pitts and Warren McCulloch indicated a practical field of application (which was not mentioned in their work from 1943), namely the recognition of special patterns by neural networks[18].

-1949: Donald O. Hebb formulated the classical Hebbian rule ,which represents in its more generalized form the basis of nearly all neural learning procedures. The rule implies that the connection between two neurons is strengthened when both neurons are active at the same time. This change in strength is proportional to the product of the two activities. Hebb could postulate this rule ,but due to the absence of neurological research he was not able to verify it[19].

-1950: The neuropsychologist Karl Lashley defended the thesis that brain information storage is realized as a distributed system. His thesis was based on experiments on rats, where only the extent but not the location of the destroyed nerve tissue influences the rats' performance to find their way out of a labyrinth.

Golden Age :

-1951: For his dissertation Marvin Minsky developed the neurocomputer Snark, which has already been capable to adjust its weights automatically. But it has never been practically implemented, since it is capable to busily calculate, but nobody really knows what it calculates.

-1956: Well-known scientists and ambitious students met at the Dartmouth Summer Research Project and discussed, to put it crudely, how to simulate a brain. Differences between top-down and bottom-up research developed. While the early supporters of artificial intelligence wanted to

simulate capabilities by means of software, supporters of neural networks wanted to achieve system behavior by imitating the smallest parts of the system – the neurons.

-1957-1958: At the MIT, Frank Rosenblatt, Charles Wightman and their coworkers developed the first successful neurocomputer, the Mark I perceptron , which was capable to recognize simple numerics by means of a 20 × 20 pixel image sensor and electromechanically worked with 512 motor driven potentiometers - each potentiometer representing one variable weight.

-1959: Frank Rosenblatt described different versions of the perceptron, formulated and verified his perceptron convergence theorem. He described neuron layers mimicking the retina, threshold switches, and a learning rule adjusting the connecting weight.

-1960: Bernard Widrow and Marcian E. Hoff introduced the ADALINE(Adaptive Linear Neuron) ,a fast and precise adaptive learning system being the first widely commercially used neural network: It could be found in nearly every analog telephone for real-time adaptive echo filtering and was trained by menas of the Widrow-Hoff rule or delta rule. At that time Hoff, later co-founder of Intel Corporation, was a PhD student of Widrow, who himself is known as the inventor of modern microprocessors. One advantage the delta rule had over the original perceptron learning algorithm was its adaptivity : If the difference between the actual output and the correct solution was large, the connecting weights also changed in larger steps – the smaller the steps, the closer the target was. Disadvantage: miss application led to infinitesimal small steps close to the target. In the following stagnation and out of fear of scientific unpopularity of the neural networks ADALINE was renamed in adaptive linear element – which was undone again later on[20].

-1961: Karl Steinbuch introduced technical realizations of associative memory, which can be seen as predecessors of today’s neural associative memories. Additionally, he described concepts for neural techniques and analyzed their possibilities and limits[21].

-1965: In his book Learning Machines, Nils Nilsson gave an overview of the progress and works of this period of neural network research. It was assumed that the basic principles of self-learning and therefore, generally speaking, "intelligent" systems had already been discovered. Today this assumption seems to be an exorbitant overestimation, but at that time it provided for high popularity and sufficient research funds.

-1969: Marvin Minsky and Seymour Papert published a precise mathematical analysis of the perceptron to show that the perceptron model was not capable of representing many important problems and so put an end to overestimation, popularity and research funds. The implication that more powerful models would show exactly the same problems and the forecast that the entire field would be a research dead end resulted in a nearly complete decline in research funds for the next 15 years– no matter how incorrect these forecasts were from today's point of view[22].

Long silence and slow reconstruction :

The research funds were, as previously-mentioned, extremely short. Everywhere research went on, but there were neither conferences nor other events and therefore only few publications. This isolation of individual researchers provided for many independently developed neural network paradigms: They researched, but there was no discourse among them.

In spite of the poor appreciation the field received, the basic theories for the still continuing renaissance were laid at that time:

-1972: Teuvo Kohonen introduced a model of the linear associator, a model of an associative memory [23]. In the same year, such a model was presented independently and from a neurophysiologist's point of view by James A. Anderson [24].

-1973: Christoph von der Malsburg used a neuron model that was non-linear and biologically more motivated [25].

-1974: For his dissertation in Harvard Paul Werbos developed a learning procedure called back propagation of error, but it was not until one decade later that this procedure reached today's importance[26].

- 1976-1980 and thereafter: Stephen Grossberg presented many papers in which numerous neural models are analyzed mathematically .Furthermore, he dedicated himself to the problem of keeping a neural network capable of learning without destroying already learned associations. Under cooperation of Gail Carpenter this led to models of adaptive resonance theory (ART)[27].

-1982: Teuvo Kohonen described the self-organizing feature maps (SOM) – also known as Kohonen maps. He was looking for the mechanisms involving self-organization in the brain (He knew that the information about the creation of a being is stored in the genome, which has, however, not enough memory for a structure like the brain. As a consequence, the brain has to organize and create itself for the most part)[28][29].

John Hopfield also invented the so-called Hopfield networks which are inspired by the laws of magnetism in physics. They were not widely used in technical applications, but the field of neural networks slowly regained importance[30].

-1983: Fukushima, Miyake and Ito introduced the neural model of the Neocognitron which could recognize handwritten characters and was an extension of the Cognitron network already developed in 1975 [31].

Renaissance:

Through the influence of John Hopfield, who had personally convinced many researchers of the importance of the field, and the wide publication of back propagation by Rumelhart, Hinton and Williams, the field of neural networks slowly showed signs of upswing.

-1985: John Hopfield published an article describing a way of finding acceptable solutions for the Travelling Salesman problem by using Hopfield nets.

-1986: The back propagation of error learning procedure as a generalization of the delta rule was separately developed and widely published by the Parallel Distributed Processing Group: Non-linearly-separable problems could be solved by multilayer perceptrons, and Marvin Minsky's negative evaluations were disproven at a single blow. At the same time a certain kind of fatigue spread in the field of artificial intelligence, caused by a series of failures and unfulfilled hope [32].

From this time on, the development of the field of research has almost been explosive.

3.3 Structure Neural Networks

Neural Networks are basically consist of a group of simple units and set of elementary neurons that are usually connected in biologically inspired architectures and organized in several layers. The neurons and the connections that connect those neurons with specific weight of each connection. The structure of a feed-forward ANN, also called as the perceptron is shown in Fig 3.1 There are Ni numbers of neurons in each i^{th} layer and the inputs to these neurons are connected to the previous layer neurons. The input layer is fed with the excitation signals.

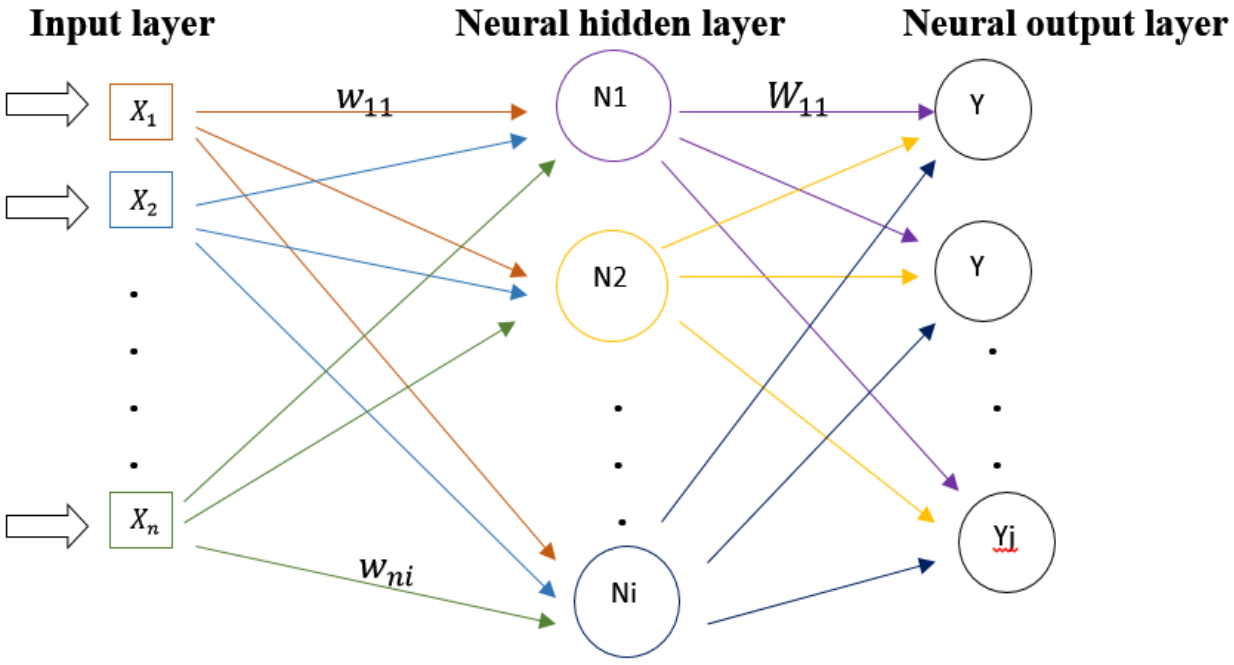

Figure 3.1: basic two-layer architecture of a feedforward ANN

In Fig 3.1, X_1, X_2… X_n is the set of inputs to the ANN. Due to their outstanding pattern recognition abilities ANNs are used for several purposes in a wide variety of fields including signal processing, computers and decision making.

One of the biggest drawbacks of applications that make use of artificial neural networks is that no well-defined guide exists to help us choose the ideal number of hidden layers to be used and the number of neurons per each hidden layer. From a different perspective, it is advantageous considering the ability to generalize.

A vital feature of ANN is its dedication to parallel computing. Hence it can produce a correct output corresponding to any input even if the concerned input was not fed into the ANN during the training process [15][16].

3.4 Components of Neural Networks

- **Connections :**

Connections carry information that is processed by neurons , and transfer data between neurons with the connecting weight.

- **Propagation Function :**

It converts vector inputs to a scalar network inputs . Any neuron in the network is connected to many other neurons that transfers its outputs to this neuron .The propagation function receives the outputs of those neurons and transform them in consideration of the connecting weights into the network input net . The weighted sum is the most common and popular propagation function .

- **Activation function :**

The activation function transforms the network input net into a new activation state . The activation is the switching status of a neuron , which indicates the extent of the neuron's activity and results from the activation function .Neurons get activated if the input exceeds their threshold value, and the activation function reacts particularly sensitive near this value .

The simplest activation function is **the binary threshold function (Step function)** , which can only take on two values .If the input is above a certain threshold, the function changes from one value to another, but otherwise remains constant which means that the function is not differentiable .

A very popular activation function are the **Piece wise linear activation function** and the **Sigmoid unipolar function.** Both functions are differentiable.

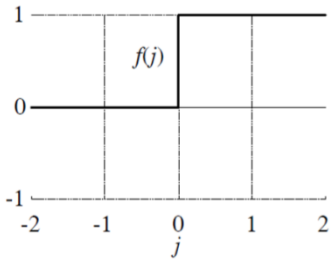

Figure 3.2: Step activation function

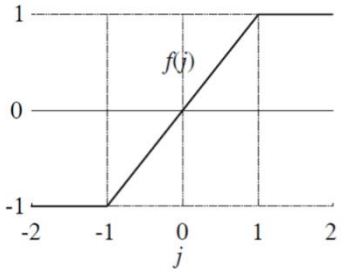

Figure 3.3: Piece wise linear activation function.

$$f(\emptyset) = \begin{cases} 1 & if\varphi \geq 0 \\ 0 & if\varphi < 0 \end{cases}$$

$$f(\emptyset) = \begin{cases} 1 & if\varphi \geq 1 \\ -1 & if\varphi < -1 \\ \varphi & if|\varphi| < 1 \end{cases}$$

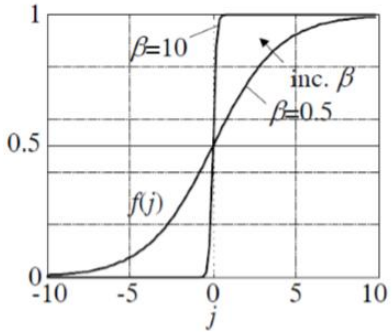

Figure 3.4: Sigmoid unipolar activation function

$$f(\emptyset) = \frac{1}{1+e^{-\beta\varphi}}$$

- **Output function :**

The output function calculates the values which are transferred from the neuron to other neurons , which means that it calculates the output values of a neuron from its activation state . Also the output function may be used to process the activation once again .

Any basic neuron model as shown in Fig 3.5 can be described by a function that Calculates the output as a function of X_m inputs to it.

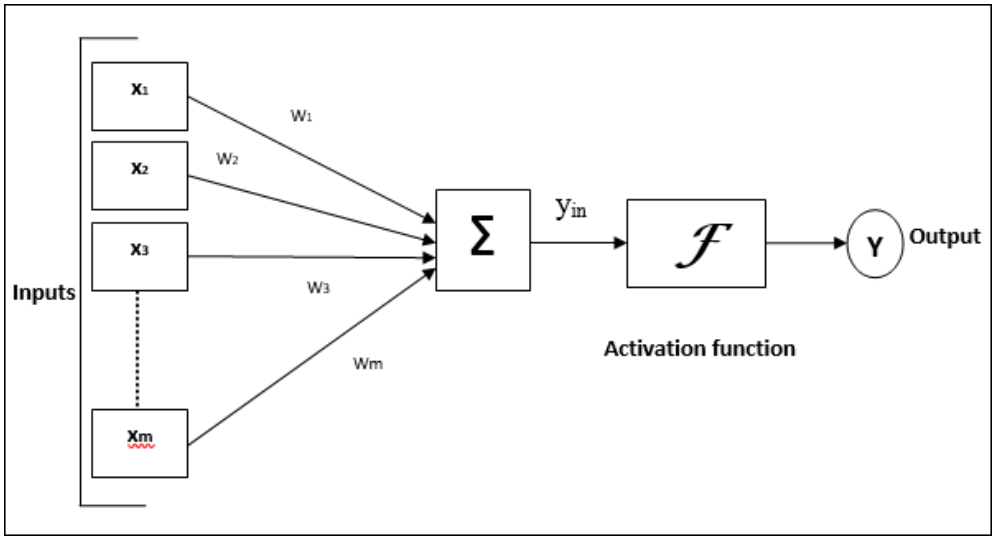

Figure 3.5: Typical model of a neuron.

The output of the neuron is given by Y = F (Yɕ) = $\left(\sum_{i=1}^{X_m} W_i X_i\right)$ (3.1)

where: W_i X_i is the input value multiplied by its weight , F (Yɕ) is the neuron activation function of Yɕ , Yɕ is the summation output signal (Propagation function) and Y is the neuron output.

$Yɕ=X^TW$ (3.2)

$W = [W_1 W_2 W_3 \dots W_m]$ (3.3)

$X = [X_1 X_2 X_3 \dots X_m]^T$ (3.4)

3.5 Working algorithm of ANN'

The neural network receives the inputs from the outside world . After that each input is multiplied by its connection weight .Where the weight of each connection gives an indication of the strength of interconnection between neurons .Then The weighted inputs are all summed up inside computing unit, and a bias is added to make the output not- zero, in case the input was zero or to scale up the system response. The activation function is set of the transfer function used to get desired output.

$$Y=F\left[\sum_{i=1}^{n}(X_i\, w_{im})-\theta\right] \quad (3.5)$$

Where;

Y= output

X= input

w= The weight of connection between the input and the next layer .

θ= Threshold value (activation value that the input must be more than).

F= The activation function.

Using sigmoid activation function as an example :

$$Y=sig\left[\sum_{i=1}^{n}(X_i\, w_{im})-\theta\right] \quad (3.6)$$

3.5.1 Learning in Artificial Neural Networks

There are several used learning methods for the ANN's . One of the most used methods is Back Propagation.

Based on delta learning rule. After determining an error (the difference between desired and target), the error is propagated backward from output layer to the input layer via hidden layer. At least for back propagation of error we need, a differentiable or even a semi-linear activation function. Back propagation procedures are shown below .

$$Y=sig\ [\sum_{i=1}^{n}(X_i\, w_{im}) - \theta] \quad (3.7)$$

$$e_j = y_d - y_a \quad (3.8)$$

$$\delta_j = dy\,[sig(y_j)] - e_j \quad (3.9)$$

$$\delta_i = dy\,[sig(y_i)].(\delta_j - W_{ij}) \quad (3.10)$$

$$\Delta W_{ij} = \propto y_i \delta_j \quad (3.11)$$

$$\Delta\theta_j = \alpha(\theta)\delta_j \quad (3.12)$$

$$W_{newij} = \Delta W_{ij} + W_{oldij} \quad (3.13)$$

$$\theta_{newij} = \Delta\theta_{ij} + \theta_{oldij} \quad (3.14)$$

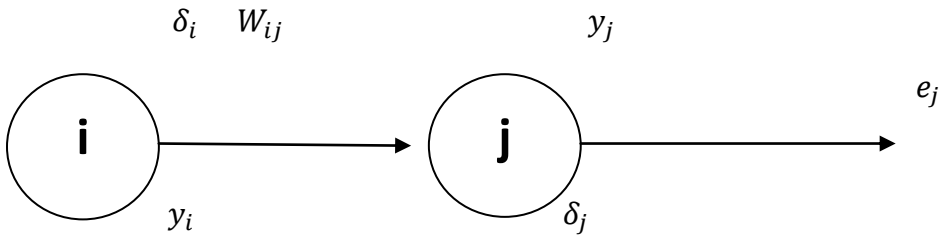

Figure 3.6: Single neuron.

where:

Sig is the sigmoid function, which is the activation function.

e_j is the error of neuron j, (the difference between the actual output data and the desired data).

δ is the error gradient .

α is the learning rate .

Y= output

X= input

w= The weight of connection between the input and the next layer .

θ= Threshold value (activation value that the input must be more than).

3.6 Number of layers and neurons that should be used in an Artificial Neural Network

First of all, a net work must have an input layer for input neurons, and an output layer for the output neurons, which make them two layers as a beginning. For the hidden layers, many sources mentioned that two or three layers may be enough, or even one layer could be enough.

Many problems can be represented by only one hidden layer but it could be very difficult to learn .Also any additional layer will generate an additional error function in which we can stuck. So the way that used in choosing the number of hidden layers is to try only one layer at first, and then if its fail a second layer should be added, and if it also fail more layers should be used.

For choosing the **number of neurons**, most sources mentioned that at first a few neurons should be used, and the number of them should be change until the desired output values appear with the best accuracy [14].

3.7 ANN's Advantages

ANNs have some key advantages that make them most suitable for certain problems and situations:

- ANNs have the ability to learn and model non-linear and complex relationships, which is really important because in real-life, many of the relationships between inputs and outputs are non-linear as well as complex.

- ANNs can generalize—after learning from the initial inputs and their relationships, it can infer unseen relationships on unseen data as well, thus making the model generalizes and predict on unseen data.

- Unlike many other prediction techniques, ANN does not impose any restrictions on the input variables (like how they should be distributed). Additionally, many studies have shown that ANNs can better model data with high volatility and non-constant variance, given its ability to learn hidden relationships in the data without imposing any fixed relationships in the data. This is something very useful in financial time series forecasting where data volatility is very high [14].

4

Chapter Four Project Design

4.1 Introduction

4.2 Ideal Data- Based Design

4.3 14 Bus System Based Design

4.4 30 Bus System Based Design

Chapter Four
Project Design

4.1 Introduction

This chapter contains a framework of three protection systems for three different electrical systems (Ideal , 14-bus system and 30-bus system) , each one consists of 6 different artificial neural networks .Tow ANN's are for faults detecting and classification , and the other four are for faults locating .

4.2 Ideal Design

This design is based on an ideal fault data , that have been generated using Hadi Saadat's power library in MATLAB .The code that has been used for data generating is presented in A1.

4.2.1 Fault Detection Neural Network

This network has been designed to detect different types of faults , based on eight different values of fault impedance (0, 0.1, 0.5, 1, 5, 10, 25, 50) Ω . It consists of an input layer of 6 neurons , a hidden layer of 10 neurons , and an output layer of a single neuron .Fig 4.1 shows the design of this network .

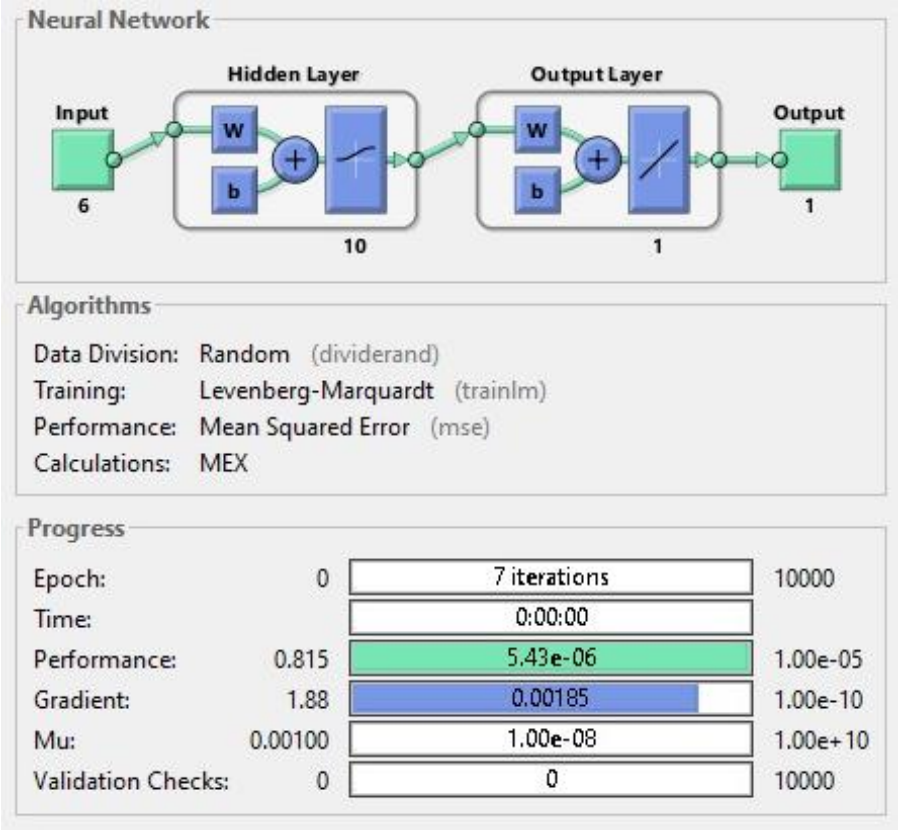

Figure 4.1: Detection Network Design

Table 4.1 shows a random sample of the data that have been generated and used as a training data for the fault detecting neural network .

Table 4.1: Detection Data Sample

Z_f	V_{af}/V_{apf}	V_{bf}/V_{bpf}	V_{cf}/V_{cpf}	I_{af}/I_{apf}	I_{bf}/I_{bpf}	I_{cf}/I_{cpf}	Output
j0	83.33333	83.33333	83.33333	0.038462	0.038462	0.038462	1
j0.1	36.11111	36.11111	36.11111	0.813258	0.813258	0.813258	1
j0.5	0.972934	0.966213	0.995758	1.01944	0.959742	0.978279	0
j1	0.72572	0.72572	2.78E-15	0.901313	0.901313	1	1
j5	1.012325	0.99643	0.973863	1.029864	1.024992	1.009799	0
j10	0.632419	0.632419	0.632419	1.403687	1.403687	1.403687	1
j25	1.002896	0.993088	1.003184	0.990894	1.034586	1.001411	0
j50	0.002588	0.002588	0.012228	1.001213	1.001213	0.996036	1

Where:

$\boldsymbol{Z_f}$ is the fault impedance that has been used while generating data .

$\boldsymbol{V_{af}}$,$\boldsymbol{V_{bf}}$,$\boldsymbol{V_{cf}}$ are the three phases voltage values after fault event .

$\boldsymbol{I_{af}}$,$\boldsymbol{I_{bf}}$,$\boldsymbol{I_{cf}}$ are the three phases current values after fault event .

$\boldsymbol{V_{apf}}$, $\boldsymbol{V_{bpf}}$, $\boldsymbol{V_{cpf}}$ are the three phases pre-fault voltage values .

$\boldsymbol{I_{apf}}$, $\boldsymbol{I_{bpf}}$, $\boldsymbol{I_{cpf}}$ are the three phases pre-fault current values.

Phase voltages and currents ratios have been used as an input for the detecting network. The output of this network has a binary value (0 or 1). Zero output indicates that there is no fault has been detected , while a one output indicates that there is a fault that has been detected .

Fig 4.2 shows the performance of the designed neural network , after 15 epochs and with an error of nearly $9.08e^{-6}$

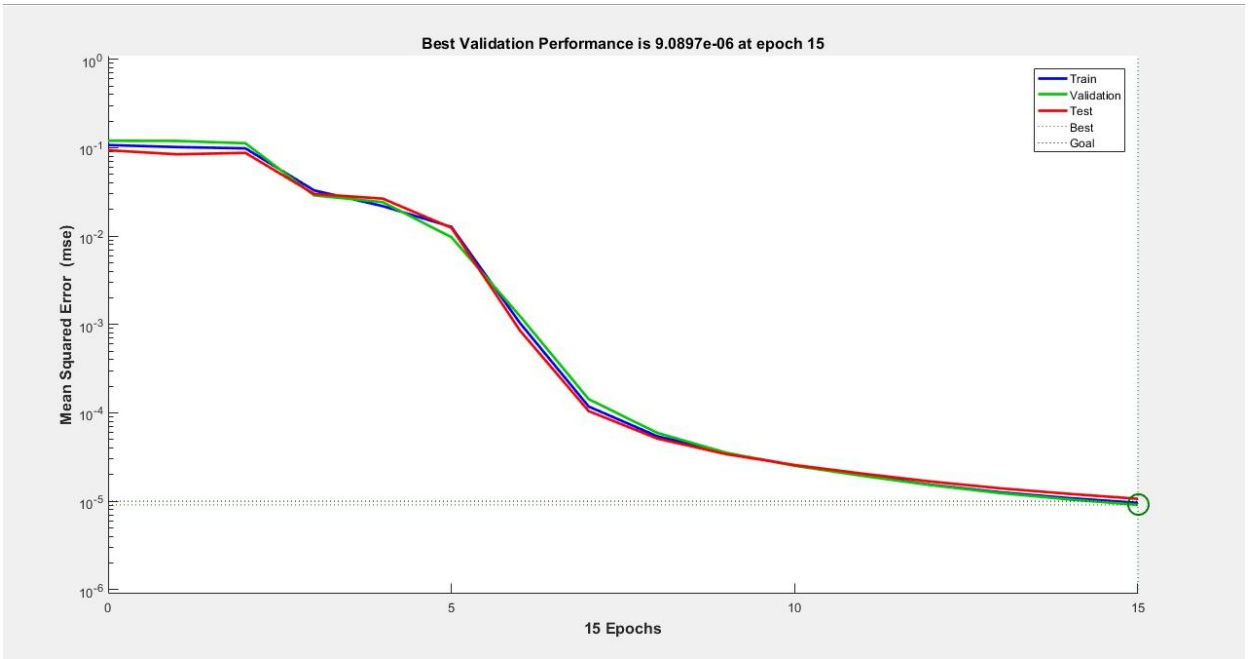

Figure 4.2: Detecting Network performance .

4.2.2 Fault Classification Neural Network

This network has been designed to classify different types of faults , based on fault impedance of (j0). It consists of an input layer of 6 neurons , a hidden layer of 35 neurons , and an output layer of 4 neurons .

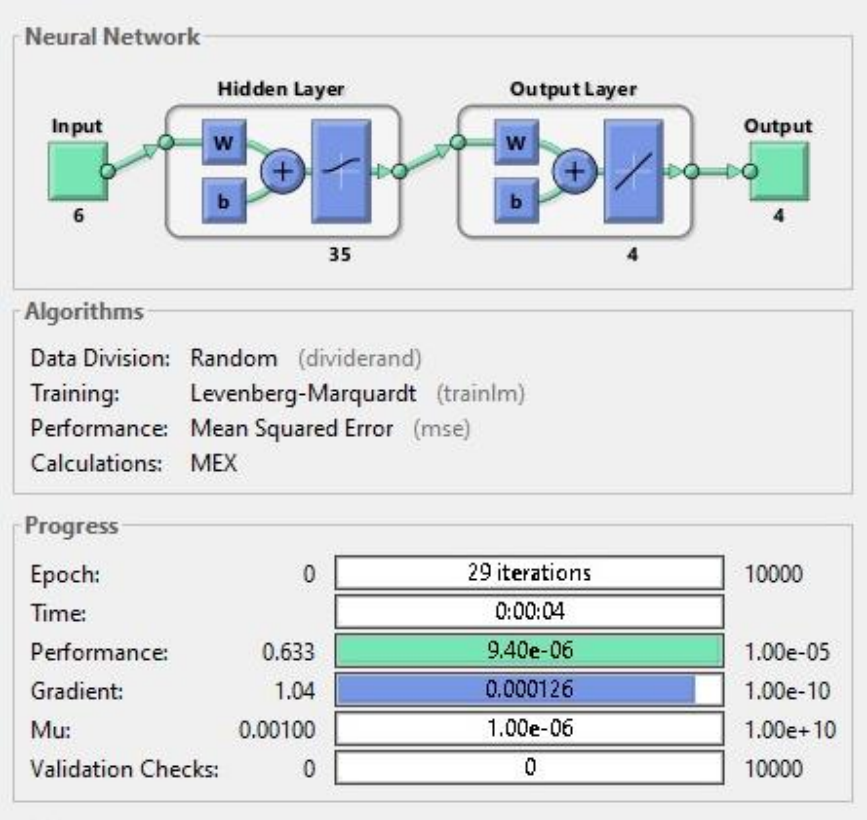

Figure 4.3: Classification Network Design

Table 4.2 shows a random sample of the data that have been generated and used as a training data for this network .

Table 4.2: Classification Data Sample

V_{af}/V_{apf}	V_{bf}/V_{bpf}	V_{cf}/V_{cpf}	I_{af}/I_{apf}	I_{bf}/I_{bpf}	I_{cf}/I_{cpf}	A	B	C	G
3.521127	3.521127	3.521127	0.652778	0.652778	0.652778	1	1	1	1
0	5.647992	5.647992	1	0.5	0.5	0	1	1	0
5.647992	0	5.647992	0.5	1	0.5	1	0	1	0
5.769134	5.769134	0.398431	1.14E-16	2.24E-16	1.380765	1	1	0	1
1.037286	0.967722	0.978338	1.016259	0.980691	1.038828	0	0	0	0
5.21971	5.21971	0.41483	1.67E-16	1.67E-16	1.377153	1	1	0	1
0.41483	5.21971	5.21971	1.377153	1.67E-16	1.67E-16	0	1	1	1
2.986433	0.666022	0.666022	5.55E-17	1.404349	1.404349	1	0	0	1

Where :

V_{af},V_{bf} ,V_{cf} are the three phases voltage values after fault event .

I_{af},I_{bf} ,I_{cf} are the three phases current values after fault event .

V_{apf}, V_{bpf}, V_{cpf} are the three phases pre-fault voltage values .

I_{apf}, I_{bpf}, I_{cpf} are the three phases pre-fault current values

A , B ,C are the three phases.

G is the ground , its value indicates if it is a ground fault .

Phase voltages and currents ratios have been used as inputs for the classification network. The outputs of this network have binary values. Zeros and ones gives an indication of having fault or not for each phase individually , also with or without ground .

As it previously mentioned zero output indicates that there is no fault has been detected , while a one output indicates that there is a fault that has been detected on a specific phase .

Fig 4.4 shows the performance of the designed neural network after 16 epochs, and with an error of nearly $7.79e^{-5}$

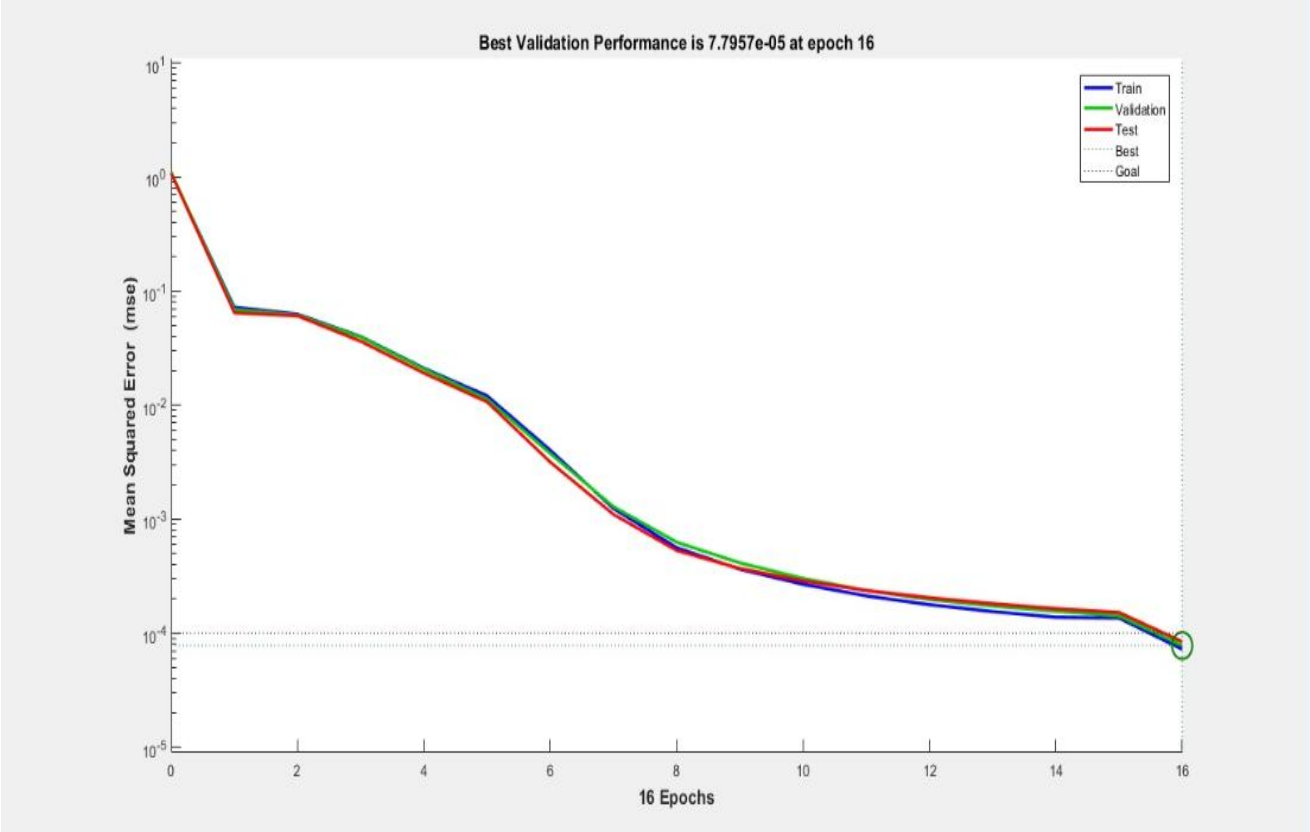

Figure 4.4: Classification Network Performance.

4.2.3 L-G Locating Neural Network

This network has been designed to locate line to ground faults , based on fault impedance of (j0). It consists of an input layer of 6 neurons , a hidden layer of 21 neurons , and an output layer of a single neuron .Fig 4.5 shows the design of this network .

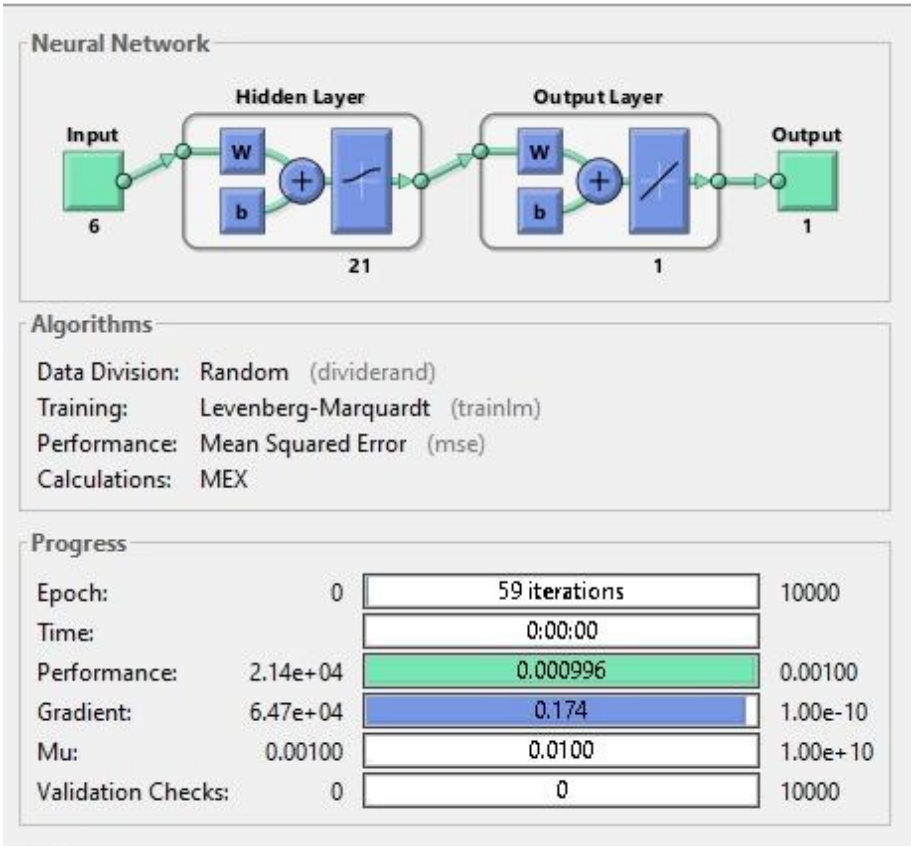

Figure 4.5: L-G Locating Network Design

Table 4.3 shows a random sample of the data that have been generated and used for the training of the L-G locating neural network . Faults data of 150 different locations have been used for training .

Table 4.3: L-G Data Sample

V_{af}/V_{apf}	V_{bf}/V_{bpf}	V_{cf}/V_{cpf}	I_{af}/I_{apf}	I_{bf}/I_{bpf}	I_{cf}/I_{cpf}	Distance
3.084859	0.653044	0.653044	1.67E-16	1.41E+00	1.408588	6000
0.684301	2.838118	0.684301	1.398393	1.67E-16	1.40E+00	22000
0.725252	2.423979	0.725252	1.385106	5.55E-17	1.39E+00	58000
2.368524	0.729356	0.729356	5.55E-17	1.38E+00	1.38378	64000
0.73916	0.73916	2.20393	1.38E+00	1.380613	5.55E-17	84000
2.104157	0.743166	0.743166	8.33E-17	1.38E+00	1.37932	98000
0.745566	1.860623	0.745566	1.378546	8.33E-17	1.38E+00	140000
0.744096	0.744096	1.793676	1.38E+00	1.37902	8.33E-17	154000

Where:

V_{af},V_{bf} ,V_{cf} are the three phases voltage values after fault event .

I_{af},I_{bf} ,I_{cf} are the three phases current values after fault event .

V_{apf}, V_{bpf}, V_{cpf} are the three phases pre-fault voltage values .

I_{apf}, I_{bpf}, I_{cpf} are the three phases pre-fault current values

Phase voltages and currents ratios have been used as inputs for the locating network. The output of this network is a distance per meter , which is the distance between the measurement location and the fault location .

Fig 4.6 shows the performance of the designed neural network after 31 epochs , and with an error of nearly 0.00053.

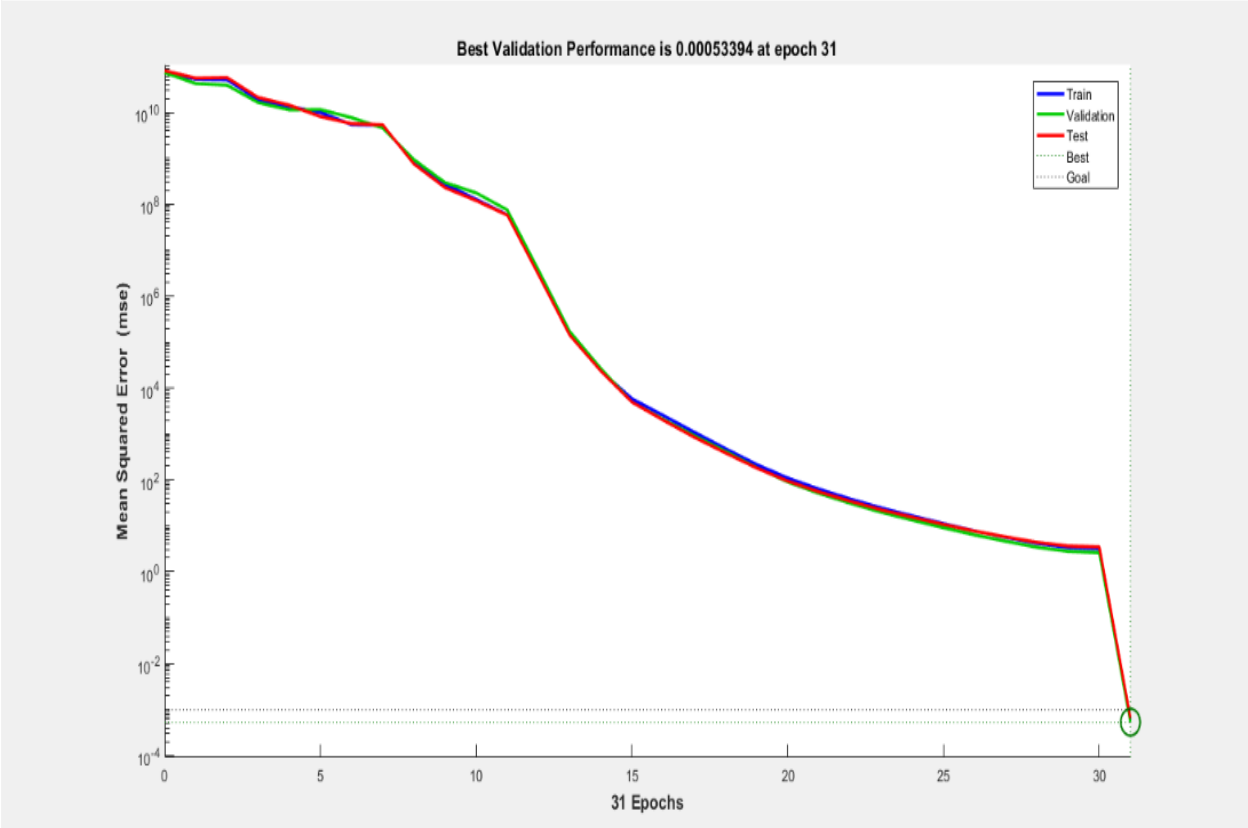

Figure 4.6: L-G Fault Locating Network Performance

4.2.4 Line To Line Fault Locating Neural Network

This network has been designed to locate line to line faults , based on fault impedance of (j0). It consists of an input layer of 6 neurons ,a hidden layer of 23 neurons, and an output layer of a single neuron .Fig 4.7 shows the design of this network .

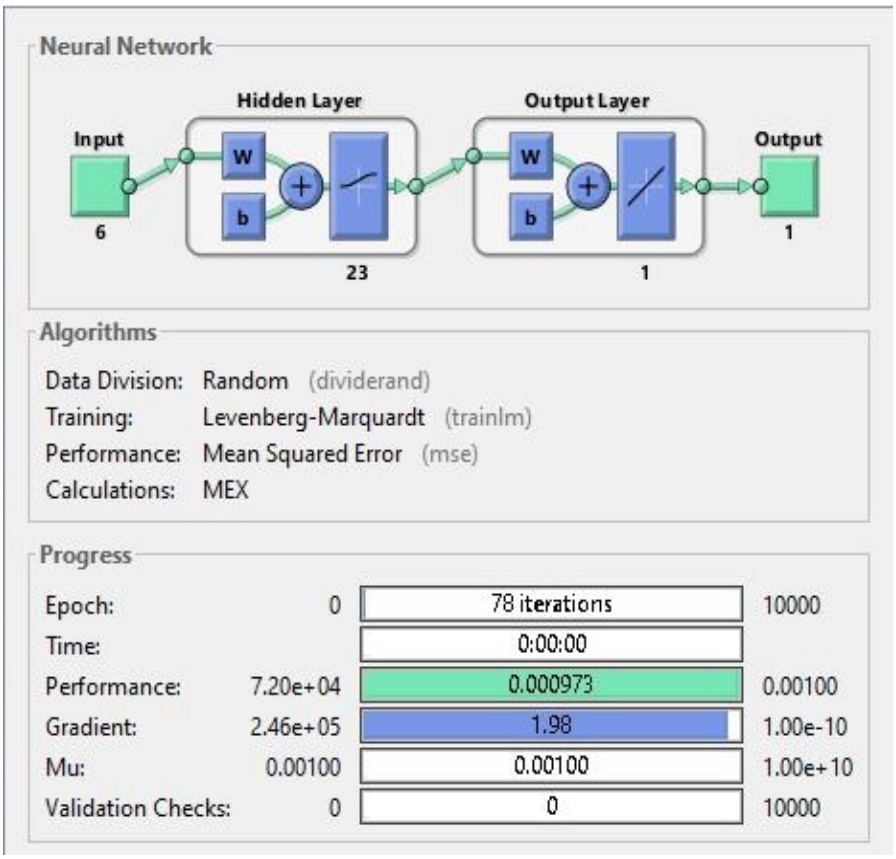

Figure 4.7: L-L Locating Network Design

Table 4.4 shows a random sample of the data that have been generated and used as a training data for L-L locating neural network . Faults data of 150 different locations have been used for training .

Table 4.4:L-L Fault Locating Data Sample

V_{af}/V_{apf}	V_{bf}/V_{bpf}	V_{cf}/V_{cpf}	I_{af}/I_{apf}	I_{bf}/I_{bpf}	I_{cf}/I_{cpf}	Distance
5.302196	5.302196	4.00E-15	0.5	0.5	1	8000
5.196152	3.11E-15	5.196152	0.5	1	0.5	10000
3.8207	0	3.8207	0.5	1	0.5	46000
3.659262	8.88E-16	3.659262	0.5	1	0.5	52000
3.608439	3.608439	4.44E-16	0.5	0.5	1	54000
3.374125	4.44E-16	3.374125	0.5	1	0.5	64000
2.763911	0	2.763911	0.5	1	0.5	98000
2.49815	2.49815	2.22E-16	0.5	0.5	1	118000

Where:

V_{af},V_{bf} ,V_{cf} are the three phases voltage values after fault event .

I_{af},I_{bf} ,I_{cf} are the three phases current values after fault event .

V_{apf}, V_{bpf}, V_{cpf} are the three phases pre-fault voltage values .

I_{apf}, I_{bpf}, I_{cpf} are the three phases pre-fault current values.

Fig 4.8 shows the performance of the designed neural network after 3584 epochs , and with an error of nearly 0.014201.

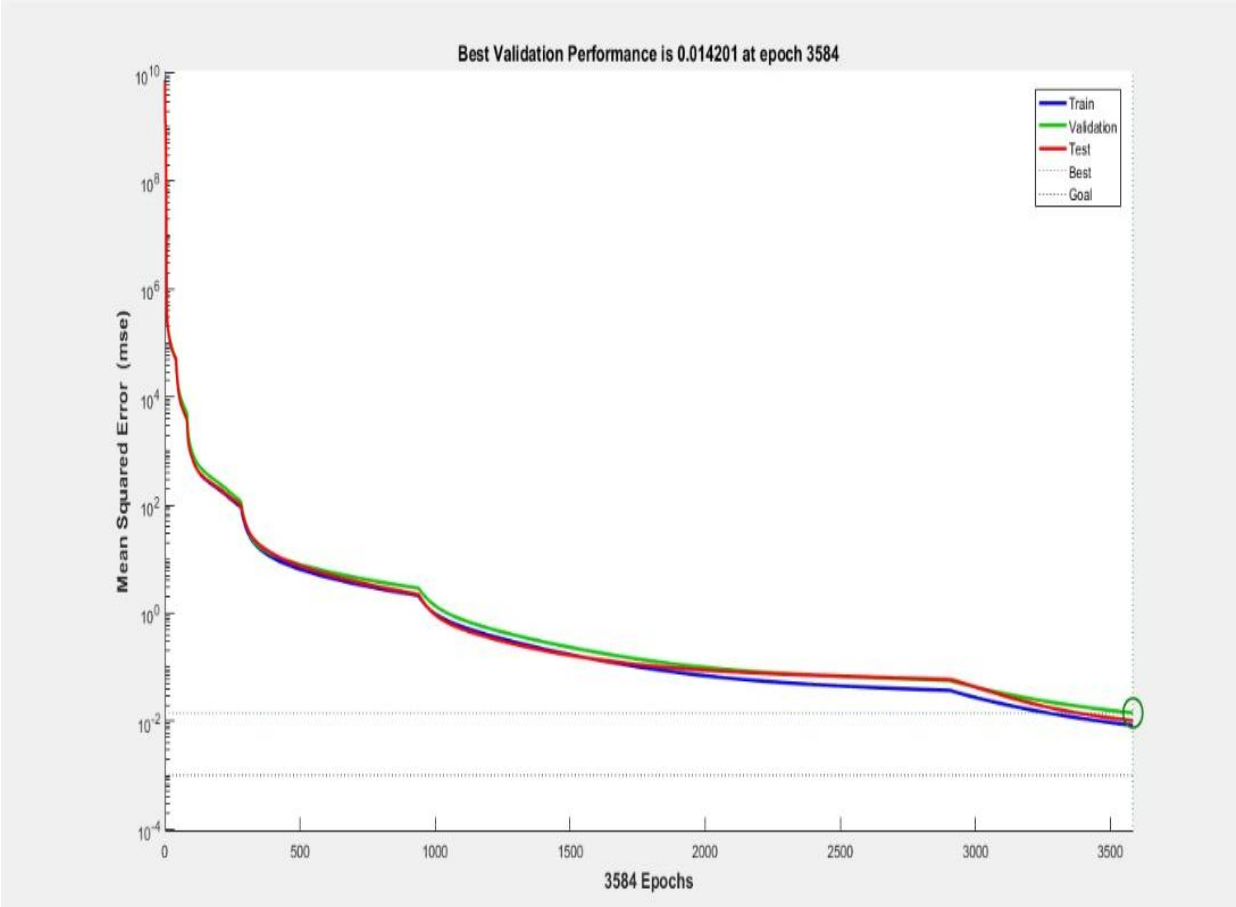

Figure 4.8: L-L Fault Locating Network Performance

4.2.5 LL-G Fault Locating Neural Network

This network has been designed to locate double line to ground faults , based on fault impedance of (j0). It consists of an input layer of 6 neurons , a hidden layer of 29 neurons , and an output layer of a single neuron .Fig 4.9 shows the design of this network .

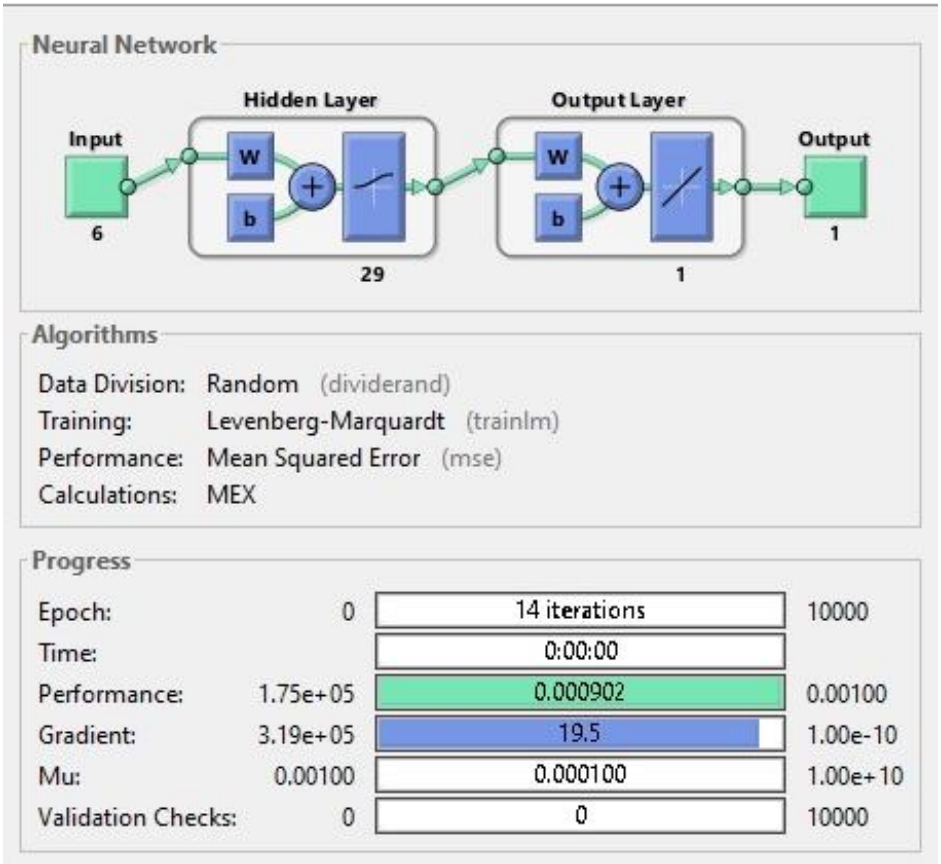

Figure 4.9: LL-G Locating Network Design

Table 4.5 shows a random sample of the data that have been generated and used as a training data for LL-G locating neural network . Faults data of 150 different locations have been used for training .

Table 4.5:LL-G Fault Locating Data Sample

V_{af}/V_{apf}	V_{bf}/V_{bpf}	V_{cf}/V_{cpf}	I_{af}/I_{apf}	I_{bf}/I_{bpf}	I_{cf}/I_{cpf}	Distance
5.769134	0.398431	5.769134	2.24E-16	1.380765	1.14E-16	2000
5.649879	5.649879	0.401979	1.14E-16	2.24E-16	1.379984	4000
2.668258	0.474202	2.668258	1.11E-16	1.364074	2.22E-16	116000
2.487425	2.487425	0.474424	1.39E-16	1.39E-16	1.364026	132000
2.161905	0.471265	2.161905	1.69E-16	1.364721	1.69E-16	168000
2.146436	2.146436	0.470975	2.22E-16	1.11E-16	1.364785	170000
1.990575	1.990575	0.467198	1.14E-16	1.14E-16	1.365617	192000
1.476941	1.476941	0.439863	1.14E-16	1.14E-16	1.371639	300000

Where:

V_{af},V_{bf} ,V_{cf} are the three phases voltage values after fault event .

I_{af},I_{bf} ,I_{cf} are the three phases current values after fault event .

V_{apf}, V_{bpf}, V_{cpf} are the three phases pre-fault voltage values .

I_{apf}, I_{bpf}, I_{cpf} are the three phases pre-fault current values.

Fig 4.10 shows the performance of the designed neural network after 265 epochs , and with an error of nearly 0.0048535.

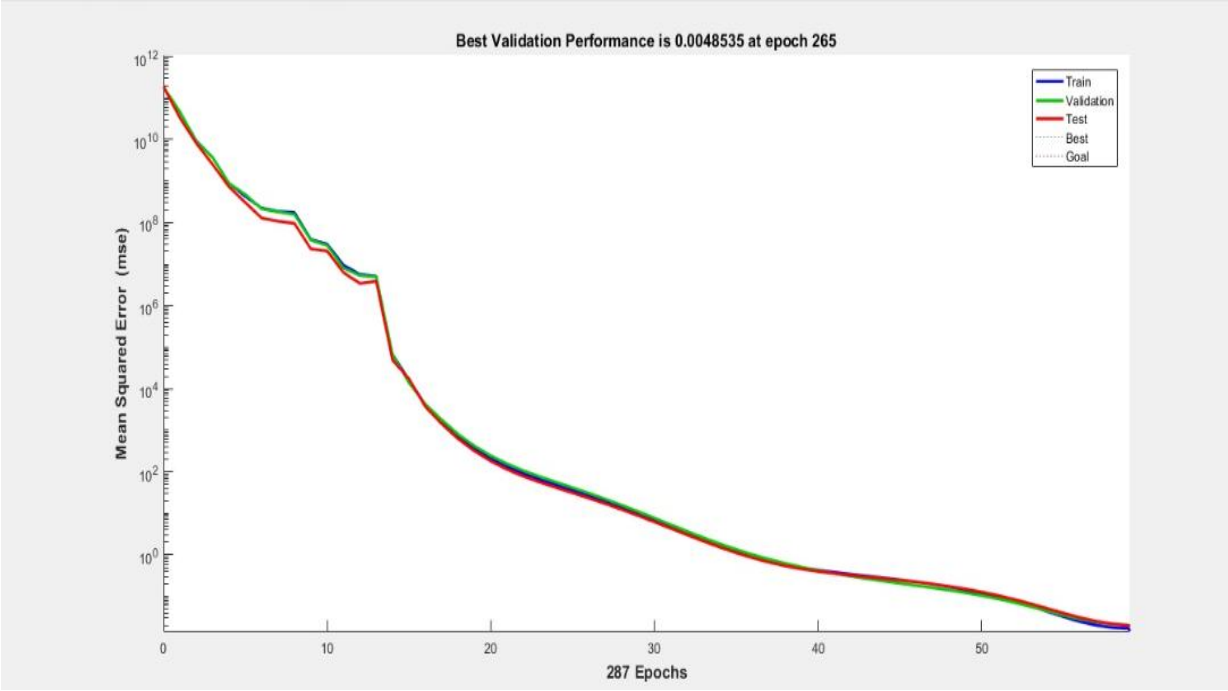

Figure 4.10: LL-G Fault Locating Network Performance

4.2.6 Three Phase Locating Neural Network

This network has been designed to locate three phase symmetrical faults , based on fault impedance of (j0.1) Ω. It consists of an input layer of 6 neurons , a hidden layer of 20 neurons , and an output layer of a single neuron .Fig 4.11 shows the design of this network .

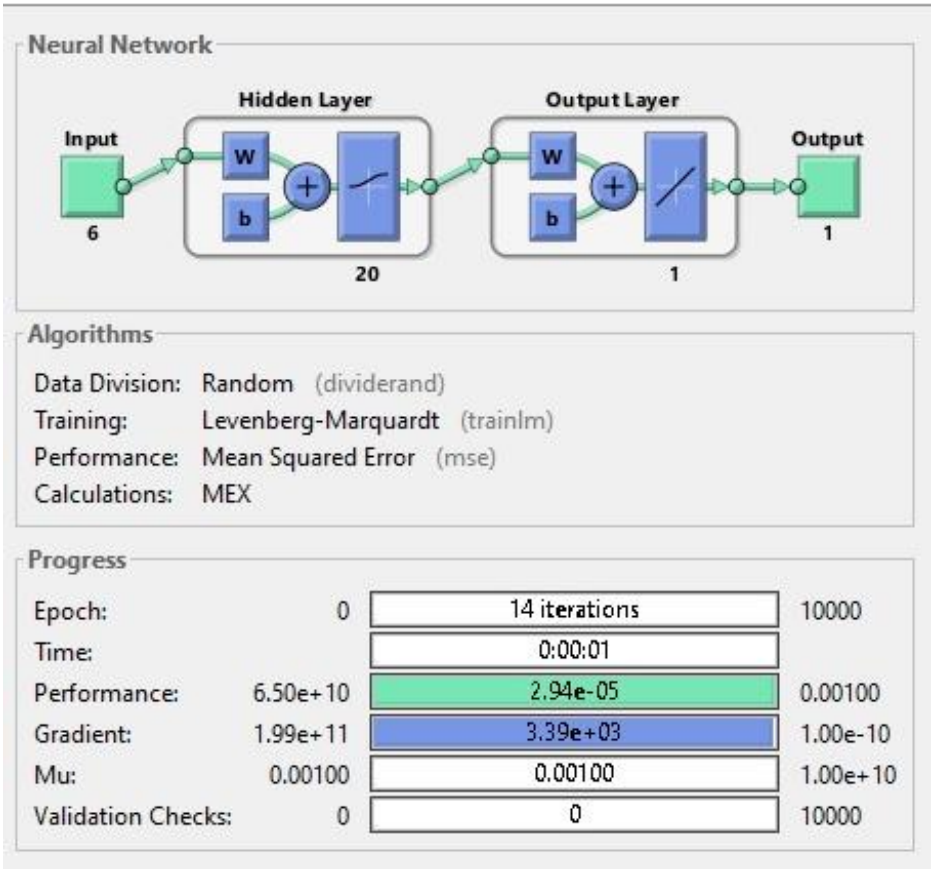

Figure 4.11: 3-Phase Faults Locating Network Design

Table 4.6 shows a random sample of the data that have been generated and used as a training data for three phase faults locating neural network . Faults data of 150 different locations have been used for training .

Table 4.6:Three Phase Fault Locating Data Sample

V_{af}/V_{apf}	V_{bf}/V_{bpf}	V_{cf}/V_{cpf}	I_{af}/I_{apf}	I_{bf}/I_{bpf}	I_{cf}/I_{cpf}	Distance
4.807692	4.807692	4.807692	5.79E-01	5.79E-01	0.578652	206000
4.761905	4.761905	4.761905	0.581006	5.81E-01	5.81E-01	208000
4.716981	4.716981	4.716981	5.83E-01	0.583333	5.83E-01	210000
4.672897	4.672897	4.672897	5.86E-01	5.86E-01	0.585635	212000
4.62963	4.62963	4.62963	0.587912	5.88E-01	5.88E-01	214000
4.587156	4.587156	4.587156	5.90E-01	0.590164	5.90E-01	216000
4.545455	4.545455	4.545455	5.92E-01	5.92E-01	0.592391	218000
4.504505	4.504505	4.504505	0.594595	5.95E-01	5.95E-01	220000

Where:

V_{af},V_{bf} ,V_{cf} are the three phases voltage values after fault event .

I_{af},I_{bf} ,I_{cf} are the three phases current values after fault event .

V_{apf}, V_{bpf}, V_{cpf} are the three phases pre-fault voltage values .

I_{apf}, I_{bpf}, I_{cpf} are the three phases pre-fault current values.

Fig 4.12 shows the performance of the designed neural network after 14 epochs , and with an error of nearly $2.8543e^{-5}$.

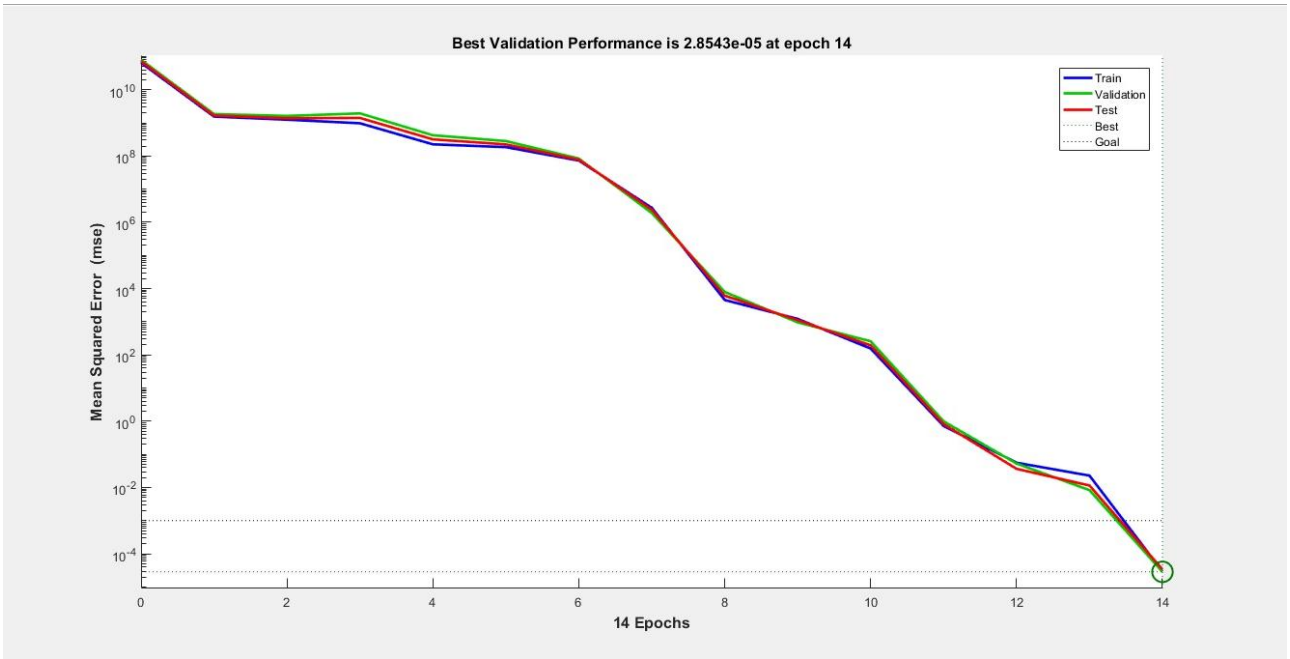

Figure 4.12 Symmetrical Faults Locating Network Performance

4.3 Fourteen- Bus System Based Design

This design is based on data that have been generated by simulating different types of faults using IEEE 14 bus system standard in SIMULINK. Only the locating networks training data have been generated after modifying the system by assuming a transmission line of 10 Km length , and 0.02 Ω /10 Km line impedance .Fig 4.13 shows the IEEE 14 bus system standard.

The output of fault locating networks is actually the values of line impedances between the measurement point and the fault location. An additional neural network was needed to determine the actual distance .

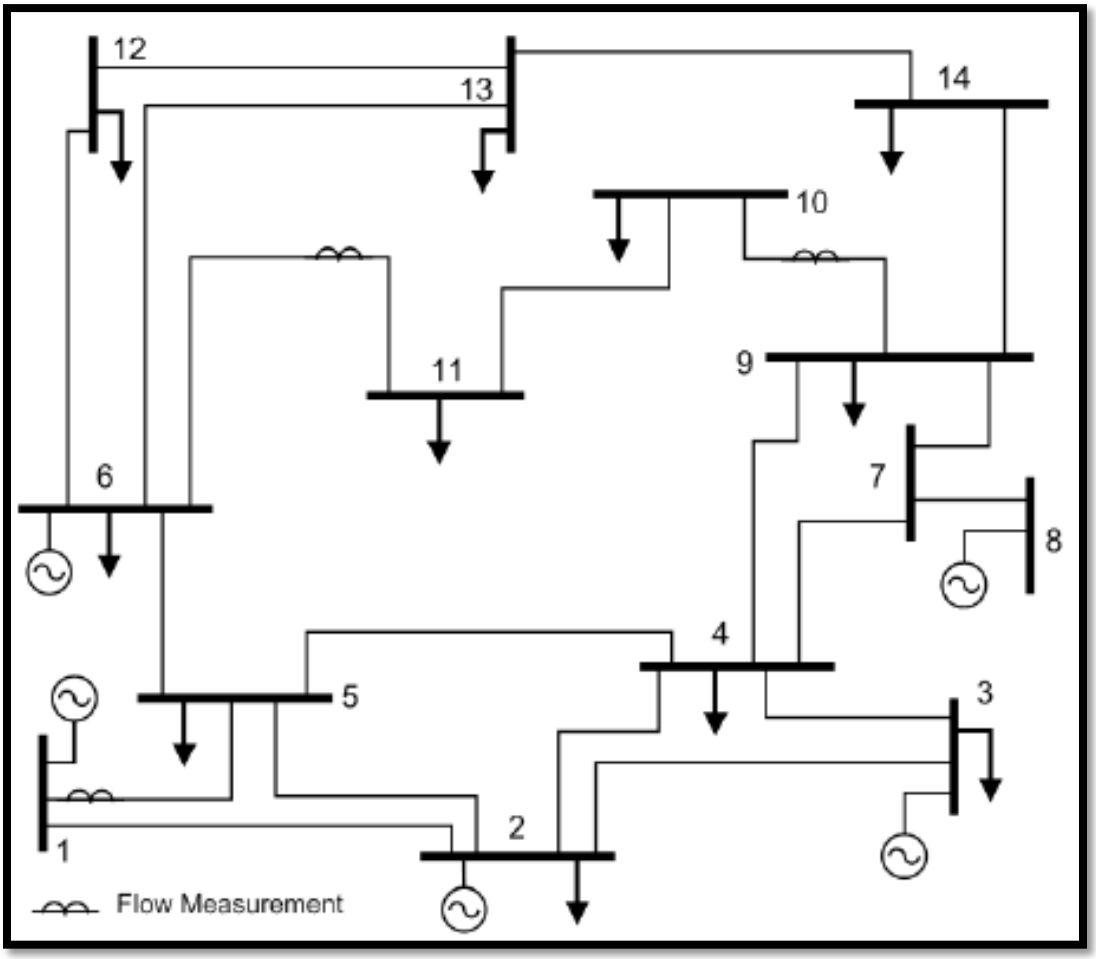

Figure 4.13: IEEE 14 Bus System Standard Single Line Diagram

4.3.1 Fault Detection Neural Network

This network has been designed to detect different types of faults. It consists of an input layer of 6 neurons , a hidden layer of 10 neurons , and an output layer of a single neuron .Fig 4.14 shows the final shape of the network design with its training progress .

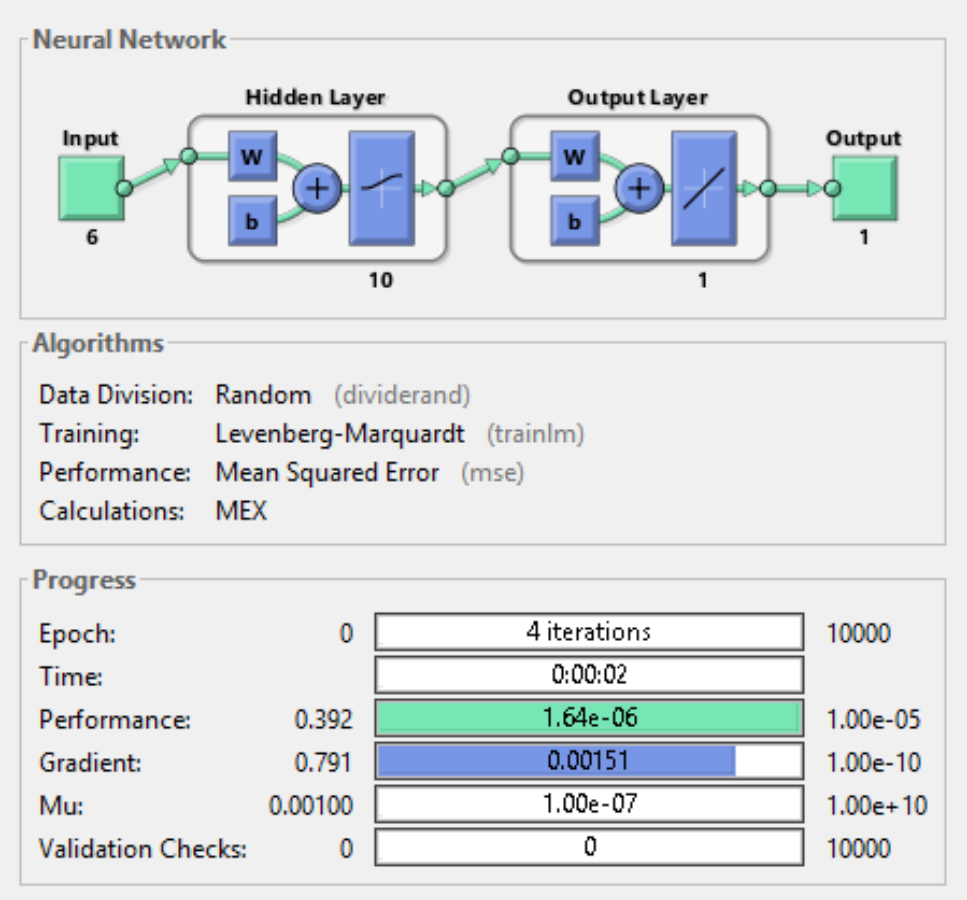

Figure 4.14: Fault Detection Network Design

Table 4.7 shows a random sample of the data that have been generated and used as a training data for the fault detecting neural network .

Table 4.7: Detection Data Sample

V_{af}/V_{apf}	V_{bf}/V_{bpf}	V_{cf}/V_{cpf}	I_{af}/I_{apf}	I_{bf}/I_{bpf}	I_{cf}/I_{cpf}	Output
0.108124	0.119955	0.101953	4.82	6.48	5.28	1
0.108638	0.120292	0.101121	4.76	6.4	5.32	1
0.988568	0.9869	0.987745	0.990098	0.990253	0.973808	0
0.297864	0.881407	0.583439	3.64	0.914	4.3	1
0.986022	0.984167	0.985111	0.989474	0.989711	1.00781	0
0.409182	0.998151	0.588878	4.88	0.976	3.58	1
1.000701	1.000672	1.000697	0.982905	0.982248	0.96543	0
0.414821	0.981241	0.566338	5.2	0.948	3.92	1

Where:

V_{af},V_{bf} ,V_{cf} are the three phases voltage values after fault event .

I_{af},I_{bf} ,I_{cf} are the three phases current values after fault event .

$V_{apf}, V_{bpf}, V_{cpf}$ are the three phases pre-fault voltage values .

$I_{apf}, I_{bpf}, I_{cpf}$ are the three phases pre-fault current values.

Fig 4.15 shows the performance of the designed neural network , after 4 epochs and with an error of nearly $1.5416e^{-6}$.

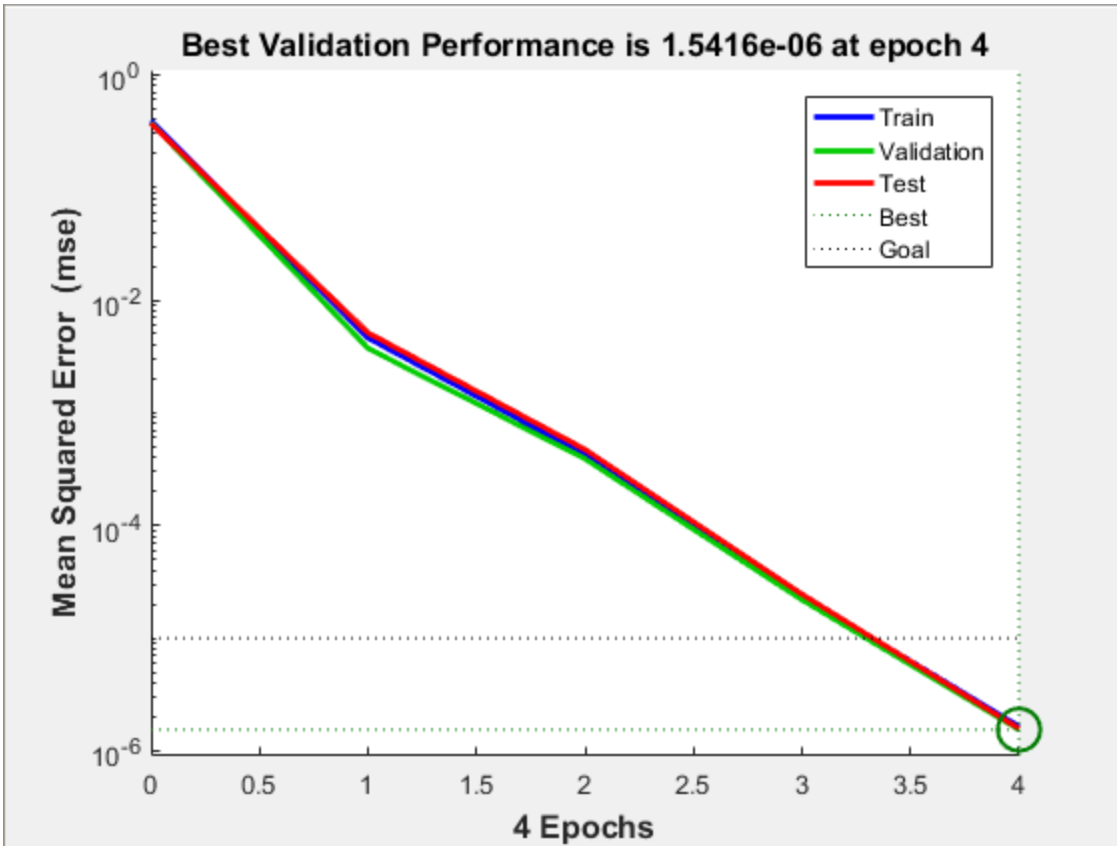

Figure 4.15: Fault Detection Network Performance

4.3.2 Fault Classification Neural Network

This network has been designed to classify different types of faults. It consists of an input layer of 6 neurons , a hidden layer of 40 neurons , and an output layer of 4 neurons .Fig 4.16 shows the final shape of the network design with its training progress .

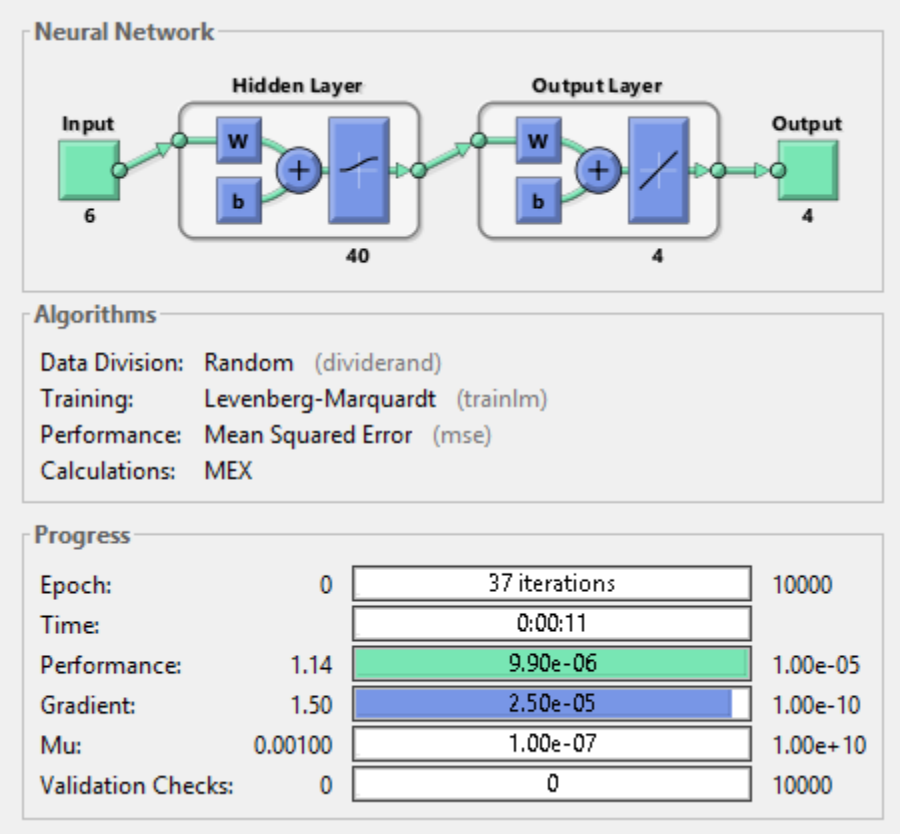

Figure 4.16: Fault Classification Network Design

Table 4.8 shows a random sample of the data that have been generated and used as a training data for the classification neural network .

Table 4.8: Fault Classification Data Sample

V_{af}/V_{apf}	V_{bf}/V_{bpf}	V_{cf}/V_{cpf}	I_{af}/I_{apf}	I_{bf}/I_{bpf}	I_{cf}/I_{cpf}	A	B	C	G
0.115692	0.851754	0.873623	1.43E-08	3.09E-09	4.61E-09	1	0	0	1
0.126625	0.019172	0.107315	2.31E-09	1.12E-08	1.35E-08	0	1	1	0
0.250292	0.805839	0.555446	1.83E-08	2.70E-09	2.10E-08	1	0	1	0
0.308909	0.796432	0.48739	2.62E-08	2.64E-09	2.88E-08	1	0	1	0
0.073547	0.122882	0.30025	1.90E-09	1.10E-08	2.63E-08	0	1	1	1
0.060223	0.123108	0.211312	1.58E-09	3.62E-09	2.84E-08	0	1	1	1
0.000532	0.712816	0.306001	1.28E-08	2.32E-09	2.64E-08	1	0	1	1
0.062609	0.180269	0.242863	1.37E-08	1.18E-08	2.55E-08	1	1	1	1

Where:

V_{af},V_{bf} ,V_{cf} are the three phases voltage values after fault event .

I_{af},I_{bf} ,I_{cf} are the three phases current values after fault event .

V_{apf}, V_{bpf}, V_{cpf} are the three phases pre-fault voltage values .

I_{apf}, I_{bpf}, I_{cpf} are the three phases pre-fault current values.

Fig 4.17 shows the performance of the designed neural network , after 37 epochs and with an error of nearly $9.4155e^{-6}$

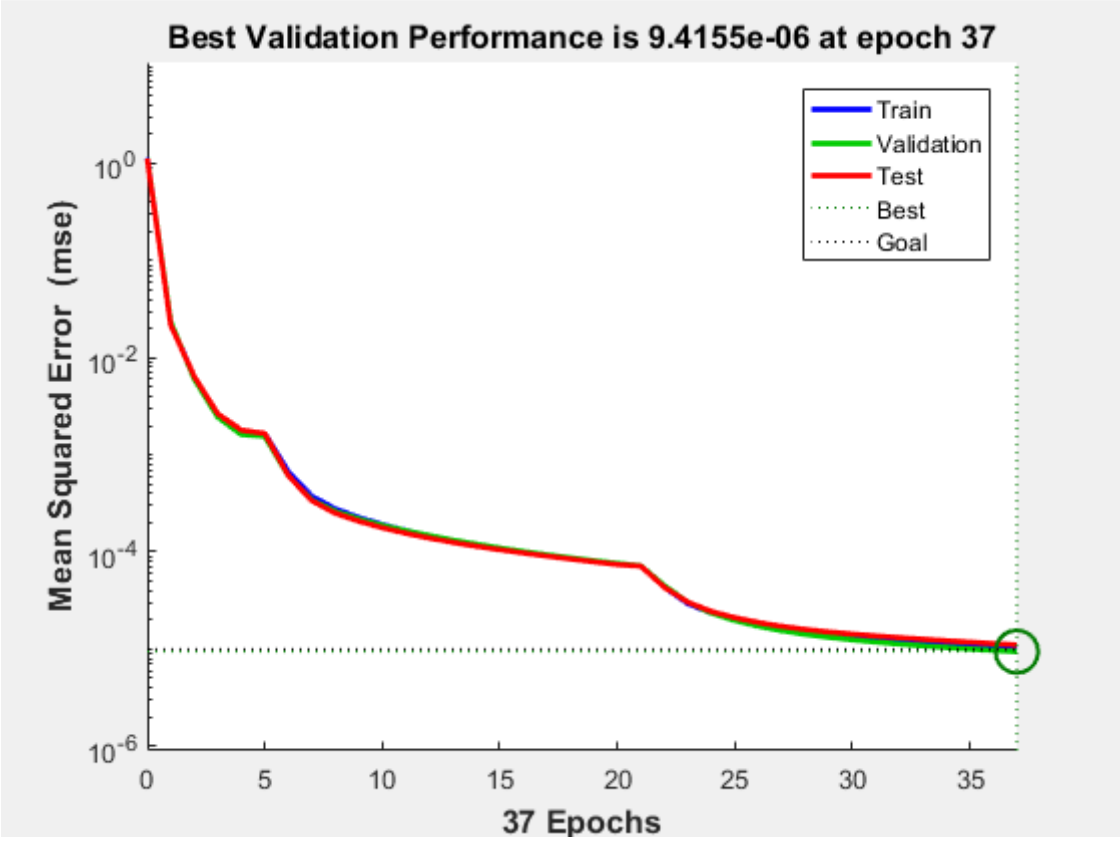

Figure 4.17: Fault Classification Network Performance

4.3.3 L-G Faults Locating Neural Network

This network has been designed to determine line impedance between the measuring point and the fault location .It consists of an input layer of 6 neurons , a hidden layer of 21 neurons , and an output layer of a single neuron .Fig 4.18 shows the final shape of the network design with its training progress.

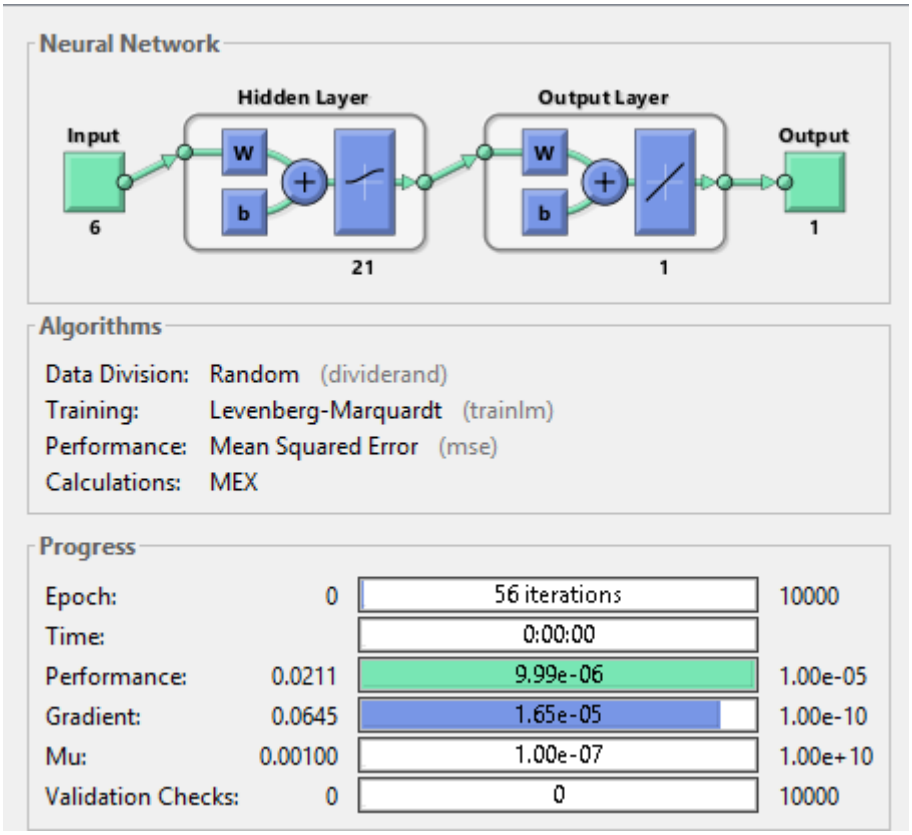

Figure 4.18: L-G Fault Locating Network Design

Table 4.9 shows a random sample of the data that have been generated and used as a training data for single line to ground locating neural network .

Table 4.9 L-G Fault Locating Data Sample

V_{af}/V_{apf}	V_{bf}/V_{bpf}	V_{cf}/V_{cpf}	I_{af}/I_{apf}	I_{bf}/I_{bpf}	I_{cf}/I_{cpf}	Z_l
0.335664	0.940493	0.878754	6.487138	0.883428	0.922329	0.02
0.404686	0.975996	0.902985	6.626994	0.977886	0.881364	0.04
0.444861	0.958539	0.907466	6.797127	0.840719	0.820609	0.06
0.479066	1.005878	0.928054	6.650383	1.021682	0.932451	0.08
0.504466	0.985487	0.927212	6.29506	0.958791	0.949313	0.1
0.526454	0.997061	0.923907	5.520278	0.902832	0.947264	0.12
0.555072	0.995773	0.93511	5.817346	0.857682	0.969786	0.14
0.577678	1.006538	0.948916	5.077187	0.780967	0.92794	0.2

Where:

V_{af},V_{bf} ,V_{cf} are the three phases voltage values after fault event .

I_{af},I_{bf} ,I_{cf} are the three phases current values after fault event .

V_{apf}, V_{bpf}, V_{cpf} are the three phases pre-fault voltage values .

I_{apf}, I_{bpf}, I_{cpf} are the three phases pre-fault current values.

Z_l is the line impedance between the measuring point and the fault location .

Fig 4.19 shows the performance of the designed neural network , after 56 epochs and with an error of nearly $8.6935e^{-6}$

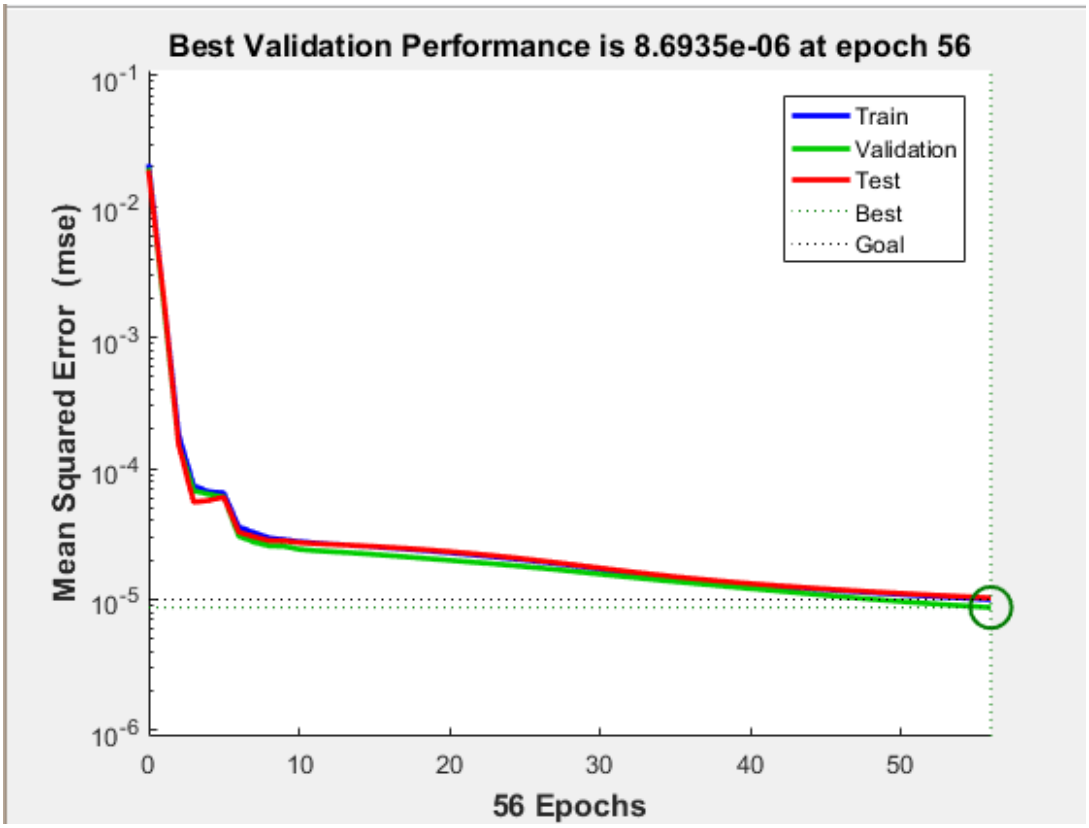

Figure 4.19: L-G Fault Locating Network

4.3.4 Line To Line Fault Locating ANN

This network has been designed to determine line impedance between the measuring point and the fault location .It consists of an input layer of 6 neurons , a hidden layer of 6 neurons , and an output layer of a single neuron .Fig 4.20 shows the final shape of the network design with its training progress.

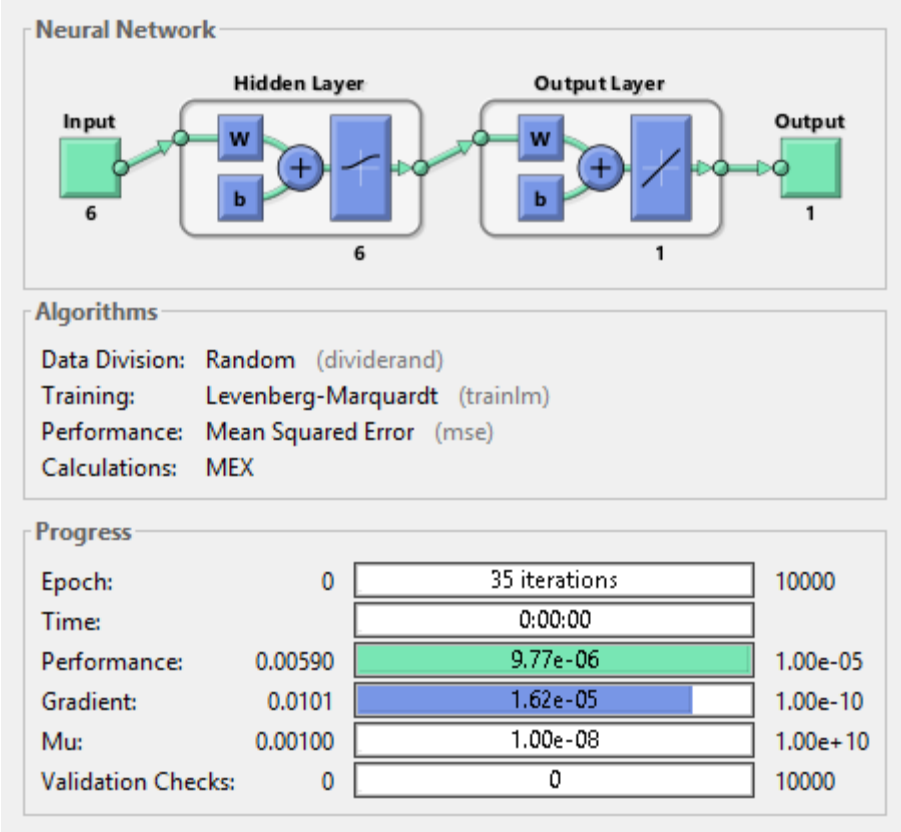

Figure 4.20: L-L Fault Locating Network

Table 4.10 shows a random sample of the data that have been generated and used as a training data for L-L locating neural network .

Table 4.10: L-L Fault Locating Data Sample

V_{af}/V_{apf}	V_{bf}/V_{bpf}	V_{cf}/V_{cpf}	I_{af}/I_{apf}	I_{bf}/I_{bpf}	I_{cf}/I_{cpf}	Z_l
0.689731	0.39567	1.009958	2.723647	2.461456	0.470193	0.08
0.710747	0.42884	1.015916	2.619584	2.388692	0.462737	0.1
0.727822	0.446704	1.018399	2.505422	2.286745	0.454972	0.12
0.735993	0.460102	1.018593	2.422848	2.199606	0.445851	0.14
0.752376	0.49804	1.023131	2.254784	2.044084	0.434429	0.18
0.764845	0.503741	1.016151	2.184568	1.97156	0.425774	0.2
0.990548	0.447141	0.563548	0.490762	2.78446	3.089475	0.02
0.40497	1.008523	0.662924	2.464709	0.478887	2.684825	0.06

Where:

V_{af},V_{bf} ,V_{cf} are the three phases voltage values after fault event .

I_{af},I_{bf} ,I_{cf} are the three phases current values after fault event .

V_{apf}, V_{bpf}, V_{cpf} are the three phases pre-fault voltage values .

I_{apf}, I_{bpf}, I_{cpf} are the three phases pre-fault current values

Fig 4.21 shows the performance of the designed neural network after 35 epochs , and with an error of nearly $9.6887e^{-6}$

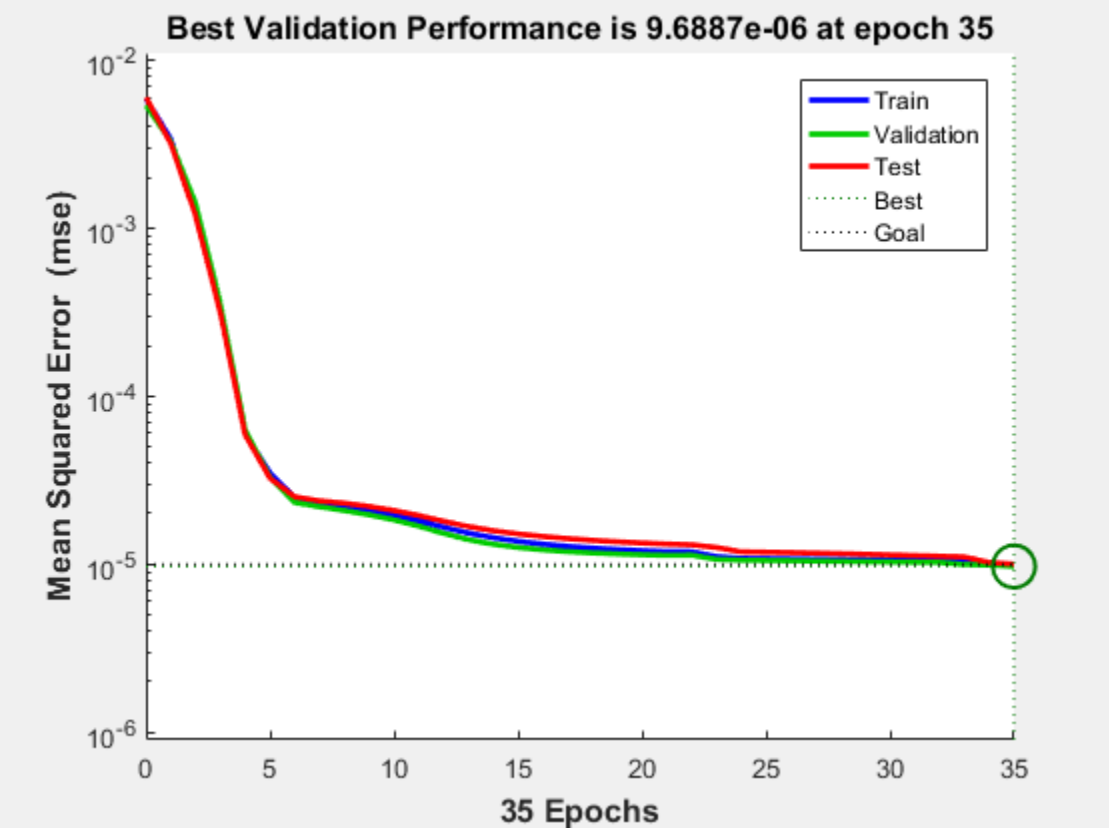

Figure 4.21: L-L Locating Network Performance

4.3.5 LL-G Fault Locating Neural Network

This network has been designed to determine line impedance between the measuring point and the fault location .It consists of an input layer of 6 neurons , a hidden layer of 6 neurons , and an output layer of a single neuron .Fig 4.22 shows the final shape of the network design with its training progress.

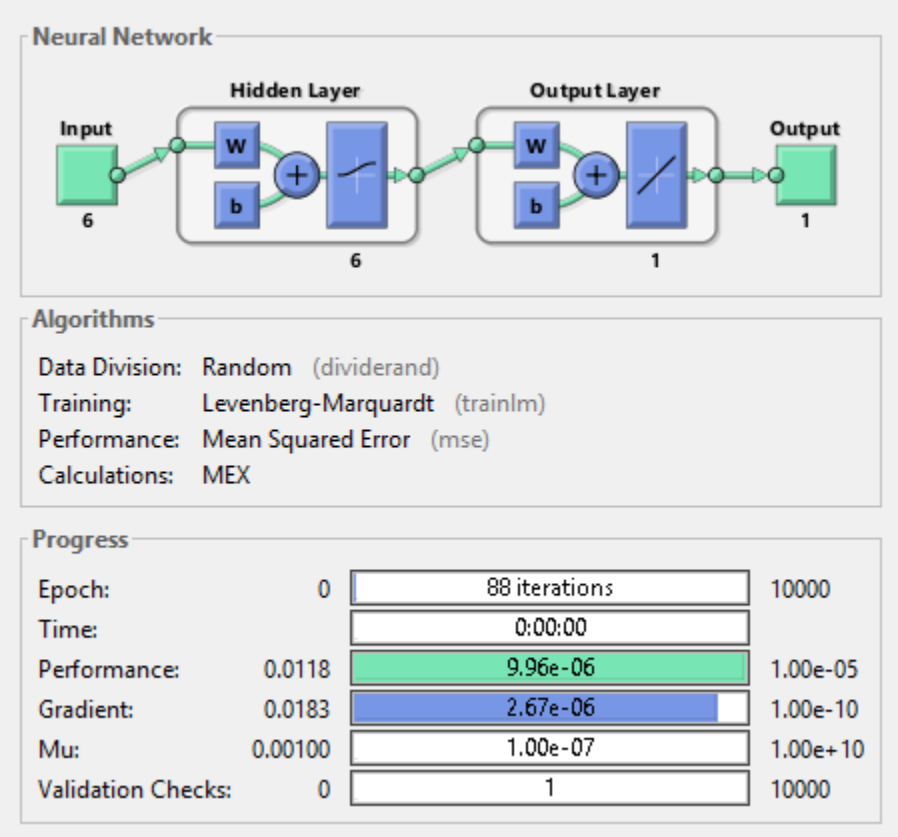

Figure 4.22: LL-G Locating Network

Table 4.11 shows a random sample of the data that have been generated and used as a training data for LL-G locating neural network .

Table 4.11: LL-G Fault Locating Data Sample

V_{af}/V_{apf}	V_{bf}/V_{bpf}	V_{cf}/V_{cpf}	I_{af}/I_{apf}	I_{bf}/I_{bpf}	I_{cf}/I_{cpf}	Z_l
0.191952	0.228057	0.869916	3.502103	3.28775	0.470984	0.02
0.332697	0.343966	0.877876	3.479306	3.11046	0.421647	0.06
0.383356	0.398266	0.887102	3.329724	2.885985	0.401819	0.08
0.408912	0.424256	0.887973	3.184515	2.80578	0.387179	0.1
0.437135	0.450487	0.894264	3.036431	2.672883	0.381883	0.12
0.493479	0.902699	0.470367	2.466548	0.371568	2.818561	0.14
0.505072	0.536055	0.902975	2.676499	2.290539	0.372348	0.18
0.512886	0.535047	0.907558	2.63371	2.274509	0.373555	0.2

Where:

V_{af},V_{bf} ,V_{cf} are the three phases voltage values after fault event .

I_{af},I_{bf} ,I_{cf} are the three phases current values after fault event .

V_{apf}, V_{bpf}, V_{cpf} are the three phases pre-fault voltage values .

I_{apf}, I_{bpf}, I_{cpf} are the three phases pre-fault current values

Fig 4.23 shows the performance of the designed neural network after 87 epochs , and with an error of nearly $1.1556e^{-5}$

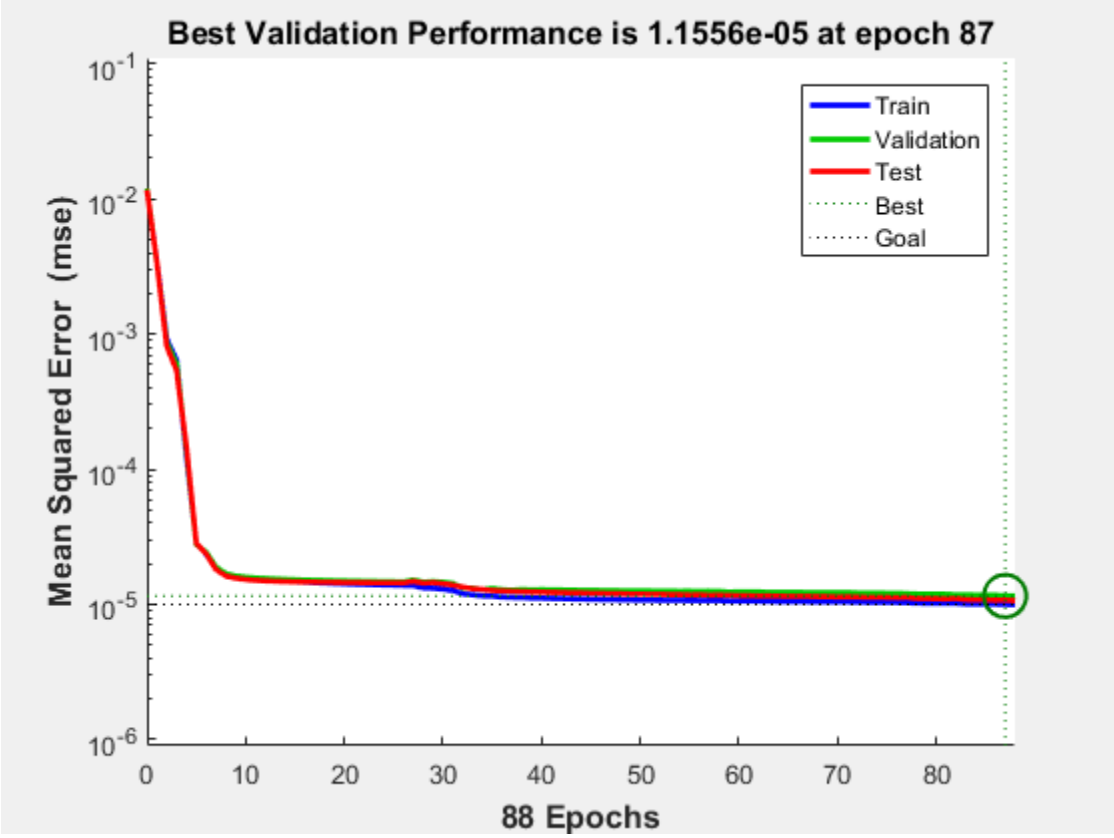

Figure 4.23: LL-G Fault Locating Network Performance

4.3.6 Three Phase Locating Neural Network

This network has been designed to determine line impedance between the measuring point and the fault location .It consists of an input layer of 6 neurons , a hidden layer of 13 neurons , and an output layer of a single neuron .Fig 4.24 shows the final shape of the network design with its training progress.

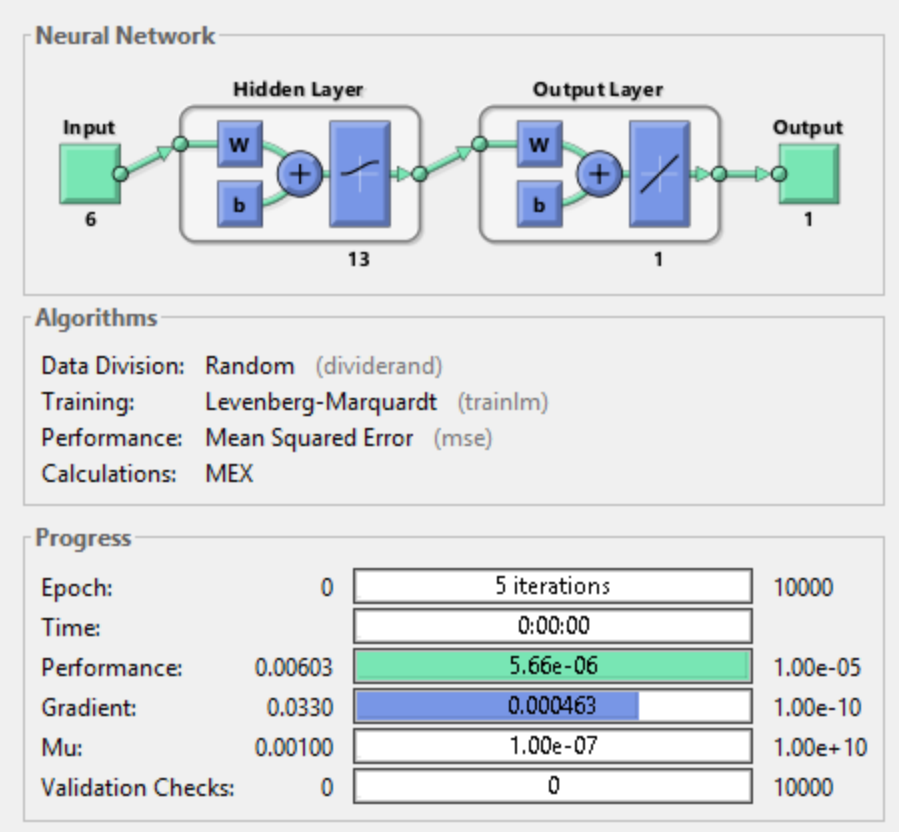

Figure 4.24: 3-Phase Faults Locating Network

Table 4.12 shows a random sample of the data that have been generated and used as a training data for three phase faults locating neural network .

Table 4.12: Three Phase Fault Locating Data Sample

V_{af}/V_{apf}	V_{bf}/V_{bpf}	V_{cf}/V_{cpf}	I_{af}/I_{apf}	I_{bf}/I_{bpf}	I_{cf}/I_{cpf}	Z_l
0.10527	0.114993	0.113107	3.207227	3.259091	3.108971	0.02
0.18085	0.190453	0.183673	3.131951	3.296212	2.950622	0.04
0.24424	0.253106	0.245766	3.081862	3.202704	2.942565	0.06
0.286094	0.293472	0.282752	2.800426	2.860372	2.739958	0.08
0.336737	0.344564	0.339004	2.781509	2.902131	2.642197	0.1
0.390409	0.395604	0.400121	2.600938	2.693469	2.511125	0.14
0.435628	0.447597	0.447144	2.405272	2.489809	2.332233	0.18
0.452245	0.458491	0.464568	2.343527	2.419688	2.282379	0.2

Where:

V_{af},V_{bf} ,V_{cf} are the three phases voltage values after fault event .

I_{af},I_{bf} ,I_{cf} are the three phases current values after fault event .

V_{apf}, V_{bpf}, V_{cpf} are the three phases pre-fault voltage values .

I_{apf}, I_{bpf}, I_{cpf} are the three phases pre-fault current values.

Fig 4.25 shows the performance of the designed neural network after 5 epochs , and with an error of nearly $5.7228e^{-6}$

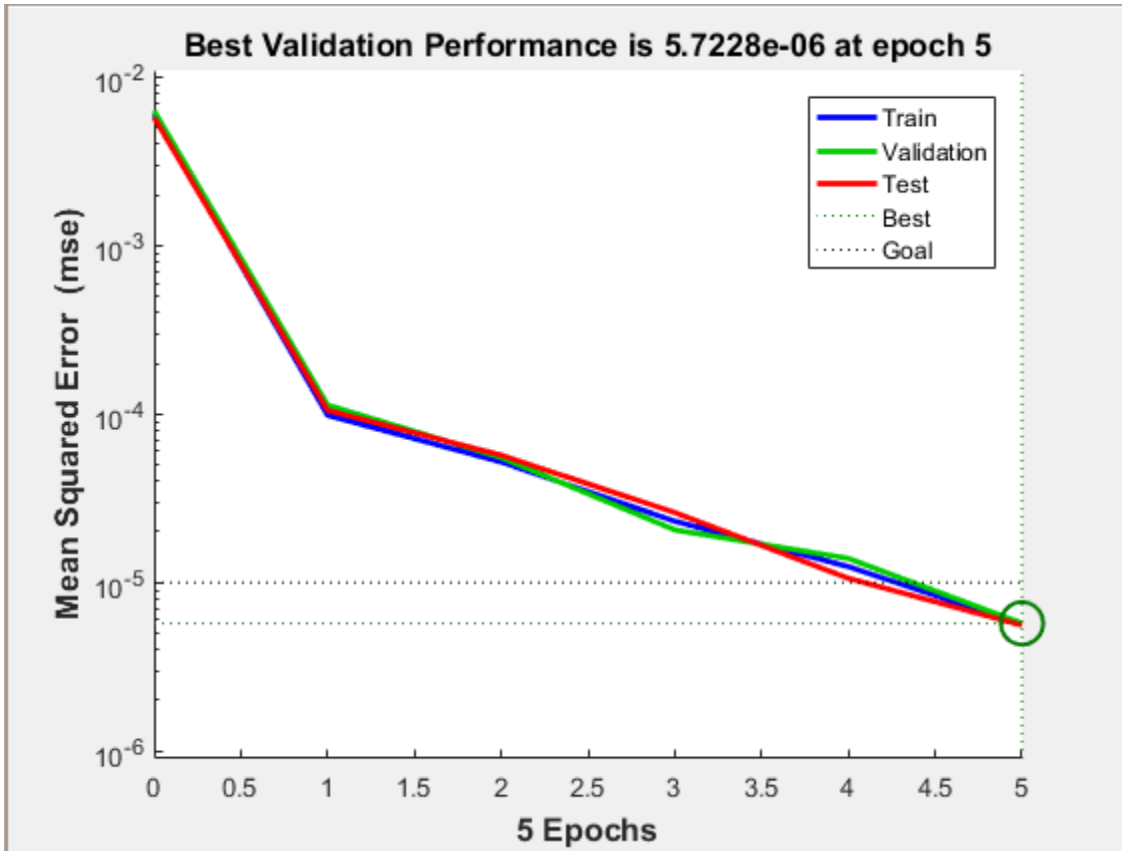

Figure 4.25: Three Phase Fault Locating Network Performance

4.3.7 Distance Network

This network has been designed to convert the line impedance values , that were the outputs of the different faults locating network into a distance per meter's. It consists of an input layer of a single neuron , a hidden layer of 7 neurons , and an output layer of a single neuron .Fig 4.26 shows the final shape of the network design with its training progress.

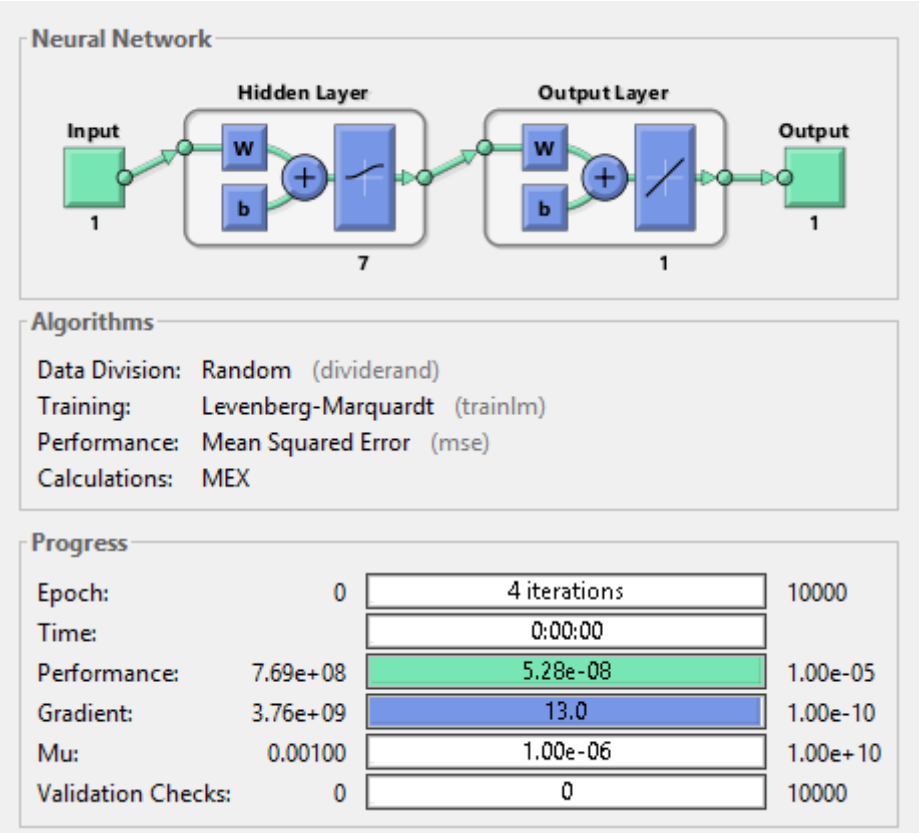

Figure 4.26: Distance Network Design

Fig 4.27shows the performance of the designed neural network after 5 epochs , and with an error of nearly $5.7228e^{-6}$

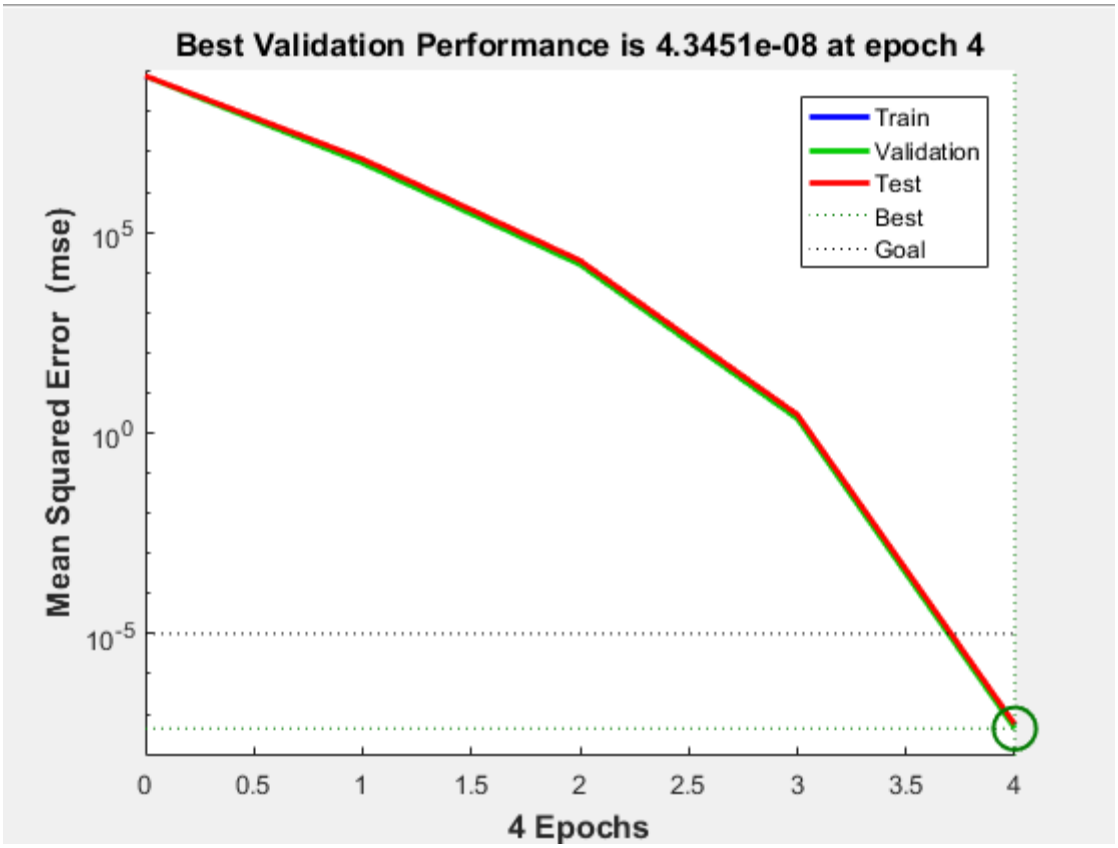

Figure 4.27: Distance Network Performance

4.4 Thirty- Bus System Based Design

This design is based on data that have been generated by simulating different types of faults using IEEE 30 bus system standard in SIMULINK. Only the locating networks training data have been generated after modifying the system lines impedances by assuming a transmission line impedance of 0.02 Ω /10 Km. The modified used data are presented in appendix A3 . Fig 4.28 shows the IEEE 30 bus system standard.

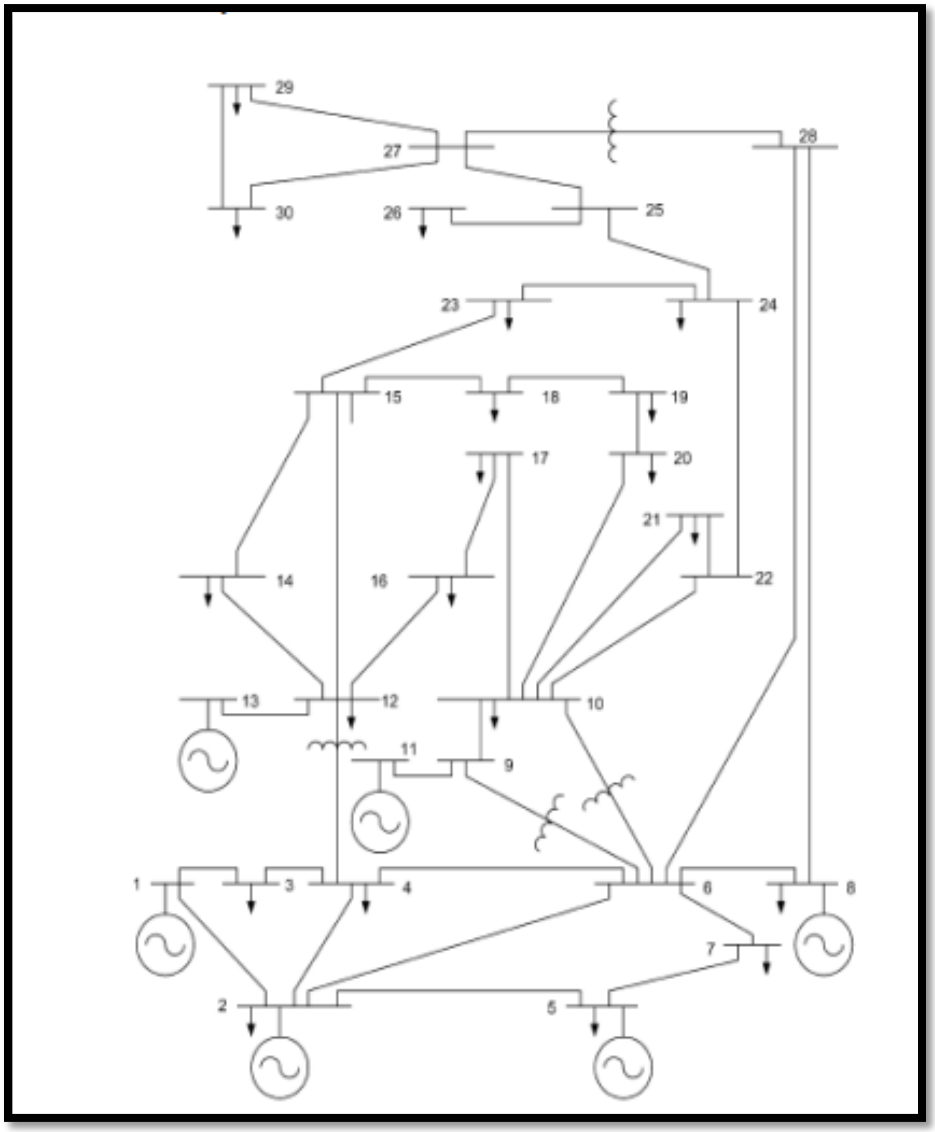

Figure 4.28: IEEE 30 Bus System Standard Single Line Diagram

4.4.1 Fault Detection Neural Network

This network has been designed to detect different types of faults. It consists of an input layer of 6 neurons , a hidden layer of 4 neurons , and an output layer of a single neuron .Fig 4.29 shows the final shape of the network design with its training progress .

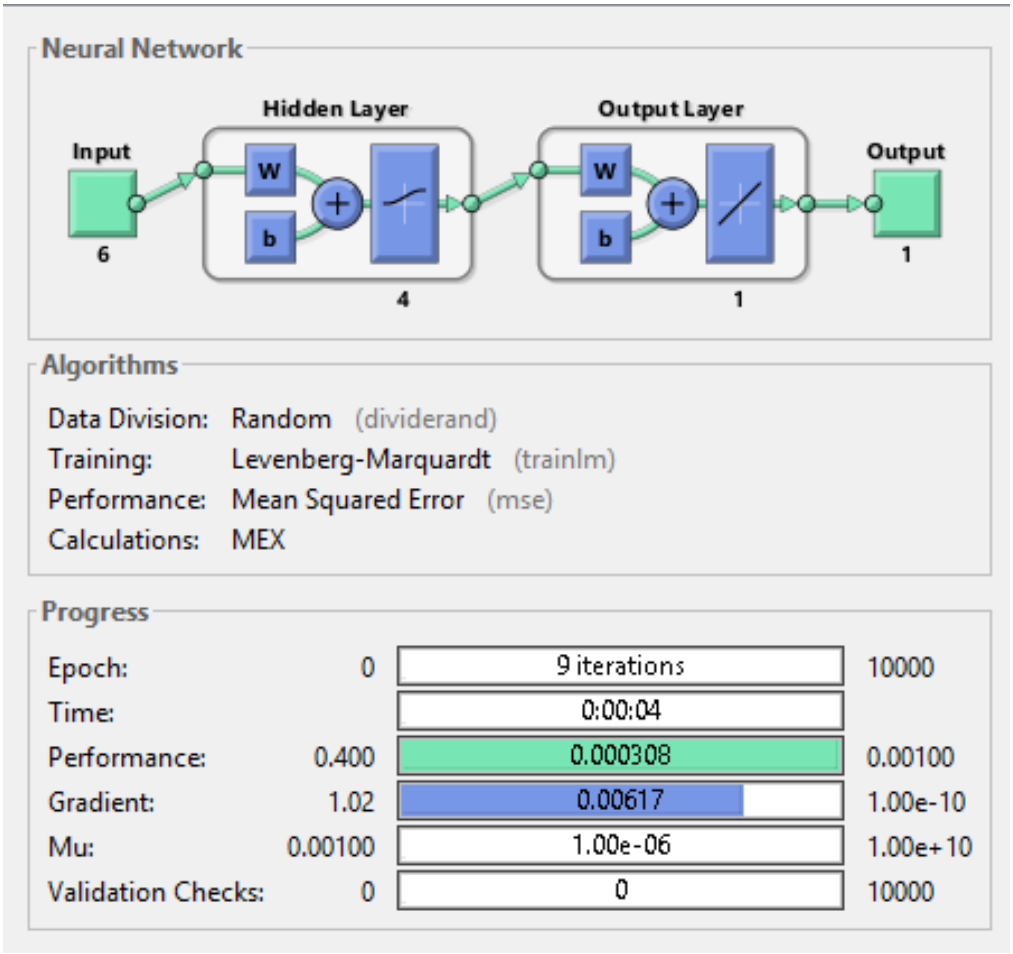

Figure 4.29: Fault Detection Network Design

Fig 4.30 shows the performance of the designed neural network , after 9 epochs and with an error of nearly 0.00028053.

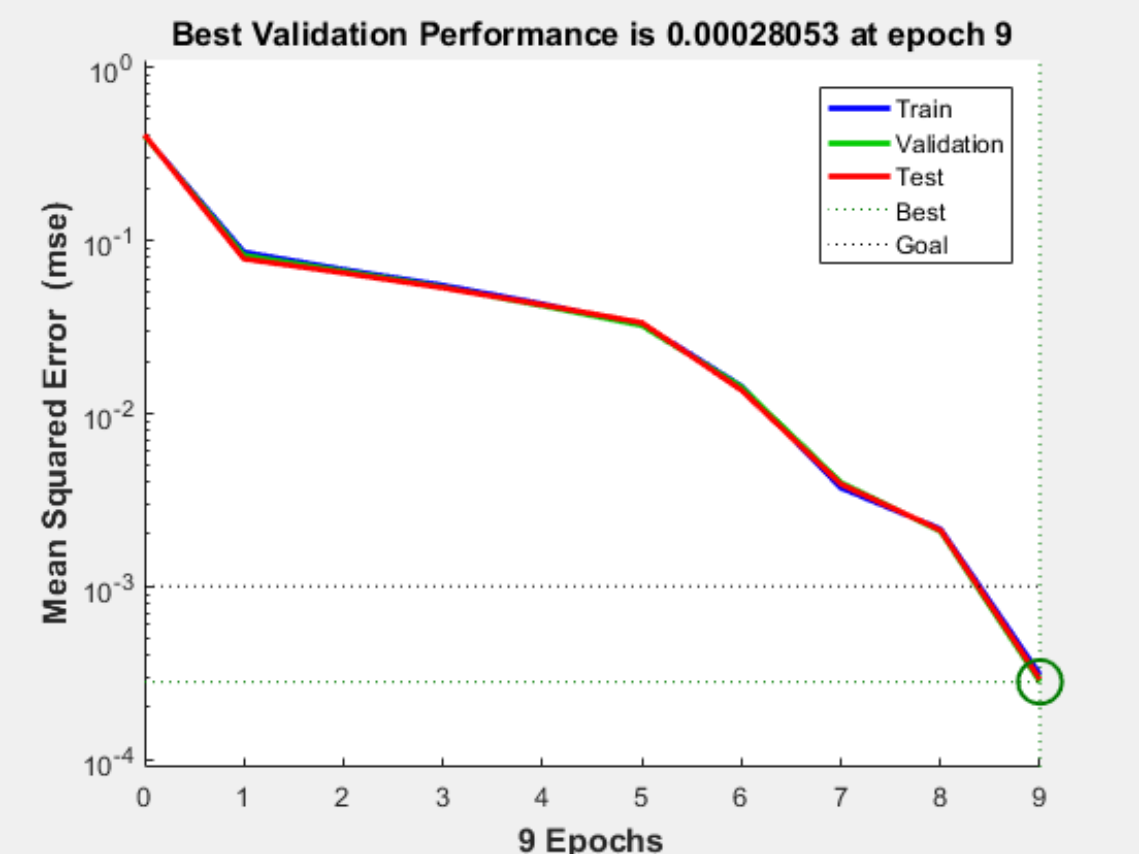

Figure 4.30: Fault Detection Network Performance

4.4.2 Fault Classification Neural Network

This network has been designed to classify different types of faults. It consists of an input layer of 6 neurons , a hidden layer of 16 neurons , and an output layer of 4 neurons .Fig 4.31 shows the final shape of the network design with its training progress .

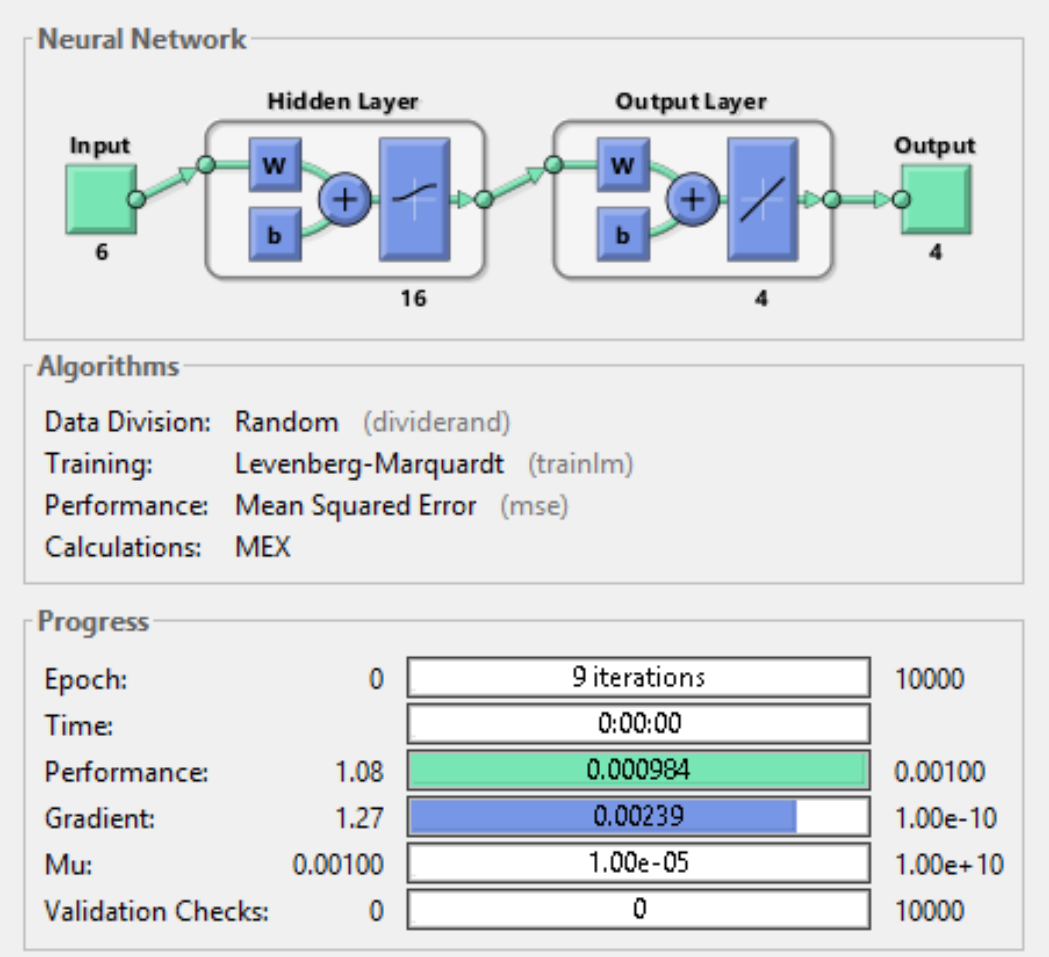

Figure 4.31: Fault Classification Network Design

Fig 4.32 shows the performance of the designed neural network , after 9 epochs and with an error of nearly 0.00097988.

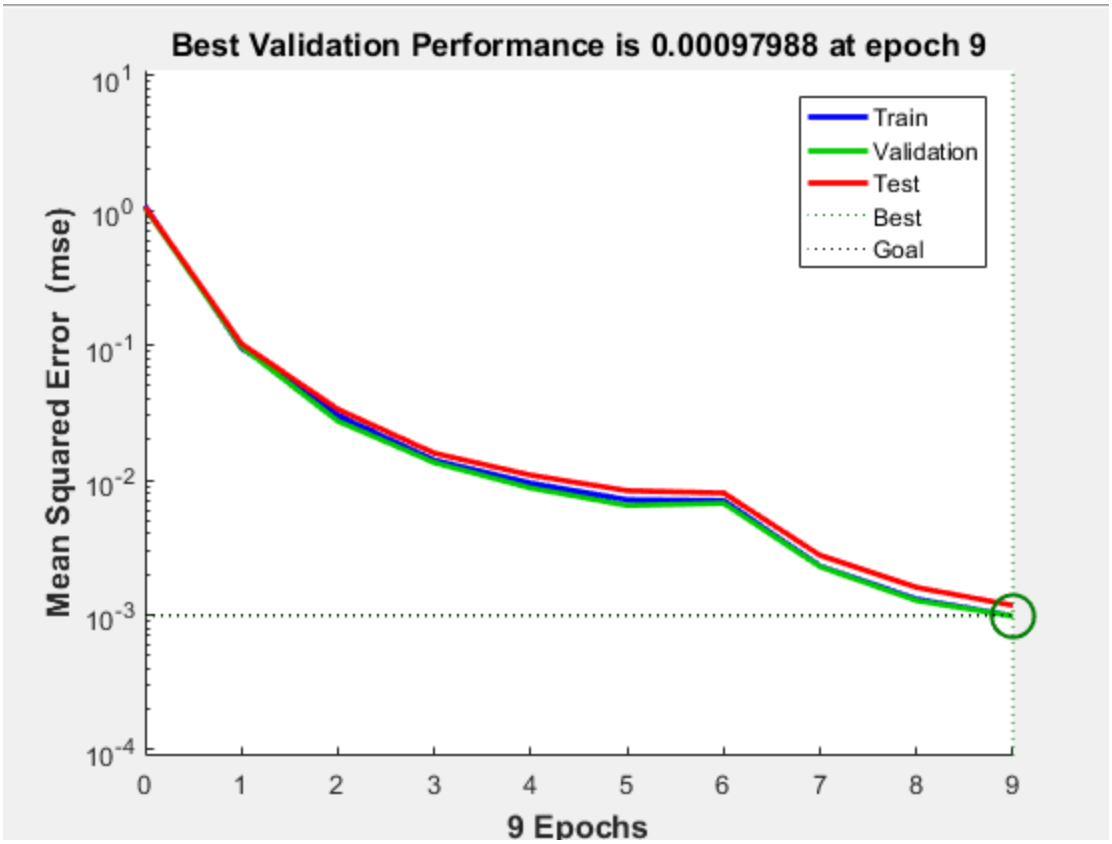

Figure 4.32: Fault Classification Network Performance

4.4.3 L-G Faults Locating Neural Network

This network has been designed to determine line impedance between the measuring point and the fault location .It consists of an input layer of 6 neurons , two hidden layers of 4,6 neurons , and an output layer of a single neuron .Fig 4.33 shows the final shape of the network design with its training progress.

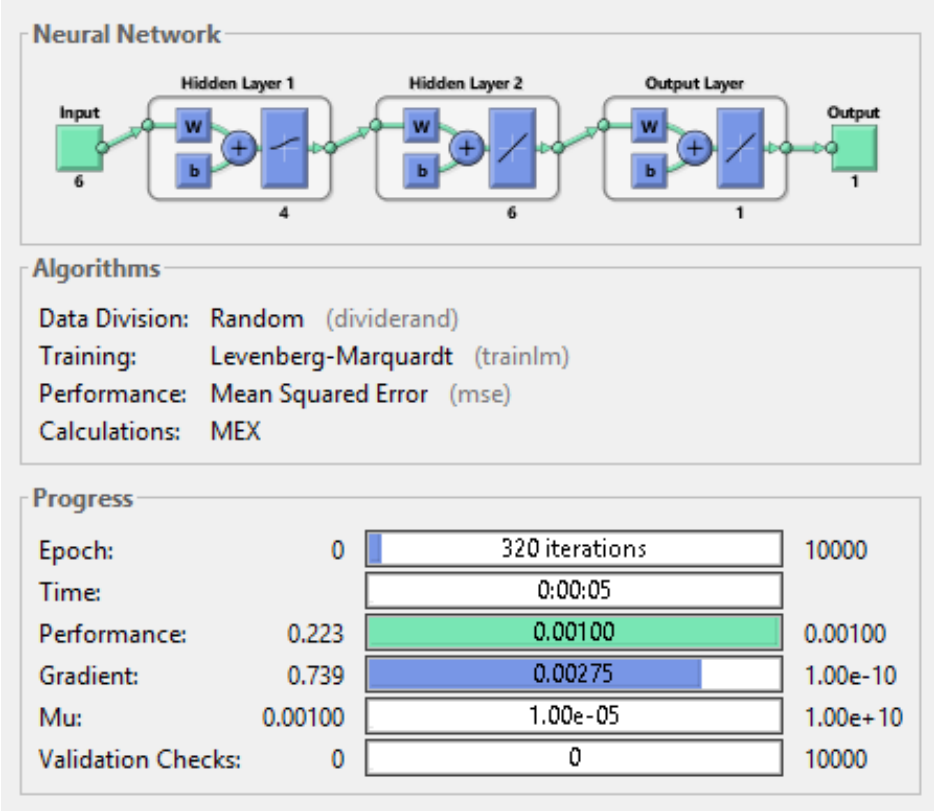

Figure 4.33: L-G Fault Locating Network Design

Fig 4.34 shows the performance of the designed neural network , after 320 epochs and with an error of nearly 0.00092101.

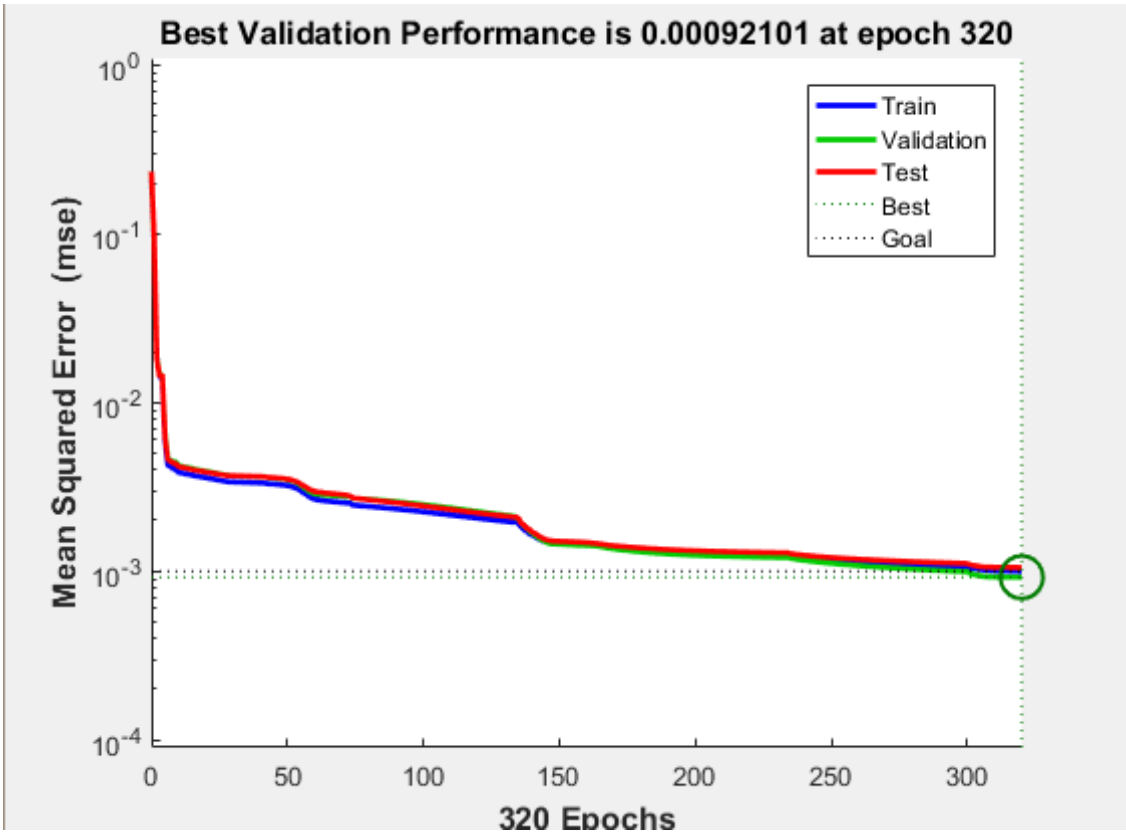

Figure 4.34: L-G Fault Locating Network Performance

4.4.4 Line To Line Fault Locating ANN

This network has been designed to determine line impedance between the measuring point and the fault location .It consists of an input layer of 6 neurons , a hidden layer of 10 neurons , and an output layer of a single neuron .Fig 4.35 shows the final shape of the network design with its training progress.

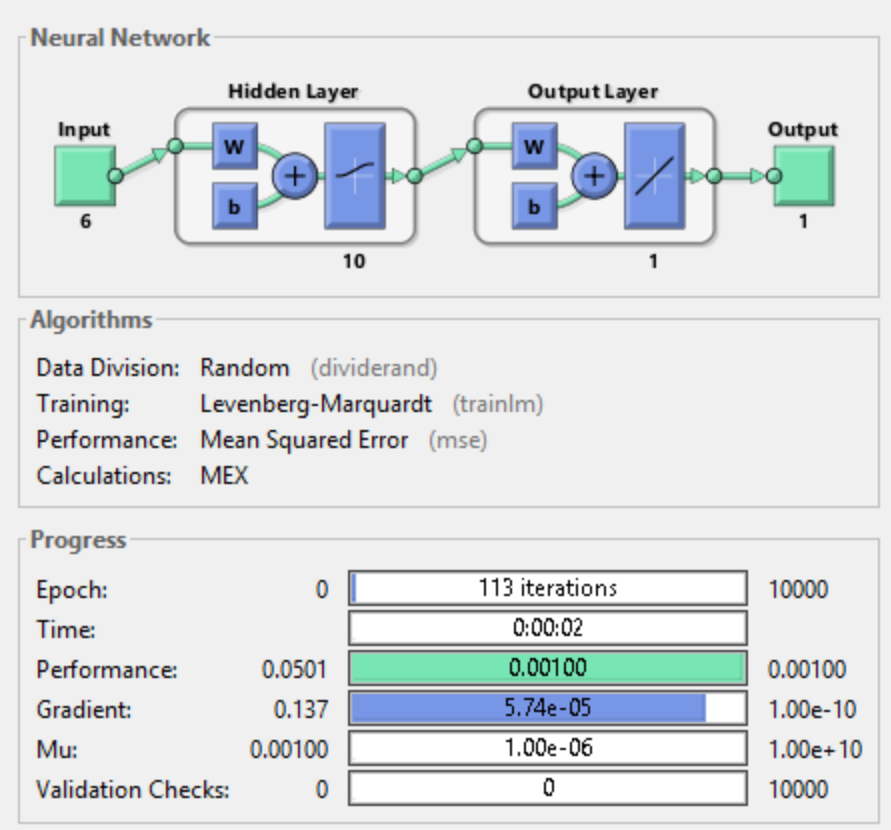

Figure 4.35: L-L Fault Locating Network Design

Fig 4.36 shows the performance of the designed neural network after 113 epochs , and with an error of nearly 0.00096263.

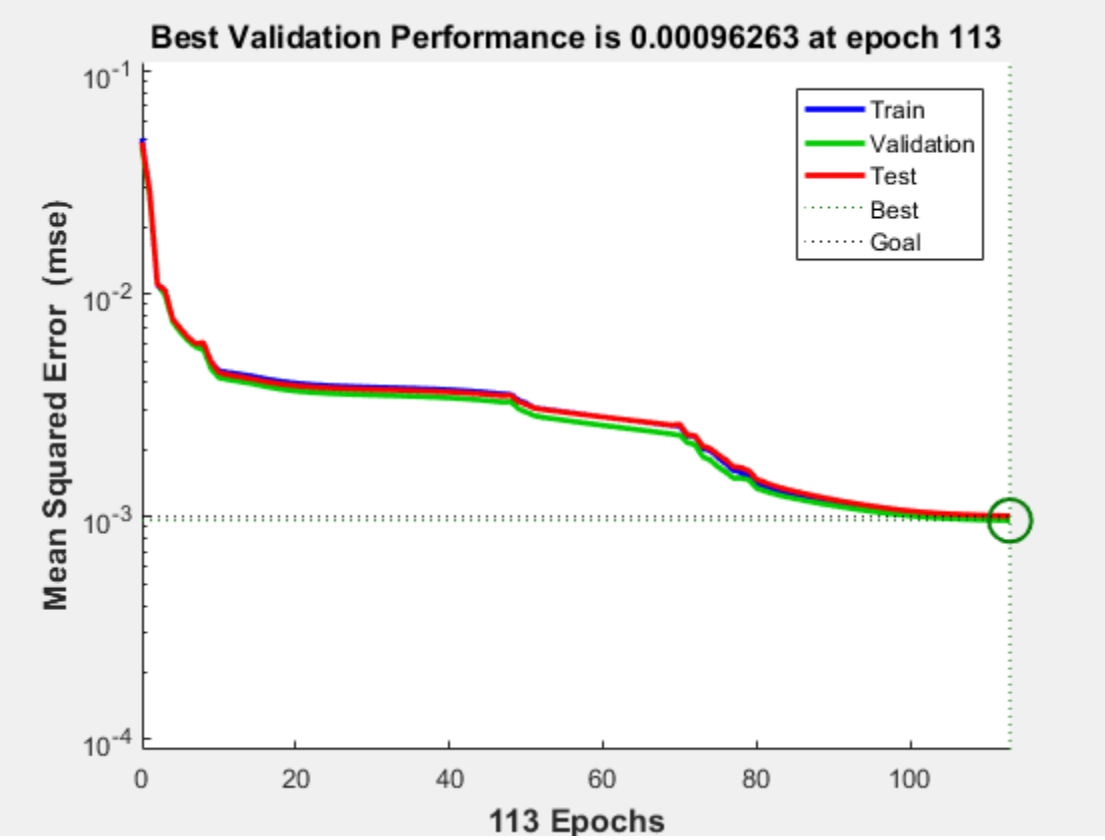

Figure 4.36: L-L Fault Locating Network Performance

4.4.5 LL-G Fault Locating Neural Network

This network has been designed to determine line impedance between the measuring point and the fault location .It consists of an input layer of 6 neurons , a hidden layer of 10 neurons , and an output layer of a single neuron .Fig 4.37shows the final shape of the network design with its training progress.

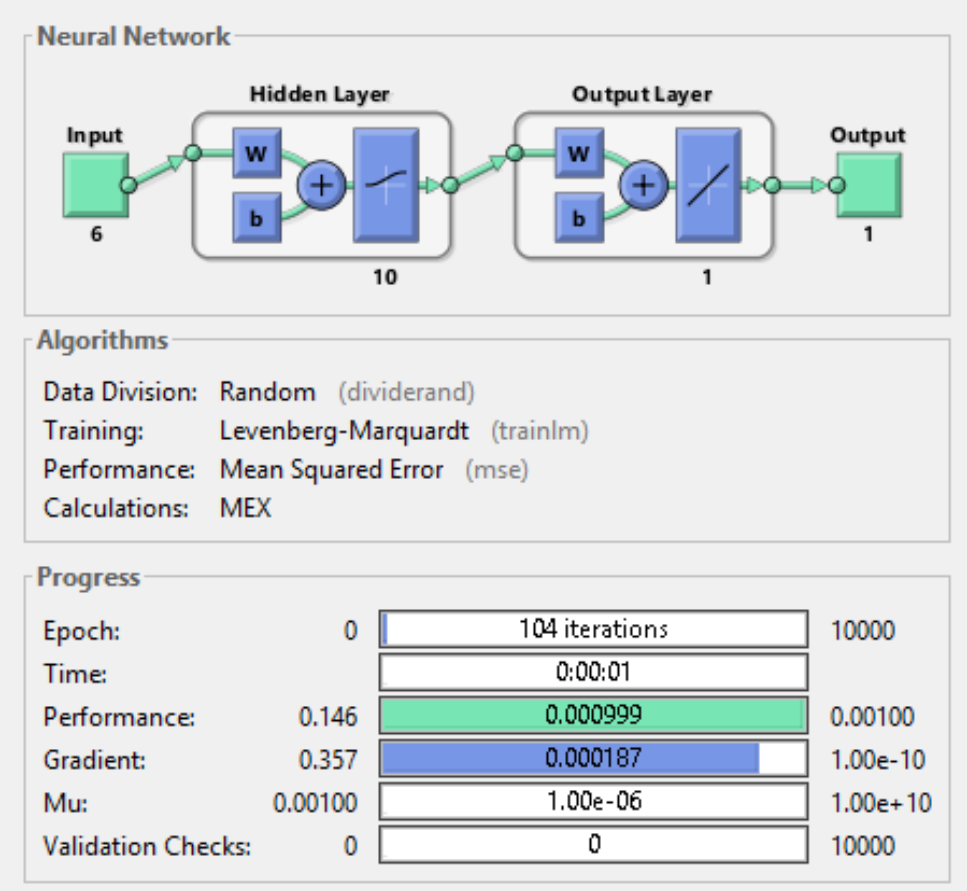

Figure 4.37: LL-G Fault Locating Network Design

Fig 4.38 shows the performance of the designed neural network after 104 epochs , and with an error of nearly 0.0010559.

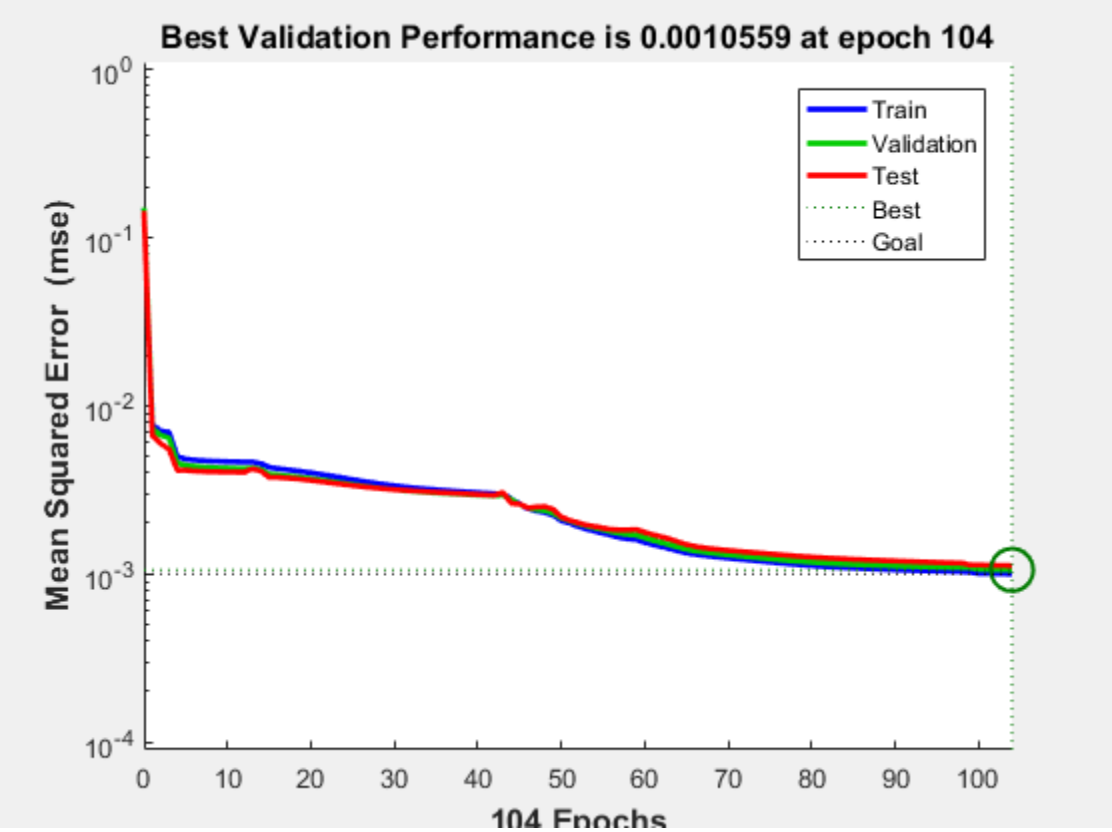

Figure 4.38: LL-G Fault Locating Network Performance

4.4.6 Three Phase Locating Neural Network

This network has been designed to determine line impedance between the measuring point and the fault location .It consists of an input layer of 6 neurons , two hidden layers of 4,8 neurons , and an output layer of a single neuron .Fig 4.39 shows the final shape of the network design with its training progress.

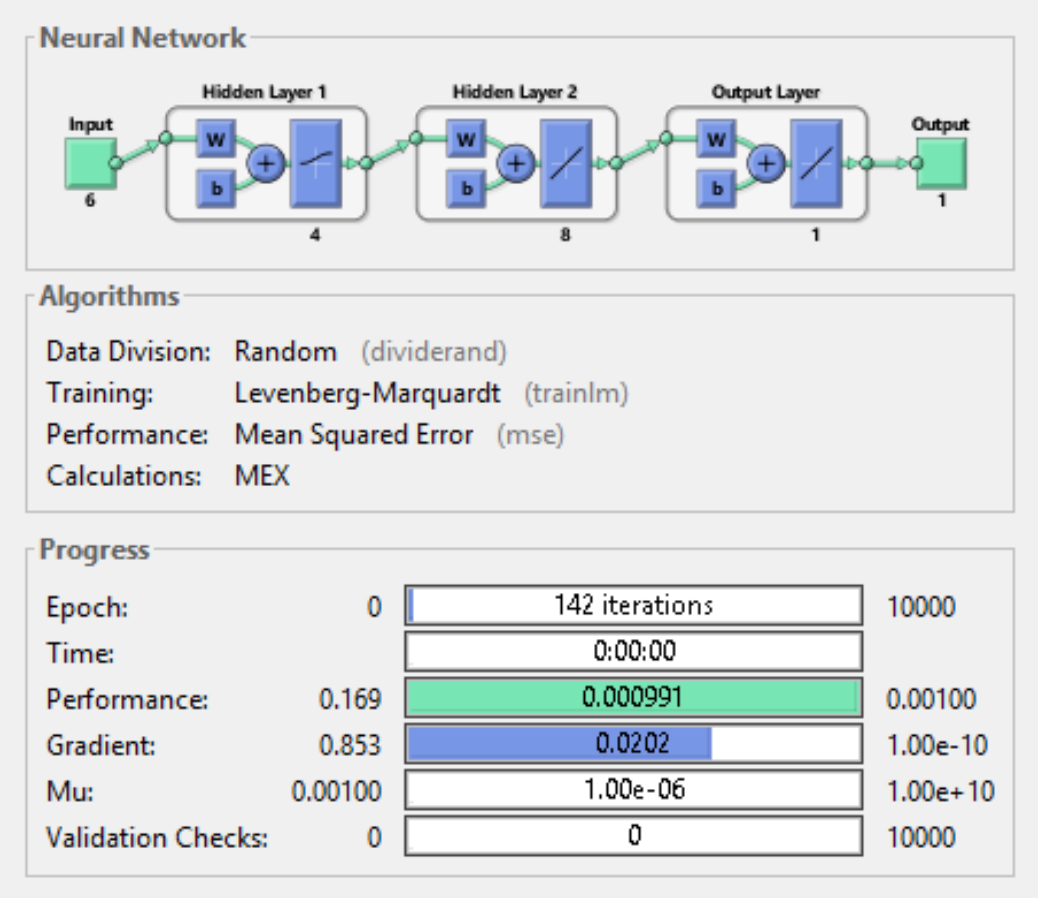

Figure 4.39: Three Phase Fault Locating Network Design

Fig 4.40 shows the performance of the designed neural network after 142 epochs , and with an error of nearly 0.0010302.

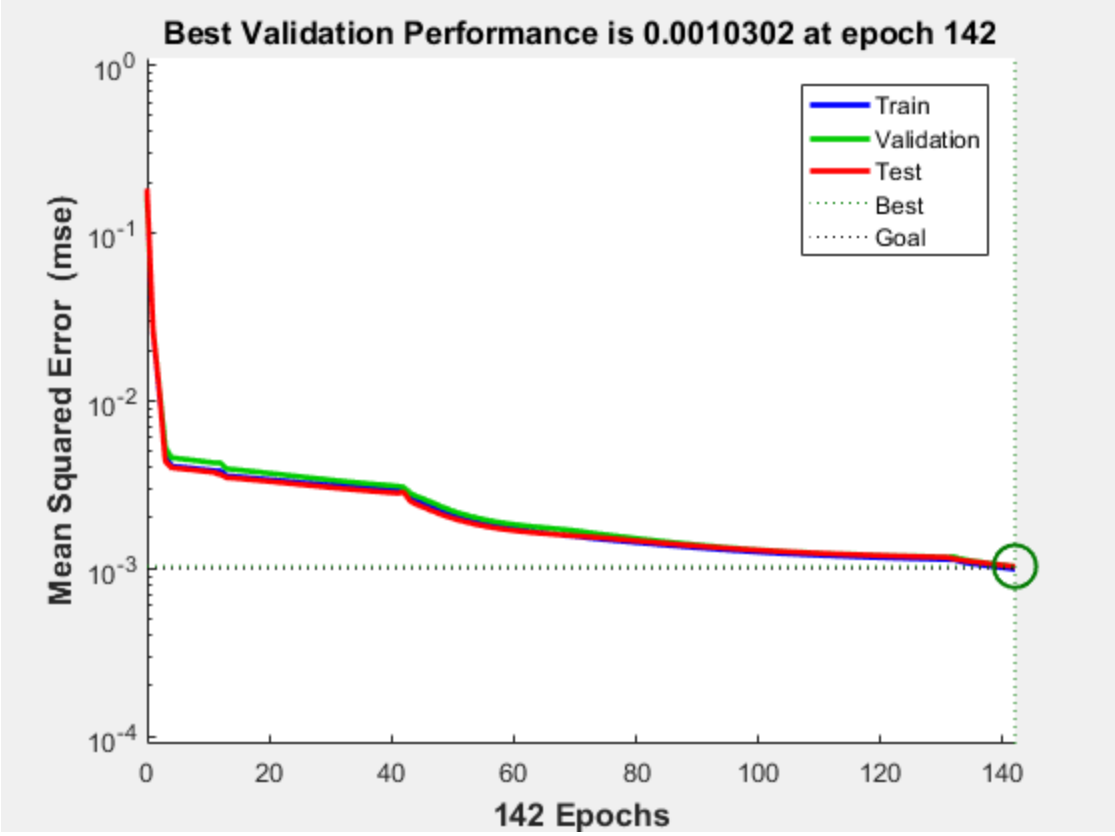

Figure 4.40: Three Phase Fault Locating Network Performance

5

Chapter Five Results And Analysis

5.1 Introduction

5.2 Ideal Data - Based Design Analysis

5.3 14 Bus System Based Design Analysis

Chapter Five
Results And Analysis

5.1 Introduction

This chapter contains results and analysis of both design scenarios , the ideal design and both 14 and 30-bus systems based design .

5.2 Ideal Design Analysis

As we have already mentioned in the previous chapter , this design is based on an ideal data that have been generated using Hadi Saadat's library in MATLAB

.

All neural networks of this system work perfectly efficient in a systems that have an ideal performance .Table 5.1 shows the results of testing the ideal fault locating neural network , with a maximum error of 0.03923 per meter. Fault detecting and classification ideal networks worked with zero error value .

Table 5.1: Ideal Locating Network Testing Sample (Ideal System).

$\boldsymbol{D_{act.}}$(m)	D_{ANN}(m)	$D_{act.} - D_{ANN}$
1500	1499.96	-0.03995
2000	2000.013	0.01293
500	499.9296	-0.07037
1000	1000.008	0.008187
28000	28000	-0.00474
28500	28500.01	0.013895
34500	34500.01	0.005064

Where ;

$\boldsymbol{D_{act.}}$ is the actual distance between the measuring point and fault location per meter .

$\boldsymbol{D_{ANN}}$ is the output of the ideal locating network per meter.

$\boldsymbol{D_{act.} - D_{ANN}}$ is the difference between the actual and predicted distances per meter.

The neural networks of this design (Ideal) have been tested in the IEEE 14-bus system in SIMULINK .The output data of this system is obviously not ideal . The detection network worked perfectly without errors , but classification and locating networks had a huge value of error. Table 5.2 shows a sample of testing data for the locating network in this system .

Table 5.2: Ideal Locating Network Testing Sample (14-Bus System)

$D_{act.}$(m)	$D_{act.} - D_{ANN}$
10000	2335258
20000	2308655
30000	2379413
90000	1219317
100000	1854439
80000	1229296

Where ;

$\boldsymbol{D_{act.}}$ is the actual distance between the measuring point and fault location per meter .

$\boldsymbol{D_{act.} - D_{ANN}}$ is the difference between the actual and predicted distances per meter.

5.3 14-Bus System and 30- Bus System Based Designs Analysis

These designs are based on data that have been generated using 14-bus system and 30-bus system in SIMULINK as it previously mentioned in chapter four .

Both detecting and classification networks of both designs work perfectly efficient in any system. The fault locating networks work quit efficient in systems that have the same lines specifications, which makes the locating system more suitable to be implemented in transmission systems than distribution systems .Table 5.3 shows the results of testing the fault classification neural network , on practical fault data of 33 kv line relates to HEPCO grid .

Table 5.3: 14-Bus System Classification Network Testing Sample.

F_c	V_{af}/V_{apf}	V_{bf}/V_{bpf}	V_{cf}/V_{cpf}	I_{af}/I_{apf}	I_{bf}/I_{bpf}	I_{cf}/I_{cpf}	A	B	C	G
BG	0.829091	0.268318	0.973273	0.672	5.69	1.308	0	1	0	1
BG	0.773727	0.278636	0.843818	0.868	5.896	0.796	0	1	0	1
AG	0.268318	0.829091	0.973273	5.69	0.672	1.308	1	0	0	1
AG	0.278636	0.773727	0.843818	5.896	0.868	0.796	1	0	0	1
No fault	1.087784	1.072887	1.041649	1.055556	0.913333	1.171111	0	0	0	0

Conclusion and Recommendations

In this project we have designed three different protection systems using artificial neural networks . The first one is based on data that have been generated using Hadi Saadat's library in MATLAB . The second design is based on a data that have been generated using SIMULINK ,IEEE 14-bus system standard . The third design is based on a data that have been generated also using SIMULINK ,IEEE 30-bus system standard .

Each design consists of several neural networks for fault detection , classification and locating . The first design detecting network has a mean squared error of (9.097e-6), classification network with mean squared error of (7.795e-5) and locating network with mean squared error of (4.90E-03). The second and the third designs detecting networks have a mean squared error of (1.54e-6)), classification networks with mean squared error of (9.415e-6) and locating networks with mean squared error of (8.73E-06).

We recommend any project group that is interested in ANN's field to design a module that can be implemented as a hardware ,developing locating networks to work in any power system, also to develop this project from a framework to a typical protection system design .

References

[1] Jiang Zhen, bao Zhong, and Tingjian Ye Mao, A fault location and realization method for overhead high voltage power transmission, Jiang Xi Vocational<Technical College Of Electricity ,Nanchang,330032,China.

[2] Pratik W. Choudhary, Saurabh S.Jadhao, Ravindra.K.Mankar, S.R.Parasakar, Classification of faults in power system using signal processing approach, Department of Electrical Engineering, SSGM,College Of Engineering Shegaon,India.

[3] Bon Nhan Nguyen, Anh Huy Quyen, Phuc Huu Nguyen and Trieu Ngoc Ton, Wavelet-based neural network for recognition of faults at NHABE power substation of the Vietnam power system, International Conference on System Science and Engineering (ICSSE),2017.

[4] Alfonso Q. Pérez Chanca, Manfred F. Bedriñana, Efficient processing of alarms avalanche using artificial neural networks and classification techniques, Power Systems Department National University of Engineering, UNI Lima, Peru.

[5] Gaganpreet Chawla, Mohinder S. Sachdev, G. Ramakrishna, Artificial neural network applications for power system protection. Power System Research Group, University of Saskatchewan 57 Campus Drive, Saskatoon, SK S7N 5A9 Canada.

[6] Ankita Nag and Anamika Yadav, Fault classification using artificial neural network in combined underground cable and overhead line, 1st IEEE International Conference on Power Electronics. Intelligent Control and Energy Systems (ICPEICES-2016).

[7] Uma Uzubi ,ArthurEkwue and Emenike Ejiogu, Artificial neural network technique for transmission line protection on Nigerian power system, IEEE PES-IAS Power Africa 2017.

[8] Edvard Csanyi, Utility reliability problems, http://electrical-engineering-portal.com/11-major-causes-of-power-system-failures.

[9] Hadi sadat , Power System Analysis, P S A Publishing,2010.

[10] Zwe-Lee Gaing, "Wavelet-Based Neural Network for Power Disturbance Recognition and Classification" iEEE Trans. Power Delivery, vol. 19, pp. IS60- I S68, Oct. 2004.

[11] L L Lai, N Rajkumar, "Wavelet Transform and Neural Networks for Fault Location of a Teed-network", IEEE International Conference on Power System Technology, POWERCON 2000, Perth, Western Australia, pp. 807-811,4-7 December, 2000.

[12] Vasilic and M. Kezunovic, "Fuzzy ART neural network algorithm for classifying the power system faults," IEEE transactions on Power Delivery, Vol. 20, No.1, 2005.

[13] Saha MM, Izykowski J, Rosolowski E, Fault Location on Power Networks, Springer publications, 2010.

[14] Magnago FH, Abur A, "Advanced techniques for transmission and distribution system fault location", Proceedings of CIGRE – Study committee 34 Colloquium and Meeting, Florence, 1999.

[15] D. Anguita, G. Parodi, and R. Zunino. Speed improvement of the backpropagation on current-generation workstations. In WCNN'93, Portland:World Congress on Neural Networks, July 11-15, 1993, Oregon ConventionCenter, Portland, Oregon, volume 1. Lawrence Erlbaum, 1993.

[16] K. Fukushima, S. Miyake, and T. Ito. Neocognitron: A neural networkmodel for a mechanism of visual pattern recognition. IEEE Transactionson Systems, Man, and Cybernetics, 13(5):826–834, September/October1983.

[17] W.S. McCulloch and W. Pitts. A logical calculus of the ideas immanent in nervous activity. Bulletin of Mathematical Biology.

[18] W. Pitts and W.S. McCulloch. How we know universals the perception of auditory and visual forms. Bulletin of Mathematical Biology.

[19] Donald O. Hebb. The Organization of Behavior: A Neuropsychological Theory. Wiley, New York, 1949.

[20] B. Widrow and M. E. Hoff. Adaptive switching circuits. In Proceedings WESCON.

[21] K. Steinbuch. Die lernmatrix. Kybernetik (Biological Cybernetics)..

[22] M. Minsky and S. Papert. Perceptrons. MIT Press, Cambridge, Mass,1969.

[23] T. Kohonen. Correlation matrix memories. IEEEtC.

[24] James A. Anderson. A simple neural network generating an interactive memory. Mathematical Biosciences..

[25] C. von der Malsburg. Self-organizing of orientation sensitive cells in striate cortex. Kybernetik.

[26] P. J. Werbos. Beyond Regression: New Tools for Prediction and Analysis in the Behavioral Sciences. PhD thesis, Harvard University, 1974.

[27] S. Grossberg. Adaptive pattern classification and universal recoding, I:Parallel development and coding of neural feature detectors. Biological Cybernetics.

[28] Teuvo Kohonen. Self-organized formation of topologically correct feature maps. Biological Cybernetics.

[29] T. Kohonen. The self-organizing map. Neurocomputing.

[30] John J. Hopfield. Neural networks and physical systems with emergent collective computational abilities. Proc. of the National Academy of Science, USA.

[31] K. Fukushima, S. Miyake, and T. Ito. Neocognitron: A neural network model for a mechanism of visual pattern recognition. IEEE Transactions on Systems, Man, and Cybernetics.

[32] D. Rumelhart, G. Hinton, and R. Williams. Learning representations by back-propagating errors. Nature, October 1986.

Appendix A1

```
Zdata= [0 1 0 0.15
        0 2 0 0.15
        1 2 0 0.3 ];

Zdata1=[0 1 0 0.15
        0 2 0 0.15
        1 2 0 0.5 ];

Zdata0=[0 1 0 0.5
        0 2 0 3.5
        1 2 0 0.3];
Zdata2=Zdata1;


block=500; % the total length is 300 Km .... block is 2000m
              % so we have 150 block
ndata=600;
Zf=0*i;
nf=2;

LLLFI=LLLFimat(Zdata, nf, Zf, ndata);
LLLFV=LLLFvmat(Zdata, nf, Zf, ndata);
LLFI=LLFimat(Zdata1, Zdata2, nf, Zf, ndata);
LLFV=LLFvmat(Zdata1, Zdata2, nf, Zf, ndata);
LLGFI=DLGFimat(Zdata0, Zdata1, Zdata2, nf, Zf, ndata);
LLGFV=DLGFvmat(Zdata0, Zdata1, Zdata2, nf, Zf, ndata);
LGFI=LGFimat(Zdata0, Zdata1, Zdata2, nf, Zf, ndata);
LGFV=LGFvmat(Zdata0, Zdata1, Zdata2, nf, Zf, ndata);

AG=[1,0,0,1];
BG=[0,1,0,1];
CG=[0,0,1,1];
AB=[1,1,0,0];
BC=[0,1,1,0];
CA=[1,0,1,0];
ABG=[1,1,0,1];
BCG=[0,1,1,1];
CAG=[1,0,1,1];
ABC=[1,1,1,1];

I0=1;
V0=I0;
 loop=1;
 Tloop=1;
while Tloop<=ndata*3;
 % No Fault Case*************************
   NFC=rand(1,6);
   NFC=NFC/10;
   NFC=NFC+0.95;
   NFC(:, 7:10)=0;
   TrainingData(Tloop, 1:6)=NFC(:, 1:6);
   TrainingData(Tloop, 8)= 0;
  Tloop=Tloop+1;

 % three phase fault*********************
```

```
    ABCCR(loop, 1) =abs(LLLFI(loop, 1))/I0;
    ABCCR(loop, 2) =abs(LLLFI(loop, 1))/I0;
    ABCCR(loop, 3) =abs(LLLFI(loop, 1))/I0;
    ABCVR(loop, 1) =abs(LLLFV(loop, 1))/V0;
    ABCVR(loop, 2) =abs(LLLFV(loop, 1))/V0;
    ABCVR(loop, 3) =abs(LLLFV(loop, 1))/V0;
    TrainingData(Tloop, 1)= ABCCR(loop, 1);
    TrainingData(Tloop, 2)= ABCCR(loop, 2);
    TrainingData(Tloop, 3)= ABCCR(loop, 3);
    TrainingData(Tloop, 4)= ABCVR(loop, 1);
    TrainingData(Tloop, 5)= ABCVR(loop, 2);
    TrainingData(Tloop, 6)= ABCVR(loop, 3);
    TrainingData(Tloop, 8)= block;
    TrainingData(Tloop, 7)= ABC(1, 1);
    TrainingData(Tloop, 8)= ABC(1, 2);
    TrainingData(Tloop, 9)= ABC(1, 3);
    TrainingData(Tloop, 10)=ABC(1, 4);
    Tloop=Tloop+1;
%   % A to B current fault******************
    ABCR(loop, 1) =abs(LLFI(loop, 3))/I0;
    ABCR(loop, 2) =abs(LLFI(loop, 2))/I0;
    ABCR(loop, 3) =abs(LLFI(loop, 1))/I0;
 % A to B voltage fault
    ABVR(loop, 1) =abs(LLFV(loop, 3))/V0;
    ABVR(loop, 2) =abs(LLFV(loop, 2))/V0;
    ABVR(loop, 3) =abs(LLFV(loop, 1))/V0;
    ABout(loop, 1)=AB(1, 1);
     ABout(loop, 2)=AB(1, 2);
      ABout(loop, 3)=AB(1, 3);
       ABout(loop, 4)=AB(1, 4);

    TrainingData(Tloop, 1)= ABCR(loop, 1);
    TrainingData(Tloop, 2)= ABCR(loop, 2);
    TrainingData(Tloop, 3)= ABCR(loop, 3);
    TrainingData(Tloop, 4)= ABVR(loop, 1);
    TrainingData(Tloop, 5)= ABVR(loop, 2);
    TrainingData(Tloop, 6)= ABVR(loop, 3);
%     TrainingData(Tloop, 8)= block;
    TrainingData(Tloop, 7)= AB(1, 1);
    TrainingData(Tloop, 8)= AB(1, 2);
    TrainingData(Tloop, 9)= AB(1, 3);
    TrainingData(Tloop, 10)=AB(1, 4);
    Tloop=Tloop+1;
%   % B to C current fault******************
    BCCR(loop, 1) =abs(LLFI(loop, 1))/I0;
    BCCR(loop, 2) =abs(LLFI(loop, 2))/I0;
    BCCR(loop, 3) =abs(LLFI(loop, 3))/I0;
%   % B to C voltage fault
    BCVR(loop, 1) =abs(LLFV(loop, 1))/V0;
    BCVR(loop, 2) =abs(LLFV(loop, 2))/V0;
    BCVR(loop, 3) =abs(LLFV(loop, 3))/V0;
    BCout(loop, 1)=BC(1, 1);
     BCout(loop, 2)=BC(1, 2);
      BCout(loop, 3)=BC(1, 3);
       BCout(loop, 4)=BC(1, 4);
    TrainingData(Tloop, 1)= BCCR(loop, 1);
    TrainingData(Tloop, 2)= BCCR(loop, 2);
```

```
    TrainingData(Tloop, 3)= BCCR(loop, 3);
    TrainingData(Tloop, 4)= BCVR(loop, 1);
    TrainingData(Tloop, 5)= BCVR(loop, 2);
    TrainingData(Tloop, 6)= BCVR(loop, 3);
    TrainingData(Tloop, 8)= block;
    TrainingData(Tloop, 7)= BC(1, 1);
    TrainingData(Tloop, 8)= BC(1, 2);
    TrainingData(Tloop, 9)= BC(1, 3);
    TrainingData(Tloop, 10)=BC(1, 4);
    Tloop=Tloop+1;
% %  % C to A current fault******************
    CACR(loop, 1) =abs(LLFI(loop, 2))/I0;
    CACR(loop, 2) =abs(LLFI(loop, 1))/I0;
    CACR(loop, 3) =abs(LLFI(loop, 3))/I0;
 % C to A voltage fault
    CAVR(loop, 1) =abs(LLFV(loop, 2))/V0;
    CAVR(loop, 2) =abs(LLFV(loop, 1))/V0;
    CAVR(loop, 3) =abs(LLFV(loop, 3))/V0;
    CAout(loop, 1)=CA(1, 1);
     CAout(loop, 2)=CA(1, 2);
      CAout(loop, 3)=CA(1, 3);
       CAout(loop, 4)=CA(1, 4);
    TrainingData(Tloop, 1)= CACR(loop, 1);
    TrainingData(Tloop, 2)= CACR(loop, 2);
    TrainingData(Tloop, 3)= CACR(loop, 3);
    TrainingData(Tloop, 4)= CAVR(loop, 1);
    TrainingData(Tloop, 5)= CAVR(loop, 2);
    TrainingData(Tloop, 6)= CAVR(loop, 3);
    TrainingData(Tloop, 8)= block;
    TrainingData(Tloop, 7)= CA(1, 1);
    TrainingData(Tloop, 8)= CA(1, 2);
    TrainingData(Tloop, 9)= CA(1, 3);
    TrainingData(Tloop, 10)=CA(1, 4);
    Tloop=Tloop+1;
%  % AB to G current fault******************
    ABGCR(loop, 1) =abs(LLGFI(loop, 3))/I0
    ABGCR(loop, 2) =abs(LLGFI(loop, 2))/I0
    ABGCR(loop, 3) =abs(LLGFI(loop, 1))/I0
% AB to G voltage fault;
    ABGVR(loop, 1) =abs(LLGFV(loop, 3))/V0
    ABGVR(loop, 2) =abs(LLGFV(loop, 2))/V0
    ABGVR(loop, 3) =abs(LLGFV(loop, 1))/V0
    ABGout(loop, 1)=ABG(1, 1);
     ABGout(loop, 2)=ABG(1, 2);
      ABGout(loop, 3)=ABG(1, 3);
       ABGout(loop, 4)=ABG(1, 4);
    TrainingData(Tloop, 1)= ABGCR(loop, 1);
    TrainingData(Tloop, 2)= ABGCR(loop, 2);
    TrainingData(Tloop, 3)= ABGCR(loop, 3);
    TrainingData(Tloop, 4)= ABGVR(loop, 1);
    TrainingData(Tloop, 5)= ABGVR(loop, 2);
    TrainingData(Tloop, 6)= ABGVR(loop, 3);
    TrainingData(Tloop, 8)= block;
    TrainingData(Tloop, 7)= ABG(1, 1);
    TrainingData(Tloop, 8)= ABG(1, 2);
    TrainingData(Tloop, 9)= ABG(1, 3);
    TrainingData(Tloop, 10)=ABG(1, 4);
```

```
    Tloop=Tloop+1;
% %  % BC to G current fault*******************
    BCGCR(loop, 1) =abs(LLGFI(loop, 1))/I0
    BCGCR(loop, 2) =abs(LLGFI(loop, 2))/I0
    BCGCR(loop, 3) =abs(LLGFI(loop, 3))/I0
 % BC to G voltage fault
    BCGVR(loop, 1) =abs(LLGFV(loop, 1))/V0
    BCGVR(loop, 2) =abs(LLGFV(loop, 2))/V0
    BCGVR(loop, 3) =abs(LLGFV(loop, 3))/V0
    BCGout(loop, 1)=BCG(1, 1);
     BCGout(loop, 2)=BCG(1, 2);
      BCGout(loop, 3)=BCG(1, 3);
       BCGout(loop, 4)=BCG(1, 4);
    TrainingData(Tloop, 1)= BCGCR(loop, 1);
    TrainingData(Tloop, 2)= BCGCR(loop, 2);
    TrainingData(Tloop, 3)= BCGCR(loop, 3);
    TrainingData(Tloop, 4)= BCGVR(loop, 1);
    TrainingData(Tloop, 5)= BCGVR(loop, 2);
    TrainingData(Tloop, 6)= BCGVR(loop, 3);
    TrainingData(Tloop, 8)= block;
    TrainingData(Tloop, 7)= BCG(1, 1);
    TrainingData(Tloop, 8)= BCG(1, 2);
    TrainingData(Tloop, 9)= BCG(1, 3);
    TrainingData(Tloop, 10)=BCG(1, 4);
    Tloop=Tloop+1;
% %  % CA to G current fault*********************
    CAGCR(loop, 1) =abs(LLGFI(loop, 2))/I0
    CAGCR(loop, 2) =abs(LLGFI(loop, 1))/I0
    CAGCR(loop, 3) =abs(LLGFI(loop, 3))/I0
 % CA to G voltage Fault
    CAGVR(loop, 1) =abs(LLGFV(loop, 2))/V0
    CAGVR(loop, 2) =abs(LLGFV(loop, 1))/V0
    CAGVR(loop, 3) =abs(LLGFV(loop, 3))/V0
    CAGout(loop, 1)=CAG(1, 1);
     CAGout(loop, 2)=CAG(1, 2);
      CAGout(loop, 3)=CAG(1, 3);
       CAGout(loop, 4)=CAG(1, 4);
    TrainingData(Tloop, 1)= CAGCR(loop, 1);
    TrainingData(Tloop, 2)= CAGCR(loop, 2);
    TrainingData(Tloop, 3)= CAGCR(loop, 3);
    TrainingData(Tloop, 4)= CAGVR(loop, 1);
    TrainingData(Tloop, 5)= CAGVR(loop, 2);
    TrainingData(Tloop, 6)= CAGVR(loop, 3);
    TrainingData(Tloop, 8)= block;
    TrainingData(Tloop, 7)= CAG(1, 1);
    TrainingData(Tloop, 8)= CAG(1, 2);
    TrainingData(Tloop, 9)= CAG(1, 3);
    TrainingData(Tloop, 10)=CAG(1, 4);
    Tloop=Tloop+1;
%  % A to G current fault**********************
    AGCR(loop, 1) = abs(LGFI(loop, 1))/I0
    AGCR(loop, 2) = abs(LGFI(loop, 2))/I0
    AGCR(loop, 3) = abs(LGFI(loop, 3))/I0
 % A to G voltage fault
    AGVR(loop, 1) = abs(LGFV(loop, 1))/V0
    AGVR(loop, 2) = abs(LGFV(loop, 2))/V0
    AGVR(loop, 3) = abs(LGFV(loop, 3))/V0
```

```
    AGout(loop, 1)=AG(1, 1);
     AGout(loop, 2)=AG(1, 2);
      AGout(loop, 3)=AG(1, 3);
       AGout(loop, 4)=AG(1, 4);
    TrainingData(Tloop, 1)= AGCR(loop, 1);
    TrainingData(Tloop, 2)= AGCR(loop, 2);
    TrainingData(Tloop, 3)= AGCR(loop, 3);
    TrainingData(Tloop, 4)= AGVR(loop, 1);
    TrainingData(Tloop, 5)= AGVR(loop, 2);
    TrainingData(Tloop, 6)= AGVR(loop, 3);
      TrainingData(Tloop, 8)= block;
    TrainingData(Tloop, 7)= AG(1, 1);
    TrainingData(Tloop, 8)= AG(1, 2);
    TrainingData(Tloop, 9)= AG(1, 3);
    TrainingData(Tloop, 10)=AG(1, 4);
      Tloop=Tloop+1;
%  % B to G cuurent fault**********************
    BGCR(loop, 1) = abs(LGFI(loop, 2))/I0
    BGCR(loop, 2) = abs(LGFI(loop, 1))/I0
    BGCR(loop, 3) = abs(LGFI(loop, 3))/I0
 % B to G voltage fault
    BGVR(loop, 1) = abs(LGFV(loop, 2))/V0
    BGVR(loop, 2) = abs(LGFV(loop, 1))/V0
    BGVR(loop, 3) = abs(LGFV(loop, 3))/V0
    BGout(loop, 1)=BG(1, 1);
     BGout(loop, 2)=BG(1, 2);
      BGout(loop, 3)=BG(1, 3);
       BGout(loop, 4)=BG(1, 4);
    TrainingData(Tloop, 1)= BGCR(loop, 1);
    TrainingData(Tloop, 2)= BGCR(loop, 2);
    TrainingData(Tloop, 3)= BGCR(loop, 3);
    TrainingData(Tloop, 4)= BGVR(loop, 1);
    TrainingData(Tloop, 5)= BGVR(loop, 2);
    TrainingData(Tloop, 6)= BGVR(loop, 3);
    TrainingData(Tloop, 8)= block;
    TrainingData(Tloop, 7)= BG(1, 1);
    TrainingData(Tloop, 8)= BG(1, 2);
    TrainingData(Tloop, 9)= BG(1, 3);
    TrainingData(Tloop, 10)=BG(1, 4);
    Tloop=Tloop+1;
% % C to G current fault**********************
    CGCR(loop, 1) = abs(LGFI(loop, 3))/I0
    CGCR(loop, 2) = abs(LGFI(loop, 2))/I0
    CGCR(loop, 3) = abs(LGFI(loop, 1))/I0
 % c to G voltage fault
    CGVR(loop, 1) = abs(LGFV(loop, 3))/V0
    CGVR(loop, 2) = abs(LGFV(loop, 2))/V0
    CGVR(loop, 3) = abs(LGFV(loop, 1))/V0
    CGout(loop, 1)=CG(1, 1);
     CGout(loop, 2)=CG(1, 2);
      CGout(loop, 3)=CG(1, 3);
       CGout(loop, 4)=CG(1, 4);
    TrainingData(Tloop, 1)= CGCR(loop, 1);
    TrainingData(Tloop, 2)= CGCR(loop, 2);
    TrainingData(Tloop, 3)= CGCR(loop, 3);
    TrainingData(Tloop, 4)= CGVR(loop, 1);
    TrainingData(Tloop, 5)= CGVR(loop, 2);
```

```
    TrainingData(Tloop, 6)= CGVR(loop, 3);
    TrainingData(Tloop, 8)= block;
    TrainingData(Tloop, 7)= CG(1, 1);
    TrainingData(Tloop, 8)= CG(1, 2);
    TrainingData(Tloop, 9)= CG(1, 3);
    TrainingData(Tloop, 10)=CG(1, 4);
      Tloop = Tloop+1;
         loop=loop+1;
      block = block + 500;
end
```

==========

```
net = newff(input',out', [20], { 'logsig','purelin'},'trainlm',
'learngdm','mse');
 % Define learning parameters
 net.trainParam.epochs=10000;   % Maximum number of epochs to train   ,
Training stops when the condition occu
 net.trainParam.goal = 0.001; %Performance goal ,Training stops when the
condition occu
net.trainParam.lr=0.2;%Learning rate
net.trainParam.mc=0.6;%Momentum constant
net.trainParam.lr_inc=1.05; %Ratio to increase learning rate
net.trainParam.lr_dec=0.7; %       Ratio to decrease learning rate%
net.trainParam.max_fail=10000;  %Maximum validation failures   ,Training
stops when the condition occur
net.trainParam.max_perf_inc=1.04; %  Maximum performance increase%
net.trainParam.min_grad=1e-10; %Minimum performance gradient
,Training stops when the condition occur
 net.trainParam.show=300;  %Epochs between displays (NaN for no displays)
 net.trainParam.time=inf;%Maximum time to train in seconds
,Training stops when the condition occur

     net = train(net,input',out');


%%
predictedtesting1 = sim(net,TrainingData(:,1:6)');
predictedtesting1'-TrainingData(:,7:10);
prof=round(ans,0);
```

```
position=1;
loopA=1;
loopB=1;
loopC=1;

while position<=1200;

    if sellect(position,1) >= 3.55%&& sellect(position,1) <= 1.1;
    sellected(loopA,1)=sellect(position,1);
   % sellected(loopA,4)=current(position,4);
    loopA=loopA+1;
    end
    if sellect(position,2) >0.655%&& sellect(position,2) <= 1.2;
    sellected(loopB,2)=sellect(position,2);
   % sellected(loopB,5)=current(position,5);
    loopB=loopB+1;
    end
    if sellect(position,3) >= 0.93 && sellect(position,3) <= 1.1;
    sellected(loopC,3)=sellect(position,3);
   % sellected(loopC,6)=current(position,6);

    loopC=loopC+1;
    end
    position=position+1;
end
```

Appendix A2

V_{aF}/V_{aPF}	V_{bf}/V_{bPF}	V_{cF}/V_{cPF}	I_{aF}/I_{aPF}	I_{bF}/I_{aPF}	V_{cF}/V_{cPF}	A	B	C	G
1.022328	0.966319	1.005561	1.006895	0.99606	0.999325	0	0	0	0
0.643424	0.643424	3.154969	1.411734	1.411734	2.78E-17	0	0	1	1
5.769134	5.769134	0.398431	1.14E-16	2.24E-16	1.380765	1	1	0	1
0.398431	5.769134	5.769134	1.380765	2.24E-16	1.14E-16	0	1	1	1
5.769134	0.398431	5.769134	2.24E-16	1.380765	1.14E-16	1	0	1	1
3.154969	0.643424	0.643424	2.78E-17	1.411734	1.411734	1	0	0	1
0.643424	3.154969	0.643424	1.411734	2.78E-17	1.411734	0	1	0	1
0.643424	0.643424	3.154969	1.411734	1.411734	2.78E-17	0	0	1	1
1.037286	0.967722	0.978338	1.016259	0.980691	1.038828	0	0	0	0
166.6667	166.6667	166.6667	0.025974	0.025974	0.025974	1	1	1	1
5.649879	5.649879	0.401979	1.14E-16	2.24E-16	1.379984	1	1	0	1
0.401979	5.649879	5.649879	1.379984	2.24E-16	1.14E-16	0	1	1	1
5.649879	0.401979	5.649879	2.24E-16	1.379984	1.14E-16	1	0	1	1
3.11944	0.648337	0.648337	8.33E-17	1.410127	1.410127	1	0	0	1
0.648337	3.11944	0.648337	1.410127	8.33E-17	1.410127	0	1	0	1
0.648337	0.648337	3.11944	1.410127	1.410127	8.33E-17	0	0	1	1
1.005383	1.00266	1.006918	1.036083	0.9728	1.003457	0	0	0	0
5.535603	5.535603	0.405388	1.76E-16	1.76E-16	1.379233	1	1	0	1
0.405388	5.535603	5.535603	1.379233	1.76E-16	1.76E-16	0	1	1	1
5.535603	0.405388	5.535603	1.76E-16	1.379233	1.76E-16	1	0	1	1
3.084859	0.653044	0.653044	1.67E-16	1.408588	1.408588	1	0	0	1
0.653044	3.084859	0.653044	1.408588	1.67E-16	1.408588	0	1	0	1
0.653044	0.653044	3.084859	1.408588	1.408588	1.67E-16	0	0	1	1
0.962251	0.99342	1.008345	0.952194	0.998281	1.045761	0	0	0	0
5.426	5.426	0.408663	1.57E-16	1.57E-16	1.378511	1	1	0	1
0.408663	5.426	5.426	1.378511	1.57E-16	1.57E-16	0	1	1	1
5.426	0.408663	5.426	1.57E-16	1.378511	1.57E-16	1	0	1	1
3.051189	0.657555	0.657555	8.33E-17	1.407114	1.407114	1	0	0	1
0.657555	3.051189	0.657555	1.407114	8.33E-17	1.407114	0	1	0	1
0.657555	0.657555	3.051189	1.407114	1.407114	8.33E-17	0	0	1	1
0.997496	0.964598	1.030931	0.965395	1.0047	1.041865	0	0	0	0
83.33333	83.33333	83.33333	0.0625	0.0625	0.0625	1	1	1	1
5.320789	5.320789	0.411809	2.00E-16	2.00E-16	1.377818	1	1	0	1
0.411809	5.320789	5.320789	1.377818	2.00E-16	2.00E-16	0	1	1	1
5.320789	0.411809	5.320789	2.00E-16	1.377818	2.00E-16	1	0	1	1
3.018392	0.661878	0.661878	1.94E-16	1.405702	1.405702	1	0	0	1
0.661878	3.018392	0.661878	1.405702	1.94E-16	1.405702	0	1	0	1
0.661878	0.661878	3.018392	1.405702	1.405702	1.94E-16	0	0	1	1
1.046965	1.019028	1.031159	1.030919	0.979311	1.048177	0	0	0	0

71.42857	71.42857	71.42857	0.074074	0.074074	0.074074	1	1	1	1
5.21971	5.21971	0.41483	1.67E-16	1.67E-16	1.377153	1	1	0	1
0.41483	5.21971	5.21971	1.377153	1.67E-16	1.67E-16	0	1	1	1
5.21971	0.41483	5.21971	1.67E-16	1.377153	1.67E-16	1	0	1	1
2.986433	0.666022	0.666022	5.55E-17	1.404349	1.404349	1	0	0	1
0.666022	2.986433	0.666022	1.404349	5.55E-17	1.404349	0	1	0	1
0.666022	0.666022	2.986433	1.404349	1.404349	5.55E-17	0	0	1	1
1.032458	0.984751	0.970936	0.971546	0.980985	0.954548	0	0	0	0
5.122525	5.122525	0.417732	1.39E-16	1.86E-16	1.376513	1	1	0	1
0.417732	5.122525	5.122525	1.376513	1.86E-16	1.39E-16	0	1	1	1
5.122525	0.417732	5.122525	1.86E-16	1.376513	1.39E-16	1	0	1	1
2.955279	0.669994	0.669994	8.33E-17	1.403054	1.403054	1	0	0	1
0.669994	2.955279	0.669994	1.403054	8.33E-17	1.403054	0	1	0	1
0.669994	0.669994	2.955279	1.403054	1.403054	8.33E-17	0	0	1	1
1.00426	1.001388	1.037549	0.969815	0.986501	0.986422	0	0	0	0
55.55556	55.55556	55.55556	0.096386	0.096386	0.096386	1	1	1	1
5.029014	5.029014	0.42052	1.76E-16	1.76E-16	1.375899	1	1	0	1
0.42052	5.029014	5.029014	1.375899	1.76E-16	1.76E-16	0	1	1	1
5.029014	0.42052	5.029014	1.76E-16	1.375899	1.76E-16	1	0	1	1
2.9249	0.673802	0.673802	8.33E-17	1.401813	1.401813	1	0	0	1
0.673802	2.9249	0.673802	1.401813	8.33E-17	1.401813	0	1	0	1
0.673802	0.673802	2.9249	1.401813	1.401813	8.33E-17	0	0	1	1
0.973799	0.979138	1.001104	1.002199	1.004409	0.985121	0	0	0	0
1.022328	0.966319	1.005561	1.006895	0.99606	0.999325	0	0	0	0
0.643424	0.643424	3.154969	1.411734	1.411734	2.78E-17	0	0	1	1
5.769134	5.769134	0.398431	1.14E-16	2.24E-16	1.380765	1	1	0	1
0.398431	5.769134	5.769134	1.380765	2.24E-16	1.14E-16	0	1	1	1
5.769134	0.398431	5.769134	2.24E-16	1.380765	1.14E-16	1	0	1	1
3.154969	0.643424	0.643424	2.78E-17	1.411734	1.411734	1	0	0	1
0.643424	3.154969	0.643424	1.411734	2.78E-17	1.411734	0	1	0	1
0.643424	0.643424	3.154969	1.411734	1.411734	2.78E-17	0	0	1	1
1.037286	0.967722	0.978338	1.016259	0.980691	1.038828	0	0	0	0
166.6667	166.6667	166.6667	0.025974	0.025974	0.025974	1	1	1	1
5.649879	5.649879	0.401979	1.14E-16	2.24E-16	1.379984	1	1	0	1
0.401979	5.649879	5.649879	1.379984	2.24E-16	1.14E-16	0	1	1	1
5.649879	0.401979	5.649879	2.24E-16	1.379984	1.14E-16	1	0	1	1
3.11944	0.648337	0.648337	8.33E-17	1.410127	1.410127	1	0	0	1
0.648337	3.11944	0.648337	1.410127	8.33E-17	1.410127	0	1	0	1
0.648337	0.648337	3.11944	1.410127	1.410127	8.33E-17	0	0	1	1
1.005383	1.00266	1.006918	1.036083	0.9728	1.003457	0	0	0	0
5.535603	5.535603	0.405388	1.76E-16	1.76E-16	1.379233	1	1	0	1

0.405388	5.535603	5.535603	1.379233	1.76E-16	1.76E-16	0	1	1	1
5.535603	0.405388	5.535603	1.76E-16	1.379233	1.76E-16	1	0	1	1
3.084859	0.653044	0.653044	1.67E-16	1.408588	1.408588	1	0	0	1
0.653044	3.084859	0.653044	1.408588	1.67E-16	1.408588	0	1	0	1
0.653044	0.653044	3.084859	1.408588	1.408588	1.67E-16	0	0	1	1
0.962251	0.99342	1.008345	0.952194	0.998281	1.045761	0	0	0	0
5.426	5.426	0.408663	1.57E-16	1.57E-16	1.378511	1	1	0	1
0.408663	5.426	5.426	1.378511	1.57E-16	1.57E-16	0	1	1	1
5.426	0.408663	5.426	1.57E-16	1.378511	1.57E-16	1	0	1	1
3.051189	0.657555	0.657555	8.33E-17	1.407114	1.407114	1	0	0	1
0.657555	3.051189	0.657555	1.407114	8.33E-17	1.407114	0	1	0	1
0.657555	0.657555	3.051189	1.407114	1.407114	8.33E-17	0	0	1	1
0.997496	0.964598	1.030931	0.965395	1.0047	1.041865	0	0	0	0
83.33333	83.33333	83.33333	0.0625	0.0625	0.0625	1	1	1	1
5.320789	5.320789	0.411809	2.00E-16	2.00E-16	1.377818	1	1	0	1
0.411809	5.320789	5.320789	1.377818	2.00E-16	2.00E-16	0	1	1	1
5.320789	0.411809	5.320789	2.00E-16	1.377818	2.00E-16	1	0	1	1
3.018392	0.661878	0.661878	1.94E-16	1.405702	1.405702	1	0	0	1
0.661878	3.018392	0.661878	1.405702	1.94E-16	1.405702	0	1	0	1
0.661878	0.661878	3.018392	1.405702	1.405702	1.94E-16	0	0	1	1
1.046965	1.019028	1.031159	1.030919	0.979311	1.048177	0	0	0	0
71.42857	71.42857	71.42857	0.074074	0.074074	0.074074	1	1	1	1
5.21971	5.21971	0.41483	1.67E-16	1.67E-16	1.377153	1	1	0	1
0.41483	5.21971	5.21971	1.377153	1.67E-16	1.67E-16	0	1	1	1
5.21971	0.41483	5.21971	1.67E-16	1.377153	1.67E-16	1	0	1	1
2.986433	0.666022	0.666022	5.55E-17	1.404349	1.404349	1	0	0	1
0.666022	2.986433	0.666022	1.404349	5.55E-17	1.404349	0	1	0	1
0.666022	0.666022	2.986433	1.404349	1.404349	5.55E-17	0	0	1	1
1.032458	0.984751	0.970936	0.971546	0.980985	0.954548	0	0	0	0
5.122525	5.122525	0.417732	1.39E-16	1.86E-16	1.376513	1	1	0	1
0.417732	5.122525	5.122525	1.376513	1.86E-16	1.39E-16	0	1	1	1
5.122525	0.417732	5.122525	1.86E-16	1.376513	1.39E-16	1	0	1	1
2.955279	0.669994	0.669994	8.33E-17	1.403054	1.403054	1	0	0	1
0.669994	2.955279	0.669994	1.403054	8.33E-17	1.403054	0	1	0	1
0.669994	0.669994	2.955279	1.403054	1.403054	8.33E-17	0	0	1	1
1.00426	1.001388	1.037549	0.969815	0.986501	0.986422	0	0	0	0
55.55556	55.55556	55.55556	0.096386	0.096386	0.096386	1	1	1	1
5.029014	5.029014	0.42052	1.76E-16	1.76E-16	1.375899	1	1	0	1
0.42052	5.029014	5.029014	1.375899	1.76E-16	1.76E-16	0	1	1	1
5.029014	0.42052	5.029014	1.76E-16	1.375899	1.76E-16	1	0	1	1
2.9249	0.673802	0.673802	8.33E-17	1.401813	1.401813	1	0	0	1

0.673802	2.9249	0.673802	1.401813	8.33E-17	1.401813	0	1	0	1
0.673802	0.673802	2.9249	1.401813	1.401813	8.33E-17	0	0	1	1
0.973799	0.979138	1.001104	1.002199	1.004409	0.985121	0	0	0	0
1.022328	0.966319	1.005561	1.006895	0.99606	0.999325	0	0	0	0
0.643424	0.643424	3.154969	1.411734	1.411734	2.78E-17	0	0	1	1
5.769134	5.769134	0.398431	1.14E-16	2.24E-16	1.380765	1	1	0	1
0.398431	5.769134	5.769134	1.380765	2.24E-16	1.14E-16	0	1	1	1
5.769134	0.398431	5.769134	2.24E-16	1.380765	1.14E-16	1	0	1	1
3.154969	0.643424	0.643424	2.78E-17	1.411734	1.411734	1	0	0	1
0.643424	3.154969	0.643424	1.411734	2.78E-17	1.411734	0	1	0	1
0.643424	0.643424	3.154969	1.411734	1.411734	2.78E-17	0	0	1	1
1.037286	0.967722	0.978338	1.016259	0.980691	1.038828	0	0	0	0
166.6667	166.6667	166.6667	0.025974	0.025974	0.025974	1	1	1	1
5.649879	5.649879	0.401979	1.14E-16	2.24E-16	1.379984	1	1	0	1
0.401979	5.649879	5.649879	1.379984	2.24E-16	1.14E-16	0	1	1	1
5.649879	0.401979	5.649879	2.24E-16	1.379984	1.14E-16	1	0	1	1
3.11944	0.648337	0.648337	8.33E-17	1.410127	1.410127	1	0	0	1
0.648337	3.11944	0.648337	1.410127	8.33E-17	1.410127	0	1	0	1
0.648337	0.648337	3.11944	1.410127	1.410127	8.33E-17	0	0	1	1
1.005383	1.00266	1.006918	1.036083	0.9728	1.003457	0	0	0	0
5.535603	5.535603	0.405388	1.76E-16	1.76E-16	1.379233	1	1	0	1
0.405388	5.535603	5.535603	1.379233	1.76E-16	1.76E-16	0	1	1	1
5.535603	0.405388	5.535603	1.76E-16	1.379233	1.76E-16	1	0	1	1
3.084859	0.653044	0.653044	1.67E-16	1.408588	1.408588	1	0	0	1
0.653044	3.084859	0.653044	1.408588	1.67E-16	1.408588	0	1	0	1
0.653044	0.653044	3.084859	1.408588	1.408588	1.67E-16	0	0	1	1
0.962251	0.99342	1.008345	0.952194	0.998281	1.045761	0	0	0	0
5.426	5.426	0.408663	1.57E-16	1.57E-16	1.378511	1	1	0	1
0.408663	5.426	5.426	1.378511	1.57E-16	1.57E-16	0	1	1	1
5.426	0.408663	5.426	1.57E-16	1.378511	1.57E-16	1	0	1	1
3.051189	0.657555	0.657555	8.33E-17	1.407114	1.407114	1	0	0	1
0.657555	3.051189	0.657555	1.407114	8.33E-17	1.407114	0	1	0	1
0.657555	0.657555	3.051189	1.407114	1.407114	8.33E-17	0	0	1	1
0.997496	0.964598	1.030931	0.965395	1.0047	1.041865	0	0	0	0
83.33333	83.33333	83.33333	0.0625	0.0625	0.0625	1	1	1	1
5.320789	5.320789	0.411809	2.00E-16	2.00E-16	1.377818	1	1	0	1
0.411809	5.320789	5.320789	1.377818	2.00E-16	2.00E-16	0	1	1	1
5.320789	0.411809	5.320789	2.00E-16	1.377818	2.00E-16	1	0	1	1
3.018392	0.661878	0.661878	1.94E-16	1.405702	1.405702	1	0	0	1
0.661878	3.018392	0.661878	1.405702	1.94E-16	1.405702	0	1	0	1
0.661878	0.661878	3.018392	1.405702	1.405702	1.94E-16	0	0	1	1

1.046965	1.019028	1.031159	1.030919	0.979311	1.048177	0	0	0	0
71.42857	71.42857	71.42857	0.074074	0.074074	0.074074	1	1	1	1
5.21971	5.21971	0.41483	1.67E-16	1.67E-16	1.377153	1	1	0	1
0.41483	5.21971	5.21971	1.377153	1.67E-16	1.67E-16	0	1	1	1
5.21971	0.41483	5.21971	1.67E-16	1.377153	1.67E-16	1	0	1	1
2.986433	0.666022	0.666022	5.55E-17	1.404349	1.404349	1	0	0	1
0.666022	2.986433	0.666022	1.404349	5.55E-17	1.404349	0	1	0	1
0.666022	0.666022	2.986433	1.404349	1.404349	5.55E-17	0	0	1	1
1.032458	0.984751	0.970936	0.971546	0.980985	0.954548	0	0	0	0
5.122525	5.122525	0.417732	1.39E-16	1.86E-16	1.376513	1	1	0	1
0.417732	5.122525	5.122525	1.376513	1.86E-16	1.39E-16	0	1	1	1
5.122525	0.417732	5.122525	1.86E-16	1.376513	1.39E-16	1	0	1	1
2.955279	0.669994	0.669994	8.33E-17	1.403054	1.403054	1	0	0	1
0.669994	2.955279	0.669994	1.403054	8.33E-17	1.403054	0	1	0	1
0.669994	0.669994	2.955279	1.403054	1.403054	8.33E-17	0	0	1	1
1.00426	1.001388	1.037549	0.969815	0.986501	0.986422	0	0	0	0
55.55556	55.55556	55.55556	0.096386	0.096386	0.096386	1	1	1	1
5.029014	5.029014	0.42052	1.76E-16	1.76E-16	1.375899	1	1	0	1
0.42052	5.029014	5.029014	1.375899	1.76E-16	1.76E-16	0	1	1	1
5.029014	0.42052	5.029014	1.76E-16	1.375899	1.76E-16	1	0	1	1
2.9249	0.673802	0.673802	8.33E-17	1.401813	1.401813	1	0	0	1
0.673802	2.9249	0.673802	1.401813	8.33E-17	1.401813	0	1	0	1
0.673802	0.673802	2.9249	1.401813	1.401813	8.33E-17	0	0	1	1
0.973799	0.979138	1.001104	1.002199	1.004409	0.985121	0	0	0	0

V_{aF}/V_{aPF}	V_{bf}/V_{bPF}	V_{cF}/V_{cPF}	I_{aF}/I_{aPF}	I_{bF}/I_{aPF}	V_{cF}/V_{cPF}	Fault
0.706867	1.370413	0.706867	1.391062	2.78E-17	1.391062	1
0.706867	0.706867	1.370413	1.391062	1.391062	2.78E-17	1
0.996757	1.034993	0.957405	0.963093	1.027595	1.039965	0
3.496503	3.496503	3.496503	0.654378	0.654378	0.654378	1
1.534697	1.534697	0.444401	1.14E-16	1.14E-16	1.370639	1
0.444401	1.534697	1.534697	1.370639	1.14E-16	1.14E-16	1
1.534697	0.444401	1.534697	1.14E-16	1.370639	1.14E-16	1
1.365612	0.706114	0.706114	1.11E-16	1.391306	1.391306	1
0.706114	1.365612	0.706114	1.391306	1.11E-16	1.391306	1
0.706114	0.706114	1.365612	1.391306	1.391306	1.11E-16	1
1.02427	0.954824	0.985441	0.996103	0.954227	1.006842	0
3.472222	3.472222	3.472222	0.655963	0.655963	0.655963	1
1.527216	1.527216	0.443838	1.69E-16	1.69E-16	1.370763	1
0.443838	1.527216	1.527216	1.370763	1.69E-16	1.69E-16	1
1.527216	0.443838	1.527216	1.69E-16	1.370763	1.69E-16	1
1.360849	0.705359	0.705359	8.33E-17	1.391551	1.391551	1
0.705359	1.360849	0.705359	1.391551	8.33E-17	1.391551	1
0.705359	0.705359	1.360849	1.391551	1.391551	8.33E-17	1
0.968036	1.043413	1.009293	0.977913	1.023647	0.96829	0
3.448276	3.448276	3.448276	0.657534	0.657534	0.657534	1
1.342182	0.702318	0.702318	8.33E-17	1.392538	1.392538	1
0.702318	1.342182	0.702318	1.392538	8.33E-17	1.392538	1
0.702318	0.702318	1.342182	1.392538	1.392538	8.33E-17	1
1.519812	1.519812	0.443274	1.69E-16	1.69E-16	1.370887	1
0.443274	1.519812	1.519812	1.370887	1.69E-16	1.69E-16	1
1.519812	0.443274	1.519812	1.69E-16	1.370887	1.69E-16	1
1.356126	0.704602	0.704602	1.11E-16	1.391796	1.391796	1
0.704602	1.356126	0.704602	1.391796	1.11E-16	1.391796	1
0.704602	0.704602	1.356126	1.391796	1.391796	1.11E-16	1
0.976885	0.994536	1.039752	1.016637	0.960532	0.971154	0
3.424658	3.424658	3.424658	0.659091	0.659091	0.659091	1
1.342182	0.702318	0.702318	8.33E-17	1.392538	1.392538	1
0.702318	1.342182	0.702318	1.392538	8.33E-17	1.392538	1
0.702318	0.702318	1.342182	1.392538	1.392538	8.33E-17	1
1.512483	1.512483	0.442709	1.69E-16	1.69E-16	1.371012	1
0.442709	1.512483	1.512483	1.371012	1.69E-16	1.69E-16	1
1.512483	0.442709	1.512483	1.69E-16	1.371012	1.69E-16	1
1.351441	0.703843	0.703843	8.33E-17	1.392043	1.392043	1
0.703843	1.351441	0.703843	1.392043	8.33E-17	1.392043	1
0.703843	0.703843	1.351441	1.392043	1.392043	8.33E-17	1

0.988032	1.017249	1.00442	0.97428	0.972658	1.047684	0
3.401361	3.401361	3.401361	0.660633	0.660633	0.660633	1
1.50523	1.50523	0.442142	1.69E-16	1.69E-16	1.371137	1
0.442142	1.50523	1.50523	1.371137	1.69E-16	1.69E-16	1
1.50523	0.442142	1.50523	1.69E-16	1.371137	1.69E-16	1
1.346793	0.703081	0.703081	2.78E-17	1.39229	1.39229	1
0.703081	1.346793	0.703081	1.39229	2.78E-17	1.39229	1
0.703081	0.703081	1.346793	1.39229	1.39229	2.78E-17	1
0.965006	0.979487	0.998017	0.956501	0.986905	1.039258	0
3.378378	3.378378	3.378378	0.662162	0.662162	0.662162	1
1.49805	1.49805	0.441574	1.39E-16	1.39E-16	1.371262	1
0.441574	1.49805	1.49805	1.371262	1.39E-16	1.39E-16	1
1.49805	0.441574	1.49805	1.39E-16	1.371262	1.39E-16	1
1.342182	0.702318	0.702318	8.33E-17	1.392538	1.392538	1
0.702318	1.342182	0.702318	1.392538	8.33E-17	1.392538	1
0.702318	0.702318	1.342182	1.392538	1.392538	8.33E-17	1
0.972021	0.985989	0.959141	1.016165	1.01284	1.039208	0
3.355705	3.355705	3.355705	0.663677	0.663677	0.663677	1
1.490943	1.490943	0.441005	1.69E-16	1.69E-16	1.371387	1
0.441005	1.490943	1.490943	1.371387	1.69E-16	1.69E-16	1
1.490943	0.441005	1.490943	1.69E-16	1.371387	1.69E-16	1
1.337609	0.701552	0.701552	5.55E-17	1.392786	1.392786	1
0.701552	1.337609	0.701552	1.392786	5.55E-17	1.392786	1
0.701552	0.701552	1.337609	1.392786	1.392786	5.55E-17	1
0.985251	0.979949	0.956895	0.990047	0.978436	0.98267	0
3.333333	3.333333	3.333333	0.665179	0.665179	0.665179	1
0.706867	1.370413	0.706867	1.391062	2.78E-17	1.391062	1
0.706867	0.706867	1.370413	1.391062	1.391062	2.78E-17	1
0.996757	1.034993	0.957405	0.963093	1.027595	1.039965	0
3.496503	3.496503	3.496503	0.654378	0.654378	0.654378	1
1.534697	1.534697	0.444401	1.14E-16	1.14E-16	1.370639	1
0.444401	1.534697	1.534697	1.370639	1.14E-16	1.14E-16	1
1.534697	0.444401	1.534697	1.14E-16	1.370639	1.14E-16	1
1.365612	0.706114	0.706114	1.11E-16	1.391306	1.391306	1
0.706114	1.365612	0.706114	1.391306	1.11E-16	1.391306	1
0.706114	0.706114	1.365612	1.391306	1.391306	1.11E-16	1
1.02427	0.954824	0.985441	0.996103	0.954227	1.006842	0
3.472222	3.472222	3.472222	0.655963	0.655963	0.655963	1
1.527216	1.527216	0.443838	1.69E-16	1.69E-16	1.370763	1
0.443838	1.527216	1.527216	1.370763	1.69E-16	1.69E-16	1
1.527216	0.443838	1.527216	1.69E-16	1.370763	1.69E-16	1

1.360849	0.705359	0.705359	8.33E-17	1.391551	1.391551	1
0.705359	1.360849	0.705359	1.391551	8.33E-17	1.391551	1
0.705359	0.705359	1.360849	1.391551	1.391551	8.33E-17	1
0.968036	1.043413	1.009293	0.977913	1.023647	0.96829	0
3.448276	3.448276	3.448276	0.657534	0.657534	0.657534	1
1.342182	0.702318	0.702318	8.33E-17	1.392538	1.392538	1
0.702318	1.342182	0.702318	1.392538	8.33E-17	1.392538	1
0.702318	0.702318	1.342182	1.392538	1.392538	8.33E-17	1
1.519812	1.519812	0.443274	1.69E-16	1.69E-16	1.370887	1
0.443274	1.519812	1.519812	1.370887	1.69E-16	1.69E-16	1
1.519812	0.443274	1.519812	1.69E-16	1.370887	1.69E-16	1
1.356126	0.704602	0.704602	1.11E-16	1.391796	1.391796	1
0.704602	1.356126	0.704602	1.391796	1.11E-16	1.391796	1
0.704602	0.704602	1.356126	1.391796	1.391796	1.11E-16	1
0.976885	0.994536	1.039752	1.016637	0.960532	0.971154	0
3.424658	3.424658	3.424658	0.659091	0.659091	0.659091	1
1.342182	0.702318	0.702318	8.33E-17	1.392538	1.392538	1
0.702318	1.342182	0.702318	1.392538	8.33E-17	1.392538	1
0.702318	0.702318	1.342182	1.392538	1.392538	8.33E-17	1
1.512483	1.512483	0.442709	1.69E-16	1.69E-16	1.371012	1
0.442709	1.512483	1.512483	1.371012	1.69E-16	1.69E-16	1
1.512483	0.442709	1.512483	1.69E-16	1.371012	1.69E-16	1
1.351441	0.703843	0.703843	8.33E-17	1.392043	1.392043	1
0.703843	1.351441	0.703843	1.392043	8.33E-17	1.392043	1
0.703843	0.703843	1.351441	1.392043	1.392043	8.33E-17	1
0.988032	1.017249	1.00442	0.97428	0.972658	1.047684	0
3.401361	3.401361	3.401361	0.660633	0.660633	0.660633	1
1.50523	1.50523	0.442142	1.69E-16	1.69E-16	1.371137	1
0.442142	1.50523	1.50523	1.371137	1.69E-16	1.69E-16	1
1.50523	0.442142	1.50523	1.69E-16	1.371137	1.69E-16	1
1.346793	0.703081	0.703081	2.78E-17	1.39229	1.39229	1
0.703081	1.346793	0.703081	1.39229	2.78E-17	1.39229	1
0.703081	0.703081	1.346793	1.39229	1.39229	2.78E-17	1
0.965006	0.979487	0.998017	0.956501	0.986905	1.039258	0
3.378378	3.378378	3.378378	0.662162	0.662162	0.662162	1
1.49805	1.49805	0.441574	1.39E-16	1.39E-16	1.371262	1
0.441574	1.49805	1.49805	1.371262	1.39E-16	1.39E-16	1
1.49805	0.441574	1.49805	1.39E-16	1.371262	1.39E-16	1
1.342182	0.702318	0.702318	8.33E-17	1.392538	1.392538	1
0.702318	1.342182	0.702318	1.392538	8.33E-17	1.392538	1
0.702318	0.702318	1.342182	1.392538	1.392538	8.33E-17	1

V_{aF}/V_{aPF}	V_{bf}/V_{bPF}	V_{cF}/V_{cPF}	I_{aF}/I_{aPF}	I_{bF}/I_{aPF}	V_{cF}/V_{cPF}	distance
0.643424	0.643424	3.154969	1.41	1.411734	2.78E-17	2000
0.648337	3.11944	0.648337	1.410127	8.33E-17	1.41	4000
3.084859	0.653044	0.653044	1.67E-16	1.41	1.408588	6000
0.653044	0.653044	3.084859	1.41E+00	1.41E+00	1.67E-16	6000
0.657555	3.051189	0.657555	1.407114	8.33E-17	1.41E+00	8000
3.018392	0.661878	0.661878	1.94E-16	1.41	1.41E+00	10000
0.661878	0.661878	3.018392	1.41E+00	1.405702	1.94E-16	10000
0.666022	2.986433	0.666022	1.404349	5.55E-17	1.4	12000
2.955279	0.669994	0.669994	8.33E-17	1.4	1.40E+00	14000
0.669994	0.669994	2.955279	1.4	1.403054	8.33E-17	14000
0.673802	2.9249	0.673802	1.401813	8.33E-17	1.4	16000
2.895266	0.677451	0.677451	1.67E-16	1.40E+00	1.400623	18000
0.677451	0.677451	2.895266	1.4	1.40E+00	1.67E-16	18000
0.680949	2.866347	0.680949	1.40E+00	2.78E-17	1.40E+00	20000
2.838118	0.684301	0.684301	1.67E-16	1.4	1.398393	22000
0.684301	0.684301	2.838118	1.4	1.40E+00	1.67E-16	22000
0.687514	2.810554	0.687514	1.397348	5.55E-17	1.40E+00	24000
2.783629	0.690593	0.690593	1.67E-16	1.4	1.396347	26000
0.690593	0.690593	2.783629	1.4	1.396347	1.67E-16	26000
0.693543	2.757321	0.693543	1.40E+00	8.33E-17	1.4	28000
2.731609	0.696369	0.696369	5.55E-17	1.39E+00	1.394469	30000
0.696369	0.696369	2.731609	1.39	1.394469	5.55E-17	30000
0.699077	2.70647	0.699077	1.39E+00	1.11E-16	1.39	32000
2.681886	0.70167	0.70167	8.33E-17	1.39E+00	1.39E+00	34000
0.70167	0.70167	2.681886	1.39E+00	1.392748	8.33E-17	34000
0.704153	2.657837	0.704153	1.39E+00	1.11E-16	1.39	36000
2.634306	0.706529	0.706529	8.33E-17	1.39E+00	1.391171	38000
0.706529	0.706529	2.634306	1.39	1.391171	8.33E-17	38000
0.708804	2.611274	0.708804	1.390433	0	1.39	40000
2.588725	0.710981	0.710981	8.33E-17	1.39	1.389728	42000
0.710981	0.710981	2.588725	1.39E+00	1.389728	8.33E-17	42000
0.713062	2.566645	0.713062	1.389053	8.33E-17	1.39	44000
2.545016	0.715053	0.715053	8.33E-17	1.39	1.39E+00	46000
0.715053	0.715053	2.545016	1.39E+00	1.39E+00	8.33E-17	46000
0.716955	2.523826	0.716955	1.387792	8.33E-17	1.39E+00	48000
2.503059	0.718773	0.718773	1.39E-16	1.39	1.39E+00	50000
0.718773	0.718773	2.503059	1.39E+00	1.387203	1.39E-16	50000
0.720509	2.482704	0.720509	1.386641	5.55E-17	1.39	52000
2.462747	0.722165	0.722165	5.55E-17	1.39	1.39E+00	54000

0.722165	0.722165	2.462747	1.39	1.386105	5.55E-17	54000
0.723746	2.443176	0.723746	1.385594	8.33E-17	1.39	56000
2.423979	0.725252	0.725252	5.55E-17	1.39E+00	1.385106	58000
0.725252	0.725252	2.423979	1.39	1.39E+00	5.55E-17	58000
0.726688	2.405145	0.726688	1.38E+00	2.78E-17	1.38E+00	60000
2.386663	0.728055	0.728055	1.11E-16	1.38	1.3842	62000
0.728055	0.728055	2.386663	1.38	1.38E+00	1.11E-16	62000
0.729356	2.368524	0.729356	1.38378	5.55E-17	1.38E+00	64000
2.350716	0.730592	0.730592	1.11E-16	1.38	1.38338	66000
0.730592	0.730592	2.350716	1.38	1.38338	1.11E-16	66000
0.731766	2.333231	0.731766	1.38E+00	2.78E-17	1.38	68000
2.316059	0.732881	0.732881	2.78E-17	1.38E+00	1.38E+00	70000
0.732881	0.732881	2.316059	1.38E+00	1.38264	2.78E-17	70000
0.733937	2.299192	0.733937	1.38E+00	1.67E-16	1.38	72000
2.282621	0.734938	0.734938	2.78E-17	1.38E+00	1.381976	74000
0.734938	0.734938	2.282621	1.38	1.381976	2.78E-17	74000
0.735884	2.266338	0.735884	1.38167	2.78E-17	1.38	76000
2.250334	0.736778	0.736778	2.78E-17	1.38	1.381382	78000
0.736778	0.736778	2.250334	1.38E+00	1.38E+00	2.78E-17	78000
0.73762	2.234603	0.73762	1.38111	5.55E-17	1.38E+00	80000
2.219138	0.738414	0.738414	5.55E-17	1.38	1.38E+00	82000
0.738414	0.738414	2.219138	1.38E+00	1.380853	5.55E-17	82000
0.73916	2.20393	0.73916	1.380613	5.55E-17	1.38	84000
2.188973	0.739859	0.739859	5.55E-17	1.38	1.38E+00	86000
0.739859	0.739859	2.188973	1.38	1.380387	5.55E-17	86000
0.740514	2.174261	0.740514	1.380175	1.11E-16	1.38	88000
2.159787	0.741126	0.741126	8.33E-17	1.38E+00	1.379978	90000
0.741126	0.741126	2.159787	1.38	1.379978	8.33E-17	90000
0.741696	2.145546	0.741696	1.379794	8.33E-17	1.38	92000
2.131531	0.742225	0.742225	1.11E-16	1.38	1.379623	94000
0.742225	0.742225	2.131531	1.38E+00	1.38E+00	1.11E-16	94000
0.742715	2.117736	0.742715	1.379465	1.67E-16	1.38E+00	96000
2.104157	0.743166	0.743166	8.33E-17	1.38	1.38E+00	98000
0.743166	0.743166	2.104157	1.38E+00	1.37932	8.33E-17	98000
0.74358	2.090787	0.74358	1.379186	8.33E-17	1.38	100000
2.077623	0.743959	0.743959	0	1.38	1.38E+00	102000
0.743959	0.743959	2.077623	1.38	1.379064	0	102000
0.744302	2.064657	0.744302	1.378953	1.11E-16	1.38	104000
2.051887	0.744612	0.744612	5.55E-17	1.38E+00	1.378853	106000
0.744612	0.744612	2.051887	1.38	1.38E+00	5.55E-17	106000
0.744889	2.039307	0.744889	1.38E+00	2.78E-17	1.38E+00	108000

2.026913	0.745134	0.745134	8.33E-17	1.38	1.378685	110000
0.745134	0.745134	2.026913	1.38	1.38E+00	8.33E-17	110000
0.745349	2.0147	0.745349	1.378616	5.55E-17	1.38E+00	112000
2.002665	0.745533	0.745533	5.55E-17	1.38	1.378556	114000
0.745533	0.745533	2.002665	1.38	1.378556	5.55E-17	114000
0.745688	1.990802	0.745688	1.38E+00	1.39E-16	1.38	116000
1.979109	0.745815	0.745815	2.78E-17	1.38E+00	1.378465	118000
0.745815	0.745815	1.979109	1.38	1.378465	2.78E-17	118000
0.745915	1.96758	0.745915	1.38E+00	1.67E-16	1.38	120000
1.956214	0.745988	0.745988	8.33E-17	1.38E+00	1.38E+00	122000
0.745988	0.745988	1.956214	1.38E+00	1.37841	8.33E-17	122000
0.746035	1.945005	0.746035	1.38E+00	5.55E-17	1.38	124000
1.933951	0.746057	0.746057	1.11E-16	1.38E+00	1.378387	126000
0.746057	0.746057	1.933951	1.38	1.378387	1.11E-16	126000
0.746054	1.923048	0.746054	1.378388	5.55E-17	1.38	128000
1.912292	0.746028	0.746028	8.33E-17	1.38	1.378397	130000
0.746028	0.746028	1.912292	1.38E+00	1.378397	8.33E-17	130000
0.745979	1.901681	0.745979	1.378412	2.78E-17	1.38	132000
1.891212	0.745908	0.745908	5.55E-17	1.38	1.38E+00	134000
0.745908	0.745908	1.891212	1.38E+00	1.38E+00	5.55E-17	134000
0.745815	1.880881	0.745815	1.378465	0.00E+00	1.38E+00	136000
1.870686	0.745701	0.745701	0.00E+00	1.38	1.38E+00	138000
0.745701	0.745701	1.870686	1.38E+00	1.378502	0	138000
0.745566	1.860623	0.745566	1.378546	8.33E-17	1.38	140000
1.85069	0.745411	0.745411	2.78E-17	1.38	1.38E+00	142000
0.745411	0.745411	1.85069	1.38	1.378596	2.78E-17	142000
0.745237	1.840884	0.745237	1.378652	8.33E-17	1.38	144000
1.831203	0.745045	0.745045	5.55E-17	1.38E+00	1.378714	146000
0.745045	0.745045	1.831203	1.38	1.38E+00	5.55E-17	146000
0.744834	1.821645	0.744834	1.38E+00	5.55E-17	1.38E+00	148000
1.812205	0.744605	0.744605	2.78E-17	1.38	1.378856	150000
0.744605	0.744605	1.812205	1.38	1.38E+00	2.78E-17	150000
0.744359	1.802883	0.744359	1.378935	5.55E-17	1.38E+00	152000
1.793676	0.744096	0.744096	8.33E-17	1.38	1.37902	154000
0.744096	0.744096	1.793676	1.38	1.37902	8.33E-17	154000
0.743817	1.784581	0.743817	1.38E+00	8.33E-17	1.38	156000
1.775597	0.743522	0.743522	1.11E-16	1.38E+00	1.38E+00	158000
0.743522	0.743522	1.775597	1.38E+00	1.379205	1.11E-16	158000
0.743211	1.766721	0.743211	1.38E+00	0	1.38	160000
1.757952	0.742886	0.742886	5.55E-17	1.38E+00	1.37941	162000
0.742886	0.742886	1.757952	1.38	1.37941	5.55E-17	162000

0.742546	1.749286	0.742546	1.37952	1.11E-16	1.38	164000
1.740722	0.742191	0.742191	0	1.38	1.379634	166000
0.742191	0.742191	1.740722	1.38E+00	1.38E+00	0	166000
0.741823	1.732259	0.741823	1.379753	2.78E-17	1.38E+00	168000
1.723894	0.741442	0.741442	8.33E-17	1.38	1.38E+00	170000
0.741442	0.741442	1.723894	1.38E+00	1.379876	8.33E-17	170000
0.741048	1.715626	0.741048	1.380003	2.78E-17	1.38	172000
1.707452	0.74064	0.74064	1.94E-16	1.38	1.38E+00	174000
0.74064	0.74064	1.707452	1.38	1.380135	1.94E-16	174000
0.740221	1.699371	0.740221	1.38027	0	1.38	176000
1.691381	0.73979	0.73979	0	1.38	1.380409	178000
0.73979	0.73979	1.691381	1.38	1.380409	0	178000
0.739346	1.683481	0.739346	1.38E+00	1.11E-16	1.38	180000
1.675669	0.738892	0.738892	5.55E-17	1.38E+00	1.38E+00	182000
0.738892	0.738892	1.675669	1.38E+00	1.380699	5.55E-17	182000
0.738427	1.667944	0.738427	1.38E+00	1.67E-16	1.38	184000
1.660303	0.73795	0.73795	1.94E-16	1.38E+00	1.381003	186000
0.73795	0.73795	1.660303	1.38	1.381003	1.94E-16	186000
0.737464	1.652745	0.737464	1.38116	8.33E-17	1.38	188000
1.64527	0.736967	0.736967	2.78E-17	1.38E+00	1.38132	190000
0.736967	0.736967	1.64527	1.38	1.38E+00	2.78E-17	190000
0.736461	1.637875	0.736461	1.38E+00	1.11E-16	1.38E+00	192000
1.630559	0.735944	0.735944	5.55E-17	1.38	1.381651	194000
0.735944	0.735944	1.630559	1.38	1.38E+00	5.55E-17	194000
0.735419	1.62332	0.735419	1.38182	1.94E-16	1.38E+00	196000
1.616158	0.734885	0.734885	2.78E-17	1.38	1.381993	198000
0.734885	0.734885	1.616158	1.38E+00	1.38E+00	2.78E-17	198000
0.734341	1.609071	0.734341	1.382168	1.11E-16	1.38E+00	200000
1.602058	0.733789	0.733789	8.33E-17	1.38	1.38E+00	202000
0.733789	0.733789	1.602058	1.38E+00	1.382347	8.33E-17	202000
0.733229	1.595118	0.733229	1.382528	2.78E-17	1.38	204000
1.588248	0.732661	0.732661	5.55E-17	1.38	1.38E+00	206000
0.732661	0.732661	1.588248	1.38	1.382711	5.55E-17	206000
0.732085	1.581449	0.732085	1.382897	5.55E-17	1.38	208000
1.574719	0.731501	0.731501	1.94E-16	1.38E+00	1.383086	210000
0.731501	0.731501	1.574719	1.38	1.38E+00	1.94E-16	210000
0.73091	1.568057	0.73091	1.38E+00	1.11E-16	1.38E+00	212000
1.561461	0.730311	0.730311	1.67E-16	1.38	1.383471	214000
0.730311	0.730311	1.561461	1.38	1.38E+00	1.67E-16	214000
0.729706	1.554932	0.729706	1.383666	1.11E-16	1.38E+00	216000
1.548466	0.729094	0.729094	8.33E-17	1.38	1.383864	218000

0.729094	0.729094	1.548466	1.38	1.383864	8.33E-17	218000
0.728475	1.542065	0.728475	1.38E+00	2.78E-17	1.38	220000
1.535726	0.72785	0.72785	1.11E-16	1.38E+00	1.38E+00	222000
0.72785	0.72785	1.535726	1.38E+00	1.384266	1.11E-16	222000
0.727218	1.529448	0.727218	1.38E+00	8.33E-17	1.38	224000
1.523232	0.72658	0.72658	5.55E-17	1.38E+00	1.384677	226000
0.72658	0.72658	1.523232	1.38	1.384677	5.55E-17	226000
0.725937	1.517074	0.725937	1.384885	0	1.38	228000
1.510976	0.725288	0.725288	2.78E-17	1.39E+00	1.385095	230000
0.725288	0.725288	1.510976	1.39	1.39E+00	2.78E-17	230000
0.724633	1.504935	0.724633	1.39E+00	1.67E-16	1.39E+00	232000
1.498952	0.723973	0.723973	0.00E+00	1.39	1.38552	234000
0.723973	0.723973	1.498952	1.39	1.39E+00	0	234000
0.723307	1.493024	0.723307	1.385736	5.55E-17	1.39E+00	236000
1.487152	0.722637	0.722637	5.55E-17	1.39	1.385953	238000
0.722637	0.722637	1.487152	1.39	1.385953	5.55E-17	238000
0.721961	1.481334	0.721961	1.39E+00	8.33E-17	1.39	240000
1.47557	0.721281	0.721281	1.11E-16	1.39E+00	1.39E+00	242000
0.721281	0.721281	1.47557	1.39E+00	1.386391	1.11E-16	242000
0.720596	1.469858	0.720596	1.39E+00	1.11E-16	1.39	244000
1.464199	0.719907	0.719907	1.94E-16	1.39E+00	1.386836	246000
0.719907	0.719907	1.464199	1.39	1.386836	1.94E-16	246000
0.719213	1.45859	0.719213	1.387061	1.11E-16	1.39	248000
1.453032	0.718515	0.718515	8.33E-17	1.39	1.387287	250000
0.718515	0.718515	1.453032	1.39	1.387287	8.33E-17	250000
0.717813	1.447524	0.717813	1.387514	8.33E-17	1.39	252000
1.442065	0.717107	0.717107	1.11E-16	1.39	1.387743	254000
0.717107	0.717107	1.442065	1.39	1.387743	1.11E-16	254000
0.716397	1.436655	0.716397	1.387973	8.33E-17	1.39	256000
1.431291	0.715683	0.715683	8.33E-17	1.39	1.388204	258000
0.715683	0.715683	1.431291	1.39	1.388204	8.33E-17	258000
0.714966	1.425975	0.714966	1.388436	2.78E-17	1.39	260000
1.420705	0.714245	0.714245	2.78E-17	1.39	1.38867	262000
0.714245	0.714245	1.420705	1.39	1.38867	2.78E-17	262000
0.713521	1.415481	0.713521	1.388905	8.33E-17	1.39	264000
1.410302	0.712793	0.712793	2.78E-17	1.39	1.38914	266000
0.712793	0.712793	1.410302	1.39	1.38914	2.78E-17	266000
0.712062	1.405167	0.712062	1.389377	8.33E-17	1.39	268000
1.400075	0.711329	0.711329	8.33E-17	1.39	1.389615	270000
0.711329	0.711329	1.400075	1.39	1.389615	8.33E-17	270000
0.710592	1.395027	0.710592	1.389854	0	1.39	272000

1.390022	0.709852	0.709852	5.55E-17	1.39	1.390094	274000
0.709852	0.709852	1.390022	1.39	1.390094	5.55E-17	274000
0.70911	1.385058	0.70911	1.390334	2.78E-17	1.39	276000
1.380136	0.708365	0.708365	5.55E-17	1.39	1.390576	278000
0.708365	0.708365	1.380136	1.39	1.390576	5.55E-17	278000
0.707617	1.375254	0.707617	1.390818	1.11E-16	1.39	280000
1.370413	0.706867	0.706867	2.78E-17	1.39	1.391062	282000
0.706867	0.706867	1.370413	1.39	1.391062	2.78E-17	282000
0.706114	1.365612	0.706114	1.391306	1.11E-16	1.39	284000
1.360849	0.705359	0.705359	8.33E-17	1.39	1.391551	286000
0.705359	0.705359	1.360849	1.39	1.391551	8.33E-17	286000
0.704602	1.356126	0.704602	1.391796	1.11E-16	1.39	288000
1.351441	0.703843	0.703843	8.33E-17	1.39	1.392043	290000
0.703843	0.703843	1.351441	1.39	1.392043	8.33E-17	290000
0.703081	1.346793	0.703081	1.39229	2.78E-17	1.39	292000
1.342182	0.702318	0.702318	8.33E-17	1.39	1.392538	294000
0.702318	0.702318	1.342182	1.39	1.392538	8.33E-17	294000
0.701552	1.337609	0.701552	1.392786	5.55E-17	1.39	296000
1.333071	0.700785	0.700785	2.78E-17	1.39	1.393035	298000
0.700785	0.700785	1.333071	1.39	1.393035	2.78E-17	298000
0.700016	1.328569	0.700016	1.393285	5.55E-17	1.39	300000
5.527822	5.527822	8.44E-15	0.5	0.5	1	4000
8.44E-15	5.527822	5.527822	1	0.5	0.5	4000
5.527822	8.44E-15	5.527822	0.5	1	0.5	4000
5.412659	5.412659	5.33E-15	0.5	0.5	1	6000
5.33E-15	5.412659	5.412659	1	0.5	0.5	6000
5.412659	5.33E-15	5.412659	0.5	1	0.5	6000
5.302196	5.302196	4.00E-15	0.5	0.5	1	8000
4.00E-15	5.302196	5.302196	1	0.5	0.5	8000
5.302196	4.00E-15	5.302196	0.5	1	0.5	8000
5.196152	5.196152	3.11E-15	0.5	0.5	1	10000
3.11E-15	5.196152	5.196152	1	0.5	0.5	10000
5.196152	3.11E-15	5.196152	0.5	1	0.5	10000
5.094267	5.094267	2.66E-15	0.5	0.5	1	12000
2.66E-15	5.094267	5.094267	1	0.5	0.5	12000
5.094267	2.66E-15	5.094267	0.5	1	0.5	12000
4.9963	4.9963	2.22E-15	0.5	0.5	1	14000
2.22E-15	4.9963	4.9963	1	0.5	0.5	14000
4.9963	2.22E-15	4.9963	0.5	1	0.5	14000
4.902031	4.902031	2.22E-15	0.5	0.5	1	16000
2.22E-15	4.902031	4.902031	1	0.5	0.5	16000

4.902031	2.22E-15	4.902031	0.5	1	0.5	16000
4.811252	4.811252	2.22E-15	0.5	0.5	1	18000
2.22E-15	4.811252	4.811252	1	0.5	0.5	18000
4.811252	2.22E-15	4.811252	0.5	1	0.5	18000
4.723775	4.723775	0	0.5	0.5	1	20000
0	4.723775	4.723775	1	0.5	0.5	20000
4.723775	0	4.723775	0.5	1	0.5	20000
4.639422	4.639422	1.33E-15	0.5	0.5	1	22000
1.33E-15	4.639422	4.639422	1	0.5	0.5	22000
4.639422	1.33E-15	4.639422	0.5	1	0.5	22000
4.558028	4.558028	1.33E-15	0.5	0.5	1	24000
1.33E-15	4.558028	4.558028	1	0.5	0.5	24000
4.558028	1.33E-15	4.558028	0.5	1	0.5	24000
4.479442	4.479442	0	0.5	0.5	1	26000
0	4.479442	4.479442	1	0.5	0.5	26000
4.479442	0	4.479442	0.5	1	0.5	26000
4.403519	4.403519	1.33E-15	0.5	0.5	1	28000
1.33E-15	4.403519	4.403519	1	0.5	0.5	28000
4.403519	1.33E-15	4.403519	0.5	1	0.5	28000
4.330127	4.330127	1.33E-15	0.5	0.5	1	30000
1.33E-15	4.330127	4.330127	1	0.5	0.5	30000
4.330127	1.33E-15	4.330127	0.5	1	0.5	30000
4.259141	4.259141	1.33E-15	0.5	0.5	1	32000
1.33E-15	4.259141	4.259141	1	0.5	0.5	32000
4.259141	1.33E-15	4.259141	0.5	1	0.5	32000
4.190446	4.190446	8.88E-16	0.5	0.5	1	34000
8.88E-16	4.190446	4.190446	1	0.5	0.5	34000
4.190446	8.88E-16	4.190446	0.5	1	0.5	34000
4.12393	4.12393	8.88E-16	0.5	0.5	1	36000
8.88E-16	4.12393	4.12393	1	0.5	0.5	36000
4.12393	8.88E-16	4.12393	0.5	1	0.5	36000
4.059494	4.059494	8.88E-16	0.5	0.5	1	38000
8.88E-16	4.059494	4.059494	1	0.5	0.5	38000
4.059494	8.88E-16	4.059494	0.5	1	0.5	38000
3.99704	3.99704	0	0.5	0.5	1	40000
0	3.99704	3.99704	1	0.5	0.5	40000
3.99704	0	3.99704	0.5	1	0.5	40000
3.936479	3.936479	8.88E-16	0.5	0.5	1	42000
8.88E-16	3.936479	3.936479	1	0.5	0.5	42000
3.936479	8.88E-16	3.936479	0.5	1	0.5	42000
3.877726	3.877726	1.33E-15	0.5	0.5	1	44000

1.33E-15	3.877726	3.877726	1	0.5	0.5	44000
3.877726	1.33E-15	3.877726	0.5	1	0.5	44000
3.8207	3.8207	0	0.5	0.5	1	46000
0	3.8207	3.8207	1	0.5	0.5	46000
3.8207	0	3.8207	0.5	1	0.5	46000
3.765328	3.765328	4.44E-16	0.5	0.5	1	48000
4.44E-16	3.765328	3.765328	1	0.5	0.5	48000
3.765328	4.44E-16	3.765328	0.5	1	0.5	48000
3.711537	3.711537	8.88E-16	0.5	0.5	1	50000
8.88E-16	3.711537	3.711537	1	0.5	0.5	50000
3.711537	8.88E-16	3.711537	0.5	1	0.5	50000
3.659262	3.659262	8.88E-16	0.5	0.5	1	52000
8.88E-16	3.659262	3.659262	1	0.5	0.5	52000
3.659262	8.88E-16	3.659262	0.5	1	0.5	52000
3.608439	3.608439	4.44E-16	0.5	0.5	1	54000
4.44E-16	3.608439	3.608439	1	0.5	0.5	54000
3.608439	4.44E-16	3.608439	0.5	1	0.5	54000
3.559009	3.559009	0	0.5	0.5	1	56000
0	3.559009	3.559009	1	0.5	0.5	56000
3.559009	0	3.559009	0.5	1	0.5	56000
3.510914	3.510914	4.44E-16	0.5	0.5	1	58000
4.44E-16	3.510914	3.510914	1	0.5	0.5	58000
3.510914	4.44E-16	3.510914	0.5	1	0.5	58000
3.464102	3.464102	4.44E-16	0.5	0.5	1	60000
4.44E-16	3.464102	3.464102	1	0.5	0.5	60000
3.464102	4.44E-16	3.464102	0.5	1	0.5	60000
3.418521	3.418521	0	0.5	0.5	1	62000
0	3.418521	3.418521	1	0.5	0.5	62000
3.418521	0	3.418521	0.5	1	0.5	62000
3.374125	3.374125	4.44E-16	0.5	0.5	1	64000
4.44E-16	3.374125	3.374125	1	0.5	0.5	64000
3.374125	4.44E-16	3.374125	0.5	1	0.5	64000
3.330867	3.330867	0	0.5	0.5	1	66000
0	3.330867	3.330867	1	0.5	0.5	66000
3.330867	0	3.330867	0.5	1	0.5	66000
3.288704	3.288704	4.44E-16	0.5	0.5	1	68000
4.44E-16	3.288704	3.288704	1	0.5	0.5	68000
3.288704	4.44E-16	3.288704	0.5	1	0.5	68000
3.247595	3.247595	4.44E-16	0.5	0.5	1	70000
4.44E-16	3.247595	3.247595	1	0.5	0.5	70000
3.247595	4.44E-16	3.247595	0.5	1	0.5	70000

3.207501	3.207501	0	0.5	0.5	1	72000
0	3.207501	3.207501	1	0.5	0.5	72000
3.207501	0	3.207501	0.5	1	0.5	72000
3.168386	3.168386	0	0.5	0.5	1	74000
0	3.168386	3.168386	1	0.5	0.5	74000
3.168386	0	3.168386	0.5	1	0.5	74000
3.130212	3.130212	4.44E-16	0.5	0.5	1	76000
4.44E-16	3.130212	3.130212	1	0.5	0.5	76000
3.130212	4.44E-16	3.130212	0.5	1	0.5	76000
3.092948	3.092948	4.44E-16	0.5	0.5	1	78000
4.44E-16	3.092948	3.092948	1	0.5	0.5	78000
3.092948	4.44E-16	3.092948	0.5	1	0.5	78000
3.05656	3.05656	0	0.5	0.5	1	80000
0	3.05656	3.05656	1	0.5	0.5	80000
3.05656	0	3.05656	0.5	1	0.5	80000
3.021019	3.021019	0	0.5	0.5	1	82000
0	3.021019	3.021019	1	0.5	0.5	82000
3.021019	0	3.021019	0.5	1	0.5	82000
2.986294	2.986294	2.22E-16	0.5	0.5	1	84000
2.22E-16	2.986294	2.986294	1	0.5	0.5	84000
2.986294	2.22E-16	2.986294	0.5	1	0.5	84000
2.952359	2.952359	4.44E-16	0.5	0.5	1	86000
4.44E-16	2.952359	2.952359	1	0.5	0.5	86000
2.952359	4.44E-16	2.952359	0.5	1	0.5	86000
2.919187	2.919187	4.44E-16	0.5	0.5	1	88000
4.44E-16	2.919187	2.919187	1	0.5	0.5	88000
2.919187	4.44E-16	2.919187	0.5	1	0.5	88000
2.886751	2.886751	0	0.5	0.5	1	90000
0	2.886751	2.886751	1	0.5	0.5	90000
2.886751	0	2.886751	0.5	1	0.5	90000
2.855029	2.855029	0	0.5	0.5	1	92000
0	2.855029	2.855029	1	0.5	0.5	92000
2.855029	0	2.855029	0.5	1	0.5	92000
2.823996	2.823996	2.22E-16	0.5	0.5	1	94000
2.22E-16	2.823996	2.823996	1	0.5	0.5	94000
2.823996	2.22E-16	2.823996	0.5	1	0.5	94000
2.79363	2.79363	4.44E-16	0.5	0.5	1	96000
4.44E-16	2.79363	2.79363	1	0.5	0.5	96000
5.769134	5.769134	0.398431	1.14E-16	2.24E-16	1.380765	2000
0.398431	5.769134	5.769134	1.380765	2.24E-16	1.14E-16	2000
5.769134	0.398431	5.769134	2.24E-16	1.380765	1.14E-16	2000

5.649879	5.649879	0.401979	1.14E-16	2.24E-16	1.379984	4000
0.401979	5.649879	5.649879	1.379984	2.24E-16	1.14E-16	4000
5.649879	0.401979	5.649879	2.24E-16	1.379984	1.14E-16	4000
5.535603	5.535603	0.405388	1.76E-16	1.76E-16	1.379233	6000
0.405388	5.535603	5.535603	1.379233	1.76E-16	1.76E-16	6000
5.535603	0.405388	5.535603	1.76E-16	1.379233	1.76E-16	6000
5.426	5.426	0.408663	1.57E-16	1.57E-16	1.378511	8000
0.408663	5.426	5.426	1.378511	1.57E-16	1.57E-16	8000
5.426	0.408663	5.426	1.57E-16	1.378511	1.57E-16	8000
5.320789	5.320789	0.411809	2.00E-16	2.00E-16	1.377818	10000
0.411809	5.320789	5.320789	1.377818	2.00E-16	2.00E-16	10000
5.320789	0.411809	5.320789	2.00E-16	1.377818	2.00E-16	10000
5.21971	5.21971	0.41483	1.67E-16	1.67E-16	1.377153	12000
0.41483	5.21971	5.21971	1.377153	1.67E-16	1.67E-16	12000
5.21971	0.41483	5.21971	1.67E-16	1.377153	1.67E-16	12000
5.122525	5.122525	0.417732	1.39E-16	1.86E-16	1.376513	14000
0.417732	5.122525	5.122525	1.376513	1.86E-16	1.39E-16	14000
5.122525	0.417732	5.122525	1.86E-16	1.376513	1.39E-16	14000
5.029014	5.029014	0.42052	1.76E-16	1.76E-16	1.375899	16000
0.42052	5.029014	5.029014	1.375899	1.76E-16	1.76E-16	16000
5.029014	0.42052	5.029014	1.76E-16	1.375899	1.76E-16	16000
4.93897	4.93897	0.423197	1.78E-16	2.17E-16	1.37531	18000
0.423197	4.93897	4.93897	1.37531	2.17E-16	1.78E-16	18000
4.93897	0.423197	4.93897	2.17E-16	1.37531	1.78E-16	18000
4.852205	4.852205	0.425768	1.69E-16	1.69E-16	1.374743	20000
0.425768	4.852205	4.852205	1.374743	1.69E-16	1.69E-16	20000
4.852205	0.425768	4.852205	1.69E-16	1.374743	1.69E-16	20000
4.768543	4.768543	0.428236	1.69E-16	1.69E-16	1.3742	22000
0.428236	4.768543	4.768543	1.3742	1.69E-16	1.69E-16	22000
4.768543	0.428236	4.768543	1.69E-16	1.3742	1.69E-16	22000
4.68782	4.68782	0.430605	1.24E-16	2.29E-16	1.373678	24000
0.430605	4.68782	4.68782	1.373678	2.29E-16	1.24E-16	24000
4.68782	0.430605	4.68782	2.29E-16	1.373678	1.24E-16	24000
4.609883	4.609883	0.43288	2.22E-16	1.11E-16	1.373177	26000
0.43288	4.609883	4.609883	1.373177	1.11E-16	2.22E-16	26000
4.609883	0.43288	4.609883	1.11E-16	1.373177	2.22E-16	26000
4.53459	4.53459	0.435062	1.69E-16	1.69E-16	1.372696	28000
0.435062	4.53459	4.53459	1.372696	1.69E-16	1.69E-16	28000
4.53459	0.435062	4.53459	1.69E-16	1.372696	1.69E-16	28000
4.461809	4.461809	0.437157	1.67E-16	5.55E-17	1.372235	30000
0.437157	4.461809	4.461809	1.372235	5.55E-17	1.67E-16	30000

4.461809	0.437157	4.461809	5.55E-17	1.372235	1.67E-16	30000
4.391416	4.391416	0.439166	1.69E-16	1.69E-16	1.371792	32000
0.439166	4.391416	4.391416	1.371792	1.69E-16	1.69E-16	32000
4.391416	0.439166	4.391416	1.69E-16	1.371792	1.69E-16	32000
4.323295	4.323295	0.441092	2.22E-16	1.11E-16	1.371368	34000
0.441092	4.323295	4.323295	1.371368	1.11E-16	2.22E-16	34000
4.323295	0.441092	4.323295	1.11E-16	1.371368	2.22E-16	34000
4.257337	4.257337	0.44294	1.69E-16	1.69E-16	1.370961	36000
0.44294	4.257337	4.257337	1.370961	1.69E-16	1.69E-16	36000
4.257337	0.44294	4.257337	1.69E-16	1.370961	1.69E-16	36000
4.193442	4.193442	0.44471	1.14E-16	1.14E-16	1.370571	38000
0.44471	4.193442	4.193442	1.370571	1.14E-16	1.14E-16	38000
4.193442	0.44471	4.193442	1.14E-16	1.370571	1.14E-16	38000
4.131513	4.131513	0.446407	2.22E-16	1.11E-16	1.370197	40000
0.446407	4.131513	4.131513	1.370197	1.11E-16	2.22E-16	40000
4.131513	0.446407	4.131513	1.11E-16	1.370197	2.22E-16	40000
4.07146	4.07146	0.448032	1.69E-16	1.69E-16	1.369839	42000
0.448032	4.07146	4.07146	1.369839	1.69E-16	1.69E-16	42000
4.07146	0.448032	4.07146	1.69E-16	1.369839	1.69E-16	42000
4.0132	4.0132	0.449589	1.24E-16	2.29E-16	1.369496	44000
0.449589	4.0132	4.0132	1.369496	2.29E-16	1.24E-16	44000
4.0132	0.449589	4.0132	2.29E-16	1.369496	1.24E-16	44000
3.956653	3.956653	0.451078	1.69E-16	1.69E-16	1.369168	46000
0.451078	3.956653	3.956653	1.369168	1.69E-16	1.69E-16	46000
3.956653	0.451078	3.956653	1.69E-16	1.369168	1.69E-16	46000
3.901745	3.901745	0.452503	1.69E-16	1.69E-16	1.368854	48000
0.452503	3.901745	3.901745	1.368854	1.69E-16	1.69E-16	48000
3.901745	0.452503	3.901745	1.69E-16	1.368854	1.69E-16	48000
3.848405	3.848405	0.453866	1.69E-16	1.69E-16	1.368554	50000
0.453866	3.848405	3.848405	1.368554	1.69E-16	1.69E-16	50000
3.848405	0.453866	3.848405	1.69E-16	1.368554	1.69E-16	50000
3.796566	3.796566	0.455169	1.67E-16	1.11E-16	1.368267	52000
0.455169	3.796566	3.796566	1.368267	1.11E-16	1.67E-16	52000
3.796566	0.455169	3.796566	1.11E-16	1.368267	1.67E-16	52000
3.746166	3.746166	0.456414	1.69E-16	1.69E-16	1.367993	54000
0.456414	3.746166	3.746166	1.367993	1.69E-16	1.69E-16	54000
3.746166	0.456414	3.746166	1.69E-16	1.367993	1.69E-16	54000
3.697146	3.697146	0.457602	1.14E-16	1.14E-16	1.367731	56000
0.457602	3.697146	3.697146	1.367731	1.14E-16	1.14E-16	56000
3.697146	0.457602	3.697146	1.14E-16	1.367731	1.14E-16	56000
3.649449	3.649449	0.458736	2.22E-16	1.11E-16	1.367481	58000

0.458736	3.649449	3.649449	1.367481	1.11E-16	2.22E-16	58000
3.649449	0.458736	3.649449	1.11E-16	1.367481	2.22E-16	58000
3.603023	3.603023	0.459817	1.69E-16	1.69E-16	1.367243	60000
0.459817	3.603023	3.603023	1.367243	1.69E-16	1.69E-16	60000
3.603023	0.459817	3.603023	1.69E-16	1.367243	1.69E-16	60000
3.557816	3.557816	0.460847	1.69E-16	1.69E-16	1.367016	62000
0.460847	3.557816	3.557816	1.367016	1.69E-16	1.69E-16	62000
3.557816	0.460847	3.557816	1.69E-16	1.367016	1.69E-16	62000
3.513782	3.513782	0.461828	1.24E-16	2.29E-16	1.3668	64000
0.461828	3.513782	3.513782	1.3668	2.29E-16	1.24E-16	64000
3.513782	0.461828	3.513782	2.29E-16	1.3668	1.24E-16	64000
3.470875	3.470875	0.462761	1.14E-16	1.14E-16	1.366595	66000
0.462761	3.470875	3.470875	1.366595	1.14E-16	1.14E-16	66000
3.470875	0.462761	3.470875	1.14E-16	1.366595	1.14E-16	66000
3.429052	3.429052	0.463648	1.14E-16	1.14E-16	1.366399	68000
0.463648	3.429052	3.429052	1.366399	1.14E-16	1.14E-16	68000
3.429052	0.463648	3.429052	1.14E-16	1.366399	1.14E-16	68000
3.388273	3.388273	0.46449	1.69E-16	1.69E-16	1.366214	70000
0.46449	3.388273	3.388273	1.366214	1.69E-16	1.69E-16	70000
3.388273	0.46449	3.388273	1.69E-16	1.366214	1.69E-16	70000
3.348498	3.348498	0.465289	1.69E-16	1.69E-16	1.366038	72000
0.465289	3.348498	3.348498	1.366038	1.69E-16	1.69E-16	72000
3.348498	0.465289	3.348498	1.69E-16	1.366038	1.69E-16	72000
3.309692	3.309692	0.466045	1.14E-16	1.14E-16	1.365871	74000
0.466045	3.309692	3.309692	1.365871	1.14E-16	1.14E-16	74000
3.309692	0.466045	3.309692	1.14E-16	1.365871	1.14E-16	74000
3.271817	3.271817	0.466761	1.69E-16	1.69E-16	1.365713	76000
0.466761	3.271817	3.271817	1.365713	1.69E-16	1.69E-16	76000
3.271817	0.466761	3.271817	1.69E-16	1.365713	1.69E-16	76000
3.234843	3.234843	0.467438	7.85E-17	1.76E-16	1.365564	78000
0.467438	3.234843	3.234843	1.365564	1.76E-16	7.85E-17	78000
3.234843	0.467438	3.234843	1.76E-16	1.365564	7.85E-17	78000
3.198735	3.198735	0.468076	1.69E-16	1.69E-16	1.365424	80000
0.468076	3.198735	3.198735	1.365424	1.69E-16	1.69E-16	80000
3.198735	0.468076	3.198735	1.69E-16	1.365424	1.69E-16	80000
3.163465	3.163465	0.468678	1.24E-16	1.76E-16	1.365291	82000
0.468678	3.163465	3.163465	1.365291	1.76E-16	1.24E-16	82000
3.163465	0.468678	3.163465	1.76E-16	1.365291	1.24E-16	82000
3.129003	3.129003	0.469243	1.14E-16	1.14E-16	1.365167	84000
0.469243	3.129003	3.129003	1.365167	1.14E-16	1.14E-16	84000
3.129003	0.469243	3.129003	1.14E-16	1.365167	1.14E-16	84000

3.095321	3.095321	0.469774	1.67E-16	1.11E-16	1.36505	86000
0.469774	3.095321	3.095321	1.36505	1.11E-16	1.67E-16	86000
3.095321	0.469774	3.095321	1.11E-16	1.36505	1.67E-16	86000
3.062393	3.062393	0.470271	1.24E-16	2.29E-16	1.36494	88000
0.470271	3.062393	3.062393	1.36494	2.29E-16	1.24E-16	88000
3.062393	0.470271	3.062393	2.29E-16	1.36494	1.24E-16	88000
3.030195	3.030195	0.470735	1.24E-16	2.29E-16	1.364838	90000
0.470735	3.030195	3.030195	1.364838	2.29E-16	1.24E-16	90000
3.030195	0.470735	3.030195	2.29E-16	1.364838	1.24E-16	90000
2.998701	2.998701	0.471168	1.14E-16	1.14E-16	1.364743	92000
0.471168	2.998701	2.998701	1.364743	1.14E-16	1.14E-16	92000
2.998701	0.471168	2.998701	1.14E-16	1.364743	1.14E-16	92000
2.967889	2.967889	0.471569	1.69E-16	1.69E-16	1.364654	94000
0.471569	2.967889	2.967889	1.364654	1.69E-16	1.69E-16	94000
2.967889	0.471569	2.967889	1.69E-16	1.364654	1.69E-16	94000
250	250	250	1.32E-02	1.32E-02	0.013158	2000
166.6667	166.6667	166.6667	0.025974	2.60E-02	2.60E-02	4000
125	125	125	3.85E-02	0.038462	3.85E-02	6000
100	100	100	5.06E-02	5.06E-02	0.050633	8000
83.33333	83.33333	83.33333	0.0625	6.25E-02	6.25E-02	10000
71.42857	71.42857	71.42857	7.41E-02	0.074074	7.41E-02	12000
62.5	62.5	62.5	8.54E-02	8.54E-02	0.085366	14000
55.55556	55.55556	55.55556	0.096386	9.64E-02	9.64E-02	16000
50	50	50	1.07E-01	0.107143	1.07E-01	18000
45.45455	45.45455	45.45455	1.18E-01	1.18E-01	0.117647	20000
41.66667	41.66667	41.66667	0.127907	1.28E-01	1.28E-01	22000
38.46154	38.46154	38.46154	1.38E-01	0.137931	1.38E-01	24000
35.71429	35.71429	35.71429	1.48E-01	1.48E-01	0.147727	26000
33.33333	33.33333	33.33333	0.157303	1.57E-01	1.57E-01	28000
31.25	31.25	31.25	1.67E-01	0.166667	1.67E-01	30000
29.41176	29.41176	29.41176	1.76E-01	1.76E-01	0.175824	32000
27.77778	27.77778	27.77778	0.184783	1.85E-01	1.85E-01	34000
26.31579	26.31579	26.31579	1.94E-01	0.193548	1.94E-01	36000
25	25	25	2.02E-01	2.02E-01	0.202128	38000
23.80952	23.80952	23.80952	0.210526	2.11E-01	2.11E-01	40000
22.72727	22.72727	22.72727	2.19E-01	0.21875	2.19E-01	42000
21.73913	21.73913	21.73913	2.27E-01	2.27E-01	0.226804	44000
20.83333	20.83333	20.83333	0.234694	2.35E-01	2.35E-01	46000
20	20	20	2.42E-01	0.242424	2.42E-01	48000
19.23077	19.23077	19.23077	2.50E-01	2.50E-01	0.25	50000
18.51852	18.51852	18.51852	0.257426	2.57E-01	2.57E-01	52000

17.85714	17.85714	17.85714	2.65E-01	0.264706	2.65E-01	54000
17.24138	17.24138	17.24138	2.72E-01	2.72E-01	0.271845	56000
16.66667	16.66667	16.66667	0.278846	2.79E-01	2.79E-01	58000
16.12903	16.12903	16.12903	2.86E-01	0.285714	2.86E-01	60000
15.625	15.625	15.625	2.92E-01	2.92E-01	0.292453	62000
15.15152	15.15152	15.15152	0.299065	2.99E-01	2.99E-01	64000
14.70588	14.70588	14.70588	3.06E-01	0.305556	3.06E-01	66000
14.28571	14.28571	14.28571	3.12E-01	3.12E-01	0.311927	68000
13.88889	13.88889	13.88889	0.318182	3.18E-01	3.18E-01	70000
13.51351	13.51351	13.51351	3.24E-01	0.324324	3.24E-01	72000
13.15789	13.15789	13.15789	3.30E-01	3.30E-01	0.330357	74000
12.82051	12.82051	12.82051	0.336283	3.36E-01	3.36E-01	76000
12.5	12.5	12.5	3.42E-01	0.342105	3.42E-01	78000
12.19512	12.19512	12.19512	3.48E-01	3.48E-01	0.347826	80000
11.90476	11.90476	11.90476	0.353448	3.53E-01	3.53E-01	82000
11.62791	11.62791	11.62791	3.59E-01	0.358974	3.59E-01	84000
11.36364	11.36364	11.36364	3.64E-01	3.64E-01	0.364407	86000
11.11111	11.11111	11.11111	0.369748	3.70E-01	3.70E-01	88000
10.86957	10.86957	10.86957	3.75E-01	0.375	3.75E-01	90000
10.6383	10.6383	10.6383	3.80E-01	3.80E-01	0.380165	92000
10.41667	10.41667	10.41667	0.385246	3.85E-01	3.85E-01	94000
10.20408	10.20408	10.20408	3.90E-01	0.390244	3.90E-01	96000
10	10	10	3.95E-01	3.95E-01	0.395161	98000
9.803922	9.803922	9.803922	0.4	4.00E-01	4.00E-01	100000
9.615385	9.615385	9.615385	4.05E-01	0.404762	4.05E-01	102000
9.433962	9.433962	9.433962	4.09E-01	4.09E-01	0.409449	104000
9.259259	9.259259	9.259259	0.414063	4.14E-01	4.14E-01	106000
9.090909	9.090909	9.090909	4.19E-01	0.418605	4.19E-01	108000
8.928571	8.928571	8.928571	4.23E-01	4.23E-01	0.423077	110000
8.77193	8.77193	8.77193	0.427481	4.27E-01	4.27E-01	112000
8.62069	8.62069	8.62069	4.32E-01	0.431818	4.32E-01	114000
8.474576	8.474576	8.474576	4.36E-01	4.36E-01	0.43609	116000
8.333333	8.333333	8.333333	0.440299	4.40E-01	4.40E-01	118000
8.196721	8.196721	8.196721	4.44E-01	0.444444	4.44E-01	120000
8.064516	8.064516	8.064516	4.49E-01	4.49E-01	0.448529	122000
7.936508	7.936508	7.936508	0.452555	4.53E-01	4.53E-01	124000
7.8125	7.8125	7.8125	4.57E-01	0.456522	4.57E-01	126000
7.692308	7.692308	7.692308	4.60E-01	4.60E-01	0.460432	128000
7.575758	7.575758	7.575758	0.464286	4.64E-01	4.64E-01	130000
7.462687	7.462687	7.462687	4.68E-01	0.468085	4.68E-01	132000
7.352941	7.352941	7.352941	4.72E-01	4.72E-01	0.471831	134000

7.246377	7.246377	7.246377	0.475524	4.76E-01	4.76E-01	136000
7.142857	7.142857	7.142857	4.79E-01	0.479167	4.79E-01	138000
7.042254	7.042254	7.042254	4.83E-01	4.83E-01	0.482759	140000
6.944444	6.944444	6.944444	0.486301	4.86E-01	4.86E-01	142000
6.849315	6.849315	6.849315	4.90E-01	0.489796	4.90E-01	144000
6.756757	6.756757	6.756757	4.93E-01	4.93E-01	0.493243	146000
6.666667	6.666667	6.666667	0.496644	4.97E-01	4.97E-01	148000
6.578947	6.578947	6.578947	5.00E-01	0.5	5.00E-01	150000
6.493506	6.493506	6.493506	5.03E-01	5.03E-01	0.503311	152000
6.410256	6.410256	6.410256	0.506579	5.07E-01	5.07E-01	154000
6.329114	6.329114	6.329114	5.10E-01	0.509804	5.10E-01	156000
6.25	6.25	6.25	5.13E-01	5.13E-01	0.512987	158000
6.17284	6.17284	6.17284	0.516129	5.16E-01	5.16E-01	160000
6.097561	6.097561	6.097561	5.19E-01	0.519231	5.19E-01	162000
6.024096	6.024096	6.024096	5.22E-01	5.22E-01	0.522293	164000
5.952381	5.952381	5.952381	0.525316	5.25E-01	5.25E-01	166000
5.882353	5.882353	5.882353	5.28E-01	0.528302	5.28E-01	168000
5.813953	5.813953	5.813953	5.31E-01	5.31E-01	0.53125	170000
5.747126	5.747126	5.747126	0.534161	5.34E-01	5.34E-01	172000
5.681818	5.681818	5.681818	5.37E-01	0.537037	5.37E-01	174000
5.617978	5.617978	5.617978	5.40E-01	5.40E-01	0.539877	176000
5.555556	5.555556	5.555556	0.542683	5.43E-01	5.43E-01	178000
5.494505	5.494505	5.494505	5.45E-01	0.545455	5.45E-01	180000
5.434783	5.434783	5.434783	5.48E-01	5.48E-01	0.548193	182000
5.376344	5.376344	5.376344	0.550898	5.51E-01	5.51E-01	184000
5.319149	5.319149	5.319149	5.54E-01	0.553571	5.54E-01	186000
5.263158	5.263158	5.263158	5.56E-01	5.56E-01	0.556213	188000
5.208333	5.208333	5.208333	0.558824	5.59E-01	5.59E-01	190000
5.154639	5.154639	5.154639	5.61E-01	0.561404	5.61E-01	192000
5.102041	5.102041	5.102041	5.64E-01	5.64E-01	0.563953	194000
5.050505	5.050505	5.050505	0.566474	5.66E-01	5.66E-01	196000
5	5	5	5.69E-01	0.568966	5.69E-01	198000
4.950495	4.950495	4.950495	5.71E-01	5.71E-01	0.571429	200000
4.901961	4.901961	4.901961	0.573864	5.74E-01	5.74E-01	202000
4.854369	4.854369	4.854369	5.76E-01	0.576271	5.76E-01	204000
4.807692	4.807692	4.807692	5.79E-01	5.79E-01	0.578652	206000
4.761905	4.761905	4.761905	0.581006	5.81E-01	5.81E-01	208000
4.716981	4.716981	4.716981	5.83E-01	0.583333	5.83E-01	210000
4.672897	4.672897	4.672897	5.86E-01	5.86E-01	0.585635	212000
4.62963	4.62963	4.62963	0.587912	5.88E-01	5.88E-01	214000
4.587156	4.587156	4.587156	5.90E-01	0.590164	5.90E-01	216000

4.545455	4.545455	4.545455	5.92E-01	5.92E-01	0.592391	218000
4.504505	4.504505	4.504505	0.594595	5.95E-01	5.95E-01	220000
4.464286	4.464286	4.464286	5.97E-01	0.596774	5.97E-01	222000
4.424779	4.424779	4.424779	5.99E-01	5.99E-01	0.59893	224000
4.385965	4.385965	4.385965	0.601064	6.01E-01	6.01E-01	226000
4.347826	4.347826	4.347826	6.03E-01	0.603175	6.03E-01	228000
4.310345	4.310345	4.310345	6.05E-01	6.05E-01	0.605263	230000
4.273504	4.273504	4.273504	0.60733	6.07E-01	6.07E-01	232000
4.237288	4.237288	4.237288	6.09E-01	0.609375	6.09E-01	234000
4.201681	4.201681	4.201681	6.11E-01	6.11E-01	0.611399	236000
4.166667	4.166667	4.166667	0.613402	6.13E-01	6.13E-01	238000
4.132231	4.132231	4.132231	6.15E-01	0.615385	6.15E-01	240000
4.098361	4.098361	4.098361	6.17E-01	6.17E-01	0.617347	242000
4.065041	4.065041	4.065041	0.619289	6.19E-01	6.19E-01	244000
4.032258	4.032258	4.032258	6.21E-01	0.621212	6.21E-01	246000
4	4	4	6.23E-01	6.23E-01	0.623116	248000
3.968254	3.968254	3.968254	0.625	6.25E-01	6.25E-01	250000
3.937008	3.937008	3.937008	6.27E-01	0.626866	6.27E-01	252000
3.90625	3.90625	3.90625	6.29E-01	6.29E-01	0.628713	254000
3.875969	3.875969	3.875969	0.630542	6.31E-01	6.31E-01	256000
3.846154	3.846154	3.846154	6.32E-01	0.632353	6.32E-01	258000
3.816794	3.816794	3.816794	6.34E-01	6.34E-01	0.634146	260000
3.787879	3.787879	3.787879	0.635922	6.36E-01	6.36E-01	262000
3.759398	3.759398	3.759398	6.38E-01	0.637681	6.38E-01	264000
3.731343	3.731343	3.731343	6.39E-01	6.39E-01	0.639423	266000
3.703704	3.703704	3.703704	0.641148	6.41E-01	6.41E-01	268000
3.676471	3.676471	3.676471	6.43E-01	0.642857	6.43E-01	270000
3.649635	3.649635	3.649635	6.45E-01	6.45E-01	0.64455	272000
3.623188	3.623188	3.623188	0.646226	6.46E-01	6.46E-01	274000
3.597122	3.597122	3.597122	6.48E-01	0.647887	6.48E-01	276000
3.571429	3.571429	3.571429	6.50E-01	6.50E-01	0.649533	278000
3.546099	3.546099	3.546099	0.651163	6.51E-01	6.51E-01	280000
3.521127	3.521127	3.521127	6.53E-01	0.652778	6.53E-01	282000
3.496503	3.496503	3.496503	6.54E-01	6.54E-01	0.654378	284000
3.472222	3.472222	3.472222	0.655963	6.56E-01	6.56E-01	286000
3.448276	3.448276	3.448276	6.58E-01	0.657534	6.58E-01	288000
3.424658	3.424658	3.424658	6.59E-01	6.59E-01	0.659091	290000
3.401361	3.401361	3.401361	0.660633	6.61E-01	6.61E-01	292000
3.378378	3.378378	3.378378	6.62E-01	0.662162	6.62E-01	294000
3.355705	3.355705	3.355705	6.64E-01	6.64E-01	0.663677	296000
3.333333	3.333333	3.333333	0.665179	6.65E-01	6.65E-01	298000

Appendix A3

Line Number	From bus	To bus	Line Reactance	Total Line Resistance
1	1	2	0.0575	0.02
2	1	3	0.1652	0.04
3	2	4	0.1737	0.04
4	3	4	0.0379	0.02
5	2	5	0.1983	0.06
6	2	6	0.1763	0.08
7	4	6	0.0414	0.04
8	5	7	0.1160	0.04
9	6	7	0.082	0.02
10	6	8	0.042	0.04
11	6	9	0.208	0.06
12	6	10	0.556	0.08
13	9	11	0.208	0.04
14	9	10	0.11	0.02
15	4	15	0.256	0.20
16	12	13	0.14	0.02
17	12	14	0.2559	0.04
18	12	15	0.1304	0.06
19	12	16	0.1987	0.08
20	14	15	0.1997	0.02
21	16	17	0.1923	0.02

22	15	18	0.2185	0.06
23	18	19	0.1292	0.02
24	19	20	0.0680	0.02
25	10	20	0.209	0.20
26	10	17	0.0845	0.14
27	10	21	0.0749	0.22
28	10	22	0.1499	0.24
29	21	22	0.0236	0.02
30	15	23	0.2020	0.16
31	22	24	0.1790	0.04
32	23	24	0.2700	0.02
33	24	25	0.3292	0.02
34	25	26	0.3800	0.02
35	25	27	0.2087	0.04
36	28	27	0.296	0.02
37	27	29	0.4153	0.04
38	27	30	0.6027	0.06
39	29	30	0.4533	0.02
40	8	28	0.200	0.40
41	6	28	0.0599	0.44